

University of Massachusetts Medical School
eScholarship@UMMS

GSBS Dissertations and Theses

Graduate School of Biomedical Sciences


2012-07-27

Molecular Studies of T Cell Recognition and Cross-Reactivity: A Dissertation

Zu T. Shen
University of Massachusetts Medical School

Let us know how access to this document benefits you.

Follow this and additional works at: https://escholarship.umassmed.edu/gsbs_diss

 Part of the [Biological Factors Commons](#), [Cells Commons](#), [Genetic Phenomena Commons](#), [Hemic and Immune Systems Commons](#), [Immunology and Infectious Disease Commons](#), and the [Pathology Commons](#)

Repository Citation

Shen ZT. (2012). Molecular Studies of T Cell Recognition and Cross-Reactivity: A Dissertation. GSBS Dissertations and Theses. <https://doi.org/10.13028/ysqk-qh98>. Retrieved from https://escholarship.umassmed.edu/gsbs_diss/630

This material is brought to you by eScholarship@UMMS. It has been accepted for inclusion in GSBS Dissertations and Theses by an authorized administrator of eScholarship@UMMS. For more information, please contact Lisa.Palmer@umassmed.edu.

**MOLECULAR STUDIES OF T CELL RECOGNITION AND CROSS-
REACTIVITY**

A Dissertation Presented

By

ZU TING SHEN

Submitted to the Faculty of the
University of Massachusetts Graduate School of Biomedical Sciences, Worcester
in partial fulfillment of the requirements for the degree of

DOCTOR OF PHILOSOPHY

July 27th, 2012

MOLECULAR STUDIES OF T CELL RECOGNITION AND CROSS-REACTIVITY

A Dissertation Presented

By

ZU TING SHEN

The signatures of the Dissertation Defense Committee signify completion and approval as to style and content of the Dissertation

Lawrence J. Stern, Ph.D., Thesis Advisor

Eric S. Huseby, Ph.D., Member of Committee

Kendall L. Knight, Ph.D., Member of Committee

Sharone Green, M.D., Member of Committee

John D. Altman, Ph.D., External Member of Committee

The signature of the Chair of the Committee signifies that the written dissertation meets the requirements of the Dissertation Committee

Leslie J. Berg, Ph.D., Chair of Committee

The signature of the Dean of the Graduate School of Biomedical Sciences signifies that the student has met all graduation requirements of the school.

Anthony Carruthers, Ph.D.,
Dean of the Graduate School of Biomedical Sciences

Interdisciplinary Graduate Program

July 27th, 2012

Acknowledgements

The work presented in this thesis would not have been possible without the support from the following people who have contributed towards my personal and scientific growth. I would especially like to acknowledge:

My mentor and advisor Larry Stern, is an exceedingly intelligent and goal-oriented scientist who seems to know everything about topics ranging from immunology, structural biology, chemical cross-linking to even pig roasting. Larry has provided me with the financial and intellectual freedom to conduct any experiment I could possibly dream of. I thank you for helping me become a better scientist and for motivating me in ways I didn't think possible.

My thesis research advisory committee including Leslie Berg, Eric Huseby and Kendall Knight. All of you have contributed great ideas and have been valuable critics of my work. I would also like to acknowledge John Altman and Sharone Green for being a part of my dissertation committee.

All of my past and present lab mates have provided tons of scientific guidance, provided helpful criticism and have dealt with many of my antics. In particular, Jennifer Stone mentored me during my first year in Larry's lab and taught me how to use all of our equipment, which we now know, occupy nearly a quarter of all departmental space! More importantly, Jen taught me everything about MHC class I expression, purification and tetramer staining, which forms an integral part of my thesis work. I thank you for steering me towards MHC class I and also for your TLC during my infancy in Larry's lab. Alexander "Sasha" Sigalov is a talented scientist who helped me to think logically

about experimental results and helped me to design rational experiments to address complicated questions. Sasha also helped to troubleshoot various experimental issues in chemical cross-linking, in immunology and multiple personal matters. I've greatly benefitted from your friendship and thank you for everything you have done for me.

Walter Kim was an incredible bay mate who sat next to me for many years. We often spent more time together than with our respective significant others. During this time, we learned about technology, sports, board games and sometimes, even science. I thank you for your friendship and the unforgettable laughs and experiences we've shared over the years. Tina Nguyen is a talented structural biologist who taught me everything about protein crystallography and Pymol. I thank you for the many excursions and random occurrences over the years. Your friendship and companionship definitely made my time in Larry's lab exciting. Ivona Strug is a top notch peptide chemist who taught me everything she could about mass spectroscopy and peptide synthesis. I thank you for helping me during the time which we overlapped. Peter Trenh has provided valuable information for Pymol, technology and even sports. I thank you for your companionship during the time which we overlapped. I would like to acknowledge the rest of the Stern lab for providing helpful criticism amongst many other things. These members include but are not limited to: Prasanna Venkatraman, Sriram Chitta, Mauricio Calvo-Calle, Maria Dorothea Nastke, Abigail Guce, Kerstin Zimmerman, Sarah Mortimer, Corrie Painter, Sabrina Vollers, Liusong Yin, Pia Negroni and Kathy Bateman.

In addition, I would like to separately acknowledge all of the technicians in Larry's lab, but in particular, Guoqi Li, Liying Lu and Loretta Lee. Over the years, each

has played a pivotal role to all research conducted in our lab. I would like to specifically acknowledge Guoqi for helping me with MHC class I expression and for kindly providing purified preparations of human β 2M, which I have used throughout my thesis research.

In addition to Larry's lab, I would also like to acknowledge past and present members of the Welsh lab, who have contributed to my research over the last four years. In particular, I've greatly benefited from collaborating with Keith Daniels, Michael Brehm and Raymond Welsh, who have all been instrumental towards my understanding of T cell cross-reactivity and viral immunology. By working closely with Mike and Keith, I've learned everything from proper plate-flicking technique (who knew that needed to be taught?) to *in vivo* CTL assays. I thank you both for the patience you have exhibited over the years. Keith and I worked closely together over the final two years. I thank you for your companionship and also teaching me what I know about mice, flow cytometry and the countless immunological procedures, which you have made me proficient in.

Last but not least, I would like to acknowledge my family and friends who have always been supportive and encouraging of my endeavors. In particular, I would like to acknowledge my wife Stephanie for her love and support over the years. I would also like to acknowledge my parents and my grandparents for the numerous sacrifices they have made on my behalf.

Abstract

Intracellular pathogens are recognized by a specialized subset of lymphocytes known as CD8⁺ T cells. Pathogen recognition by CD8⁺ T cells occurs through binding of T cell receptors (TCR) to processed antigens in complex with major histocompatibility complex (MHC) class I proteins. TCR engagement of antigens in complex with MHC class I typically lead to cytotoxic CD8⁺ T cell responses, which result in pathogen clearance. Due to the large number of foreign antigens that might be encountered by any given host a diverse repertoire of TCRs must be available for immune recognition. The main source of TCR diversity is generated by somatic recombination of the TCR genes. However, it has been suggested that selection eliminates so many recombined TCR sequences, that a high degree of TCR cross-reactivity must occur for the immune system to be able to recognize a large set of foreign pathogens. The work presented in this thesis was directed towards the understanding of the molecular mechanisms of CD8⁺ T cell recognition and cross-reactivity.

Chapter I of this thesis gives an overview of the immune system, with a focus on CD8⁺ T cells.

Chapter II of this thesis describes the development of novel bi-specific MHC heterodimers that are specific towards cross-reactive CD8⁺ T cells. Classically, MHC tetramers have been used for phenotypic characterization of antigen-specific T cells. However, identification of cross-reactive T cells requires the simultaneous use of two MHC tetramers, which was found to result in MHC tetramer cross-competition. For this reason, we generated bi-specific MHC heterodimers, which would not be affected by the

affinity between the component peptide-MHC complexes for TCR. We generated T cell lines, which cross-react with antigens from lymphocytic choriomeningitis virus (LCMV) and vaccinia virus (VV), to test our bi-specific MHC heterodimers. We show that the heterobifunctional cross-linking utilized to generate bi-specific MHC heterodimers does not affect specific binding onto cross-reactive CD8⁺ T cells.

Chapter III describes a mechanism for a cross-reactive CD8⁺ T cell response between the disparate antigens, lymphocytic choriomeningitis virus (LCMV)-GP34 (AVYNFATM) and vaccinia virus (VV)-A11R (AIVNYANL), which share the three underlined residues. The recognition determinants for LCMV-GP34 and VV-A11R were compared by an alanine/lysine scanning approach for both epitopes. Functional analysis of the mutated peptides clearly indicates that the shared P4N residue between LCMV-GP34 and VV-A11R is an important TCR contact for the recognition of both epitopes. In addition, we determined the crystal structures of both K^b-VV-A11R and K^b-LCMV-GP34. Structural analysis revealed that the two complexes are nearly identical structural mimics, which was unexpected due to the primary sequence disparity. Together with the functional studies, our results highlight that structural similarities between different peptide-MHC complexes can mediate cross-reactive T cell responses.

Chapter IV of this thesis includes additional discussion, overall conclusions and future directions.

Chapter V includes the protocols and the gene constructs that were used in this work. Also included in Chapter V are results from two unrelated incomplete projects which have yielded significant findings.

Table of Contents

Title Page	i
Signature Page	ii
Acknowledgements	iii
Abstract	vi
Table of Contents	ix
List of Tables	xi
List of Figures	xii
List of Third Party Copyrighted Material	xiv
Abbreviations	xv
Preface	xvi
I: Introduction	1
A. The Vertebrate Immune System	1
B. The Major Histocompatibility Complex (MHC)	4
1. Antigen Presentation by the MHC Class I Complex	4
2. Structural Features of the MHC Class I Complex	7
C. Recombinant MHC Class I Proteins	10
1. Production of Recombinant MHC Class I Proteins	10
2. Applications for Recombinant MHC Class I Proteins	11
D. T cell Antigen Recognition	13
1. The T cell Antigen Receptor	13
2. The T cell Co-Receptor CD8	18
3. Post Translation Modifications Alter T cell Recognition	21
E. T cell Differentiation	22
1. T cell Development	22
2. T cell Activation	23
3. Formation of T cell Memory	26
F. T cell Cross-reactivity	27
1. Mechanisms of T cell Cross-reactivity	28
2. Cross-reactive T cell Responses between LCMV and VV	34
II: Bi-specific MHC Heterodimers for the Characterization of Cross-reactive T Cells	37
A. Introduction	38
B. Materials and Methods	42
1. Production of Class I H-2K ^b Complexes	42
2. Cross-linking of Soluble MHC class I H-2K ^b Complexes	42
3. Alexa 647 Labeling of H-2K ^b Monomers, Cross-linked MHC Dimers, and Tetramers	43
4. Mass Spectroscopy	44
5. Isolation of Antigen-Specific CTL	45
6. Cell Surface and MHC Staining by Flow Cytometry	46

7. <i>Intracellular Cytokine Staining (ICS)</i>	46
C. Results	48
1. <i>Isolation and Characterization of a Cross-reactive CD8+ T cell line</i>	48
2. <i>Competition between MHC Tetramers in Conventional Staining Experiments</i>	52
3. <i>Construction of Heterodimeric MHC-based Staining Reagents by Keto-Hydrazide Coupling</i>	57
4. <i>Identification of Cross-reactive TCR on T cells using MHC Heterodimers</i>	65
D. Discussion	71
III: Disparate Epitopes Mediating Protective Heterologous Immunity to Unrelated Viruses Share Peptide-MHC Structural Features that are recognized by Cross-reactive T cells	77
A. Introduction	79
B. Materials and Methods	83
1. <i>Production of Class I H-2K^b Complexes</i>	83
2. <i>Isolation of Antigen-Specific CTL</i>	83
3. <i>Cell Surface and MHC Staining by Flow Cytometry</i>	84
4. <i>Intracellular Cytokine Staining</i>	85
5. <i>In Vivo CTL Assay</i>	85
6. <i>Crystallization and Data Collection</i>	86
7. <i>Structure Determination and Refinement</i>	86
C. Results	88
1. <i>VV-A11R and LCMV-GP34 are Cross-reactive CD8+ T cell Epitopes Elicited by LCMV Infection</i>	88
2. <i>Recognition Determinants for Cross-reactive T cells</i>	95
3. <i>Analysis of the K^b-VV-A11R and K^b-LCMV-GP34 Molecular Surfaces</i>	109
4. <i>Skewing of Cross-reactive T cell Responses Against VV-A11R and LCMV-GP34</i>	113
D. Discussion	116
<u>IV: Conclusions and Future Directions</u>	119
<u>V: Appendices</u>	136
A. Protocols used in this thesis	136
B. Gene constructs used in this thesis	171
C. Glycosylation Modulates Binding of MHC Class I monomers onto Naïve CD8+ T cells	174
D. In Cellular Assays the 9mer LCMV-GP ₃₃₋₄₁ Peptide binds to H-2K ^b as the 8mer LCMV-GP ₃₄₋₄₁ Peptide	180
<u>VI: Bibliography</u>	185

List of Tables

Table I.1	Summary of some Cross-reactive CD8 ⁺ T cell Epitopes from Previous Publications	33
Table II.1	Relevant Epitopes from VV and LCMV used for the Bi-specific MHC Heterodimer work presented in Chapter II	50
Table III.1	Relevant Epitopes from VV and LCMV used for the study on GP34-A11R Cross-reactive T cell Responses presented in Chapter III	
Table III.2	Tested K ^b -binding epitopes which share either the P4N residue or the P7 residue with LCMV-GP34 or VV-A11R	108
Table III.3	Data Collection and Refinement Statistics for K ^b -A11R and K ^b -GP34	110

List of Figures

Figure I.1	The MHC Class I Antigen Presentation Pathway	6
Figure I.2	Structural Features of the MHC Class I Complex	9
Figure I.3	Structure of TCR in Complex with MHC Class I	15
Figure I.4	Arrangement and Assembly of the T Cell Antigen Receptor	17
Figure I.5	Structure of MHC Class I in Complex with CD8 $\alpha\alpha$ co-receptor	20
Figure I.6	Mechanisms for an Individual TCR to Cross-react with Different Peptide-MHC Ligands	32
Figure II.1	CD8 ⁺ T Cells Specific for VV-A11R and LCMV-GP34	51
Figure II.2	Cross-reactive T Cells Engage Cognate Peptide-MHC Tetramers in a Manner which Reveals that there Exists Cross-reactive TCR on these Cells	55
Figure II.3	Comparable Biotinylation Levels for the Different Peptide-MHC Monomers Used for Tetramer Staining	56
Figure II.4	Chemical Reaction Scheme of Heterobifunctional Cross-linkers MHPH and MTFB	59
Figure II.5	Heterobifunctional Cross-linking of Peptide-K ^b Monomers	62
Figure II.6	Peptides are not Modified After Heterobifunctional Cross-linking and Labeling	63
Figure II.7	Binding of Alexa 647 Labeled Monomers cannot be Attributed to the Formation of Disulfide Linked Dimers	64
Figure II.8	MHC Tetramer and MHC Monomer Staining of Cross-reactive T Cells	67
Figure II.9	MHC Heterodimer Staining of Cross-reactive T Cells	70
Figure III.1	VV-A11R and LCMV-GP34 are Cross-reactive CD8 ⁺ T cell Epitopes Elicited by LCMV Infection	93

Figure III.2	Mutated Peptides from LCMV-GP34 and VV-A11R Bind to H-2K ^b with Similar Affinities with the Exception of the P3A variants	96
Figure III.3	Recognition Determinants for Cross-reactive T cells	99
Figure III.4	Acute LCMV-infected mice have a Polyclonal Cross-reactive T cell Response towards VV-A11R	101
Figure III.5	Cross-reactive T cell lines have Narrowed TCR Repertoires	103
Figure III.6	Recognition Determinants for GP34-A11R Cross-reactive T cell Receptors	106
Figure III.7	Analysis of the K ^b -VV-A11R and K ^b -LCMV-GP34 Molecular Surfaces	112
Figure III.8	Skewing of Cross-reactive Responses against both VV-A11R and LCMV-GP34	115
Figure V.A.1	Concentrator Setup for Diafiltration	144
Figure V.A.2	MHC Class I Heavy Chain Expression	151
Figure V.C.1	Glycosylation Modulates MHC Class I Monomer Binding	176
Figure V.C.2	Mutation of the Conserved CD8 Binding Site Compromises the Stability of the MHC Class I Complex	179
Figure V.D.1	The 9mer LCMV-GP ₃₃₋₄₁ peptide refolds inefficiently with H-2K ^b	182
Figure V.D.2	The Processed 9mer GP ₃₃₋₄₁ Peptide Binds to H-2K ^b Molecules as either GP ₃₃₋₄₁ or the Truncated GP ₃₄₋₄₁ Peptide	184

List of Third Party Copyrighted Material

The following figures were reproduced from journals with permission

Figure Number	Publisher	License Number
Figure I.1	John Wiley and Sons	2907690372514
Figure I.3	Elsevier	2905070493387
Figure I.4	Elsevier	2910340815678
Figure I.6	Elsevier	2903190802655

Abbreviations

AICD	Activation Induced Cell Death
APC	Antigen Presenting Cell or Allophycocyanin (fluorophore)
BCR	B Cell Receptor
BSP	Biotin Signal Peptide
β_2 M	Beta-2-Microglobulin
CFSE	Carboxyfluorescein Succinimidyl Ester
DC	Dendritic cell
DTT	1,4-Dithiothreitol
ER	Endoplasmic Reticulum
FITC	Fluorescein Isothiocyanate
GP	Glycoprotein
HC	MHC Class I heavy chain
ICS	Intracellular Cytokine Staining
IFN γ	Interferon gamma
IL-2	Interleukin-2
I.P.	Intra-peritoneal immunization
I.V.	Intra-venous immunization
LCMV	Lymphocytic Choriomeningitis Virus
MALDI	Matrix Assisted Laser Desorption/Ionization Mass Spectroscopy
MHC	Major Histocompatibility Complex
MHPH	3-N-Maleimido-6-Hydraziniumpyridine Hydrochloride
MTFB	Maleimido Trioxa Formyl Benzaldehyde
Mw	Molecular Weight
NP	Nucleoprotein
PBS	Phosphate Buffered Saline
PE	R-Phycoerythrin (fluorophore)
SA	Streptavidin
SDS-PAGE	Sodium Dodecyl Sulfate-Polyacrylamide Gel Electrophoresis
TAP	Transporter Associated with Antigen Processing
TCR	T cell Receptor
TNF α	Tumor Necrosis Factor alpha
VV	Vaccinia Virus

Preface

The work presented in Chapter II on Bi-specific MHC heterodimers was done in collaboration with Alexander Sigalov from the Stern lab, Michael Brehm and Keith Daniels from the Welsh lab and Liisa Selin. Alex designed the mass spectroscopy experiment and helped to troubleshoot biochemical experiments. Mike and Keith maintained the T cell lines and worked with me to perform all of the functional experiments. Liisa Selin provided important unpublished data.

Shen ZT, Brehm MA, Daniels KA, Sigalov AB, Selin LK, Welsh RM, Stern LJ. Bi-specific MHC heterodimers for characterization of cross-reactive T cells. *J Biol Chem.* 2010 Oct 22;285(43):33144-53

The work presented in Chapter III on the mechanism of LCMV-GP₃₄₋₄₁ and VV-A11R₁₉₈₋₂₀₅ cross-reactivity was done in collaboration with Tina Nguyen from the Stern lab and Keith Daniels from the Welsh lab. Tina and I crystallized both peptide-K^b complexes. Tina solved both of the crystal structures. Keith and I performed all of the functional experiments.

Shen ZT, Nguyen TT, Daniels KA, Welsh RM, Stern LJ. Disparate Epitopes Mediating Protective Heterologous Immunity to Unrelated Viruses Share Peptide-MHC Structural Features that are recognized by Cross-reactive T cells. Manuscript in preparation.

Chapter I:

Introduction

The immune system is a multi-faceted defense mechanism which protects the host from invasion by foreign pathogens. This chapter will give an overview of the immune system, with an emphasis on CD8+ T cell recognition and CD8+ T cell Cross-reactivity.

I.A. The Vertebrate Immune System

The innate immune response is an “ancient” defense system that provides immediate protection against pathogens. The main strategy of the innate immune system is to target molecular patterns which are not found in the host. This mode of recognition is commonly known as pattern recognition and plays a major role in the quick response of the innate immune response. The receptors which act in the innate immune recognition are encoded in the germline, which predestines the recognition of these receptors towards a limited number of targets. These targets may include components of the bacterial cell wall, such as lipids or peptidoglycans (Medzhitov and Janeway 2000; Janeway 2001; Maile 2006).

The first line of defense in the innate immune system includes the physical and the chemical barriers. The physical barriers comprise of the skin and the mucus membranes which prevents entry for most foreign pathogens. The chemical barriers include metabolites that inhibit bacterial growth, such as fatty acids found in sweat, the low pH environment generated by gastric secretions or lysozyme found in tears and

saliva that functions as an antibacterial agent, by catalyzing the breakdown of the bacterial cell wall (Janeway 2001; Maile 2006). However, if a pathogen surpasses these initial barriers, recruitment of effector cells to sites of infection occurs, which is the main line of defense for the innate immune system.

Cells called phagocytes, which includes macrophages, function in the identification and removal of foreign pathogens or infected host cells through a process known as phagocytosis (Janeway 2001). Phagocytes are also capable of recruiting other cell types to sites of infection by promoting inflammation, which is stimulated by chemical factors known as cytokines. While innate immune responses are rapid, they are often ineffective against well-evolved pathogens such as viruses. In cases where pathogens persist, the innate immune system is able to recruit the better evolved adaptive immune response through a process known as antigen presentation (Janeway 2001; Janeway and Medzhitov 2002).

In contrast to the rapidly occurring innate immune response which targets a predetermined set of pathogens, the adaptive immune system generates a pathogen-specific response towards any pathogen that may arise in the host through a process known as selection. This diverse response is achieved through somatic recombination of the antigen receptors involved, which include the T cell receptor (TCR) and the B cell receptor (BCR), expressed on T cells and B cells, respectively. A broad range of specificities is generated through somatic recombination of the TCR V, D and J gene fragments, which randomly recombine with the aid of recombinase activating genes to form a competent TCR or BCR (Schatz, Oettinger et al. 1989). Additional diversity is

introduced by nucleotide addition at the V, D and J gene junctions, which results in a large repertoire of diverse TCR sequences (Leiden and Strominger 1986). Theoretical estimates indicate that 10^{15} different antigen-specific receptors can be generated through somatic recombination (Marrack and Kappler 1988).

The adaptive immune system is comprised of cells called leukocytes, better known as white blood cells. A common subset of white blood cells is lymphocytes, which constitute 20-40% of the entire white blood cell population. The major types of lymphocytes in the adaptive immune response include B lymphocytes and T lymphocytes, better known as B cells and T cells. B cells and T cells are derived from the same hematopoietic stem cells, and are indistinguishable until post-activation (Janeway 2001). B cells and T cells act in concert in the adaptive immune response, with B cells playing a major role in the humoral immune response and T cells playing a role in the cell-mediated immune response. The major effector role of B cells is to secrete antigen-specific antibodies, which bind to foreign antigens in their native form and target them for degradation, through a process known as opsonization. On the other hand, T cells recognize processed antigens in the context of Major Histocompatibility Complex (MHC) proteins. Upon recognition, the major effector role for CD8+ T cells is to eliminate any infected host cells by inducing cytotoxic responses (Janeway 2001; Pancer and Cooper 2006).

Selection for lymphocytes occurs during T cell development and will be discussed in the T cell development subsection of this chapter. Lymphocytes which survive the selection process migrate to peripheral lymphoid tissues where clonal expansion occurs,

which results in the clearance of pathogen (Pancer and Cooper 2006). After pathogen clearance, some of the responding effector cells are converted into memory cells, which can quickly respond towards the same pathogen, should re-infection occur. This hallmark feature of the adaptive immune response is known as immunological memory and will also be discussed later. An equally important aspect of the adaptive immune response is the elimination of self-reactive cells. Discrimination of foreign versus self antigens is paramount for the host, as autoimmune responses may result (Boehm 2011).

I.B. The Major Histocompatibility Complex (MHC)

The major histocompatibility complex (MHC) is a polymorphic cell surface glycoprotein that is expressed on the surface of antigen presenting cells (APCs). The main role for MHC molecules is to present antigens to T cells. There are two main classes of MHC molecules, class I and class II. The two different classes of MHC differ mainly in their intracellular processing and presentation pathways and the subtype of T cells which they present to. The MHC class I pathway generates peptide-antigens for CD8⁺ T cells, while the MHC class II pathway generates peptide-antigens from CD4⁺ T cells. The focus of this subsection will be directed towards the MHC class I complex.

I.B.1. Antigen Presentation by the MHC Class I Complex

The MHC class I complex is a trimer consisting of a polymorphic heavy chain, a beta-2-microglobulin (β_2M) light chain and an antigenic-peptide 8-10 amino acids long

(8-10mer) (See Figure I.1A). MHC class I molecules are ubiquitously expressed on the extracellular surface of all nucleated cells and their major role is to present antigenic fragments to CD8⁺ T cells. While the source of proteins is often misfolded self-proteins, sometimes foreign proteins are also displayed to CD8⁺ T cells, which alerts CD8⁺ T cells to the infection status of the host cell (Janeway 2001; Maile 2006).

Intracellular proteins are processed in the cytosol into 3-22mer peptides by the proteasome (Kisselev, Akopian et al. 1999) and subsequently translocated into the lumen of the endoplasmic reticulum (ER) by transporter associated with antigen processing (TAP) (Androlewicz, Anderson et al. 1993; Shepherd, Schumacher et al. 1993). In the lumen, MHC class I molecules are assembled and folded with the aid of several other proteins, including tapasin, calnexin, calreticulum, ERp57 and TAP (Pamer and Cresswell 1998). Initially, the MHC class I HC is stabilized by calnexin prior to β_2M association (Degen, Cohen-Doyle et al. 1992). After associating with β_2M , the unstable complex formed between the MHC class I HC and β_2M interacts with the ER chaperones calreticulin (Sadasivan, Lehner et al. 1996) and ERp57 (Silvennoinen, Myllyharju et al. 2004; Wearsch and Cresswell 2007). Next, tapasin facilitates the loading of 8-10mer peptides by linking the MHC class I complex to TAP (Ortmann, Androlewicz et al. 1994). Lastly, peptide-bound MHC class I complexes dissociate from TAP and are transported through the secretory pathway via the trans-golgi network to the plasma membrane where they present the processed antigens to CD8⁺ T cells (Suh, Cohen-Doyle et al. 1994) (See Figure I.1).

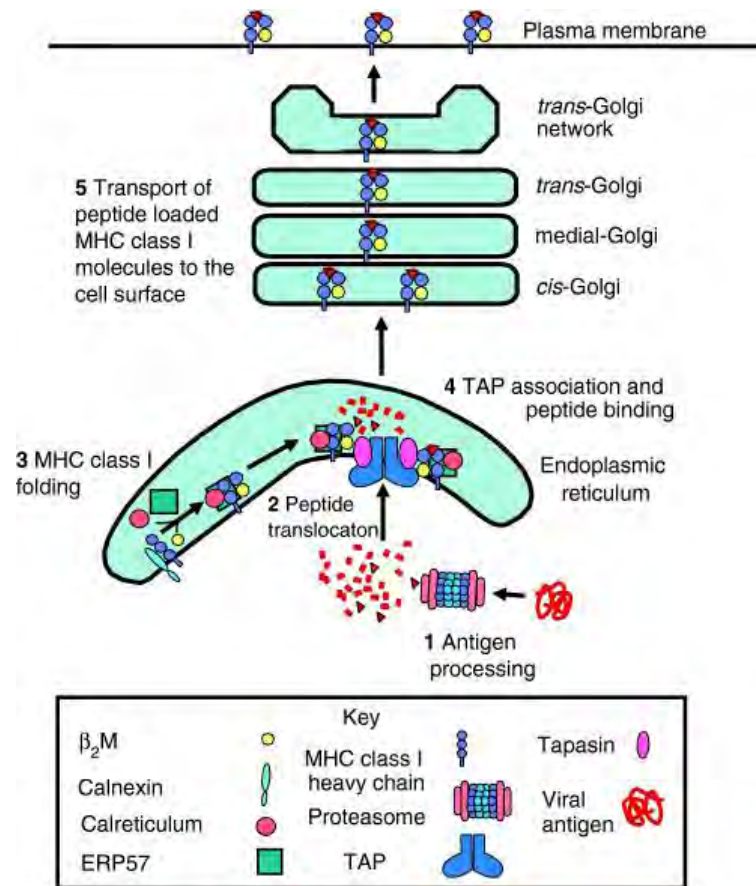


Figure I.1. The MHC Class I Antigen Presentation Pathway (Hewitt 2003). 1. Proteins are processed in the cytosol by the proteasome. 2. Peptides generated by proteolytic cleavage are translocated into the ER lumen by TAP. 3. MHC class I molecules consisting of the heavy chain and associated β_2M subunits, fold and assemble in the ER lumen with the aid of ER chaperones calnexin, calreticulum and ERp57. 4. MHC class I subunits in complex with calreticulum and ERp57 associate with TAP and tapasin facilitates peptide binding. 5. Peptide loaded MHC class I complexes dissociate from TAP and are transported through the secretory pathway via the golgi network to the plasma membrane. This figure was reproduced with permission.

I.B.2. Structural Features of the MHC Class I Complex

The MHC class I complex consists of four distinct extracellular, transmembrane domains, three of which are from the MHC class I HC with β_2M contributing a fourth domain. The three distinct extracellular domains from the MHC class I heavy chain (HC) are the $\alpha 1$, $\alpha 2$ and $\alpha 3$ domains. The $\alpha 1$ and $\alpha 2$ domains form the antigen binding site, which resembles a hotdog bun. The base of the bun consists of a single, eight-stranded β -pleated sheet and the two sides of the bun each contain a single α -helix, numbered $\alpha 1$ and $\alpha 2$ (See figure I.1). The $\alpha 3$ domain is a membrane proximal IgG-like region, which anchors the MHC class I molecule to the plasma membrane (Bjorkman, Saper et al. 1987; Janeway 2001). The β_2M light chain that's assembled with the MHC class I HC is not membrane bound, but instead, is stabilized in a non-covalent manner to the MHC class I HC via the $\alpha 3$ domain (Townsend, Elliott et al. 1990).

The vast majority of MHC class I peptides bind with both the amino and the carboxyl terminus of the peptide anchored into the MHC class I molecule through either hydrogen bonding or hydrophobic interactions (Matsumura, Fremont et al. 1992; Rammensee 1995), although exceptions for hydrogen binding at the amino terminus have been reported (Achour, Michaelsson et al. 2002; Velloso, Michaelsson et al. 2004). Due to the diversity of MHC gene locus, peptide binding motifs differ amongst the various MHC class I alleles. For example, 8mer peptides are naturally processed and presented by the murine MHC class I H-2K^b molecule (Van Bleek and Nathenson 1990). The H-2K^b molecule has two primary "pockets" or anchoring positions, which lock in the bound peptide. These pockets occur at peptide position 5 (p5) and also at peptide position 8

(p8) (Fremont, Matsumura et al. 1992; Matsumura, Fremont et al. 1992). The p8 pocket is commonly referred to as the C-terminal pocket, which prefers amino acids with hydrophobic side chains such as leucine, methionine, isoleucine or valine (Fremont, Matsumura et al. 1992; Matsumura, Fremont et al. 1992). Meanwhile, the p5 pocket has a strong preference for tyrosine or phenylalanine (Falk, Rotzschke et al. 1991). A secondary anchor residue is located at p3, which seems to have a slight preference for tyrosine (Falk, Rotzschke et al. 1991).

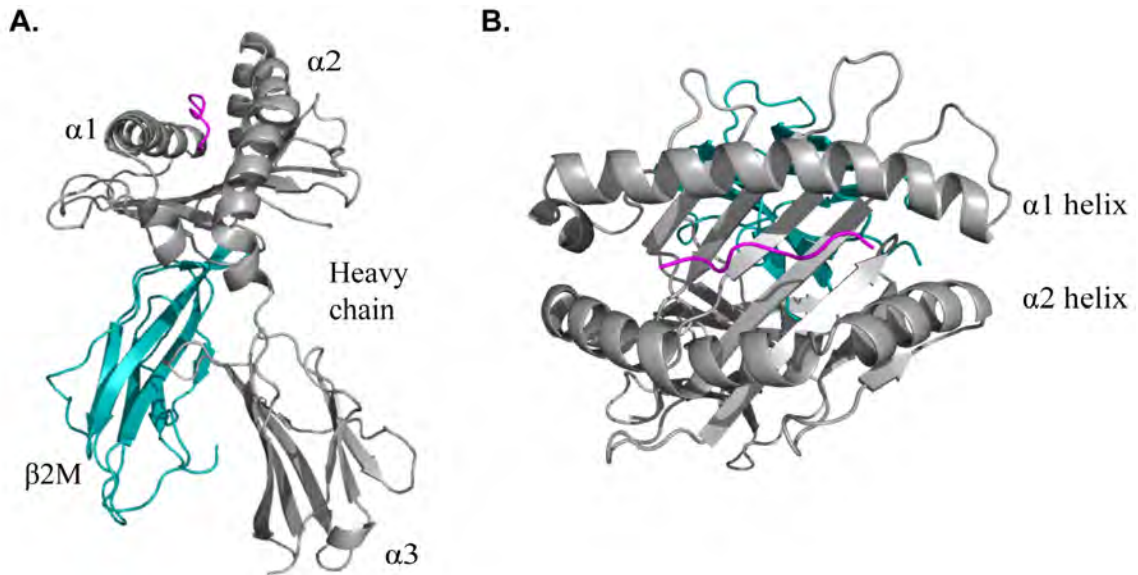


Figure I.2. Structural Features of the MHC Class I Complex. The MHC class I complex is a trimer consisting of heavy chain, $\beta 2M$ and peptide (PDBID: 3TID) and is represented as a ribbon diagram. *A.* Side view looking down the helical groove of the MHC class I molecule. The MHC class I heavy chain comprises of three distinct extracellular domains: $\alpha 1$, $\alpha 2$, and $\alpha 3$. $\beta 2M$ noncovalently associates with the heavy chain and contributes a fourth extracellular domain. The heavy chain is colored grey, $\beta 2M$ is colored cyan and peptide is colored magenta. *B.* Top view of the MHC class I molecule. The peptide binding groove is formed by the $\alpha 1$ and $\alpha 2$ domains which form helices.

I.C. Recombinant MHC Class I Proteins

The use of recombinant MHC proteins in immunology has become widespread since the invention of MHC tetramers (Altman, Moss et al. 1996). In this subsection, I will briefly review a commonly utilized method for purifying MHC class I complexes, some of the ways to generate MHC class I oligomers and the reported applications for recombinant MHC class I proteins.

1.C.1. Production of Recombinant MHC Class I Proteins

The independent expression of the MHC Class I heavy chain and beta-2-microglobulin subunits was first performed in *E. coli* (Parker, Carreno et al. 1992), which expresses these subunits as insoluble inclusion bodies (for procedure, see Chapter V.A.9). After expression, a procedure which includes washing (in the presence of detergents) and centrifugation (for procedure, see Chapter V.A.11) allows for purification of the insoluble inclusion body subunits (Garboczi, Hung et al. 1992). The solubilized MHC class I heavy chain and beta-2-microglobulin subunits are subsequently refolded *in vitro* in the presence of excess 8-10mer peptide (Parker, Carreno et al. 1992). The dilution of the urea solubilized subunits into denaturant-free buffer in the presence of peptide enables folding of the MHC class I complex (for procedure, see Chapter V.A.18). A feature specific to MHC class I complexes is that the trimolecular complex consisting of heavy chain, beta-2-microglobulin and peptide does not fold in the absence of peptide or irrelevant peptide which does not bind MHC (Garboczi, Hung et al. 1992; Parker, Carreno et al. 1992).

After refolding, there are two methods for isolating the purified complexes. Purification of the MHC class I complexes can be achieved by either size exclusion chromatography or anion exchange chromatography. For size exclusion chromatography, the refolding mixture needs to be concentrated down into a volume that can be injected onto a size exclusion column, typically less than 1 mL. Due to the large amount of refolded protein that is yielded by this particular refolding procedure (typically 10-20 mg/L, personal experience), concentrating sometimes results in protein aggregation. The method which I routinely use is buffer exchange by diafiltration (for protocol and setup, see Chapter V.A.4), which exchanges out the arginine refolding buffer for Tris pH 8, which is the buffer used in anion exchange chromatography along with its 1M NaCl salt counterpart. The selected pH at 8.0 is a pH value that is greater than the calculated isoelectric point for MHC class I complex (~6.0 for K^b-GP₃₄₋₄₁), which will result in proteins with a net negative charge. The negatively charged MHC class I complexes can then be bound onto anion exchange chromatography columns where purified MHC class I complexes can be eluted off of the column at a salt gradient at approximately 30% (for anion exchange trace, see Figure V.D.1). The arginine needs to be filtered out prior to anion exchange chromatography because it acts as a salt which causes the MHC class I complexes to self-elute.

1.C.2. Applications for Recombinant MHC Class I Proteins

A commonly utilized protocol for quantifying antigen-specific T cells is MHC oligomer staining. Commonly known as MHC tetramer staining, this method depends on

the binding of TCR to recombinant peptide-MHC complexes, assembled into tetramers to account for low affinity of individual TCR molecules for peptide-MHC complexes (Altman, Moss et al. 1996). Recombinant peptide-MHC complexes are frequently tetramerized by interaction with a fluorescently-labeled streptavidin via a biotin tag, which is incorporated into the C-terminus of the MHC class I HC construct by either chemical (i.e. thiols) or enzymatic (i.e. biotin ligase) addition (Duffy, Tsao et al. 1998). The fluorescently-labeled MHC oligomers can subsequently “stain” antigen-specific T cells by binding to their TCRs, which can be detected on the surface of T cells by flow cytometry. A similar method that has been used for detection of antigen-specific T cells is the MHC dimer-Ig (Fahmy, Bieler et al. 2002). In these molecules, the MHC class I complex is expressed as a genetic fusion at the N-terminus of an immunoglobulin heavy chain (Fahmy, Bieler et al. 2001). MHC dimer-Ig was initially designed to study T cell activation requirements, but has been adopted for phenotyping antigen-specific T cell subsets (Fahmy, Bieler et al. 2002). In addition to tracking antigen-specific T cells, MHC oligomers have been used to examine the role of multivalent TCR engagement in T cell activation (Boniface, Rabinowitz et al. 1998; Cochran, Cameron et al. 2001; Stone and Stern 2006) Most recently, peptide-MHC heterodimers have recently been utilized to study the ligand requirements of positive and negative selection during T cell development (Juang, Ebert et al. 2010). Chapter II of this thesis describes bi-specific peptide-MHC heterodimers as a novel staining reagent for visualizing cross-reactive T cells.

I.D. T cell Antigen Recognition

I.D.1. The T cell Antigen Receptor

There are several different types of TCRs (Rudolph, Stanfield et al. 2006), but those found on the CD4⁺ and CD8⁺ T cells are disulfide-linked heterodimers consisting of one alpha (α) chain and one beta (β) chain, which forms the antigen binding site. Each TCR α and TCR β chain consists of variable and constant Ig-like domains, followed by a transmembrane domain and a short cytoplasmic tail. TCR $\alpha\beta$ heterodimers are found on all CD4⁺ and CD8⁺ T cells, which are the major T cell subsets. The role for TCR is to bind to peptide-MHC complexes, hence the term “MHC restriction”. The variable regions of the TCR $\alpha\beta$ heterodimers which bind to peptide-MHC ligands are known as the complementarity-determining region (CDR) loops, and are numbered 1, 2 and 3 (Janeway 2001).

Structural analysis of TCR and peptide-MHC co-crystal structures revealed that TCR $\alpha\beta$ interacts with peptide-MHC using six different loops (Garboczi, Ghosh et al. 1996; Garcia, Degano et al. 1996): CDR1 α , CDR1 β , CDR2 α , CDR2 β , CDR3 α and CDR3 β . Interactions with the variable peptide occur primarily with the CDR3 α and CDR3 β loops, while interactions with the MHC occur with the germline encoded CDR1 and CDR2 loops (See Figure I.3) (Garboczi, Ghosh et al. 1996; Garcia, Degano et al. 1996). As a general rule of thumb, TCRs are positioned diagonally across the peptide-MHC, such that the CDR1 and CDR2 loops of the TCR α chain are positioned over the MHC α 1 helix and the CDR1 and CDR2 loops of the TCR β chain are positioned over the

MHC $\alpha 2$ helix (Garboczi, Ghosh et al. 1996) (See Figure I.3). A productive interaction between TCR and peptide-MHC results in downstream signaling cascades which have different biological consequences, ranging from positive selection to T cell activation, depending on the developmental state of the T cell (Janeway 2001).

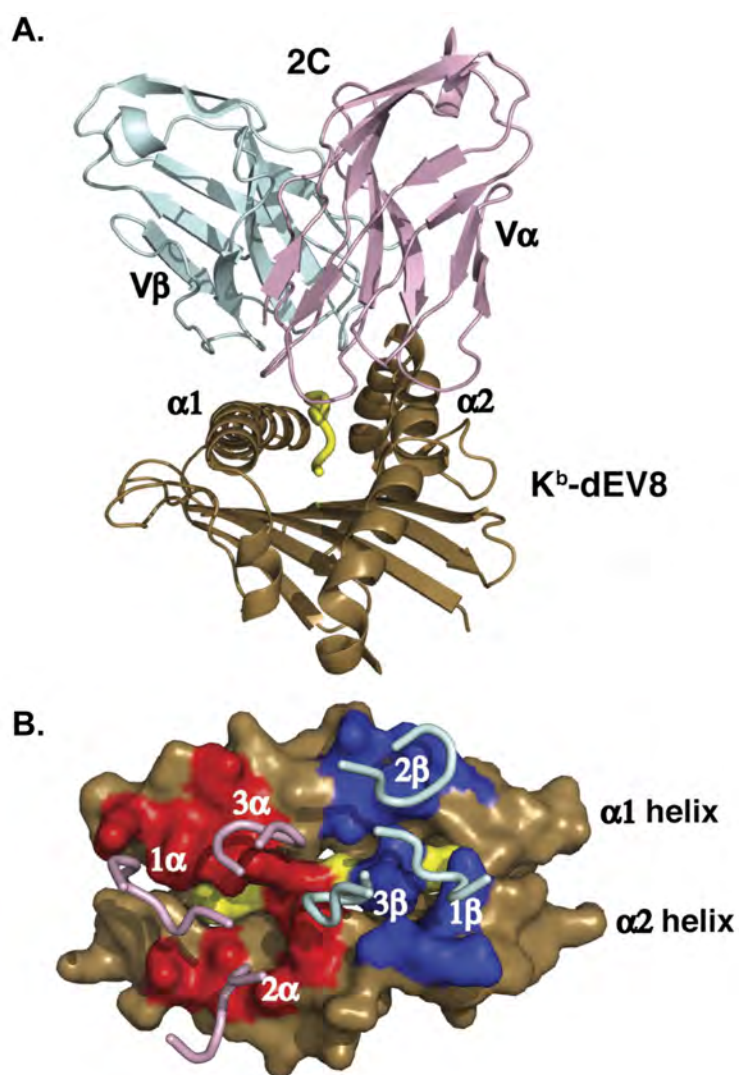


Figure I.3. Structure of TCR in Complex with MHC Class I (Garcia, Degano et al. 1998). A. Ribbon diagram of the 2C TCR V α V β domains complexed with the α 1 α 2 domains of K^b-dEV8. A portion of the 2C TCR and H-2K^b structures are not displayed (PDBID: 2CKB). 2C TCR V α is colored pink, 2C TCR V β is colored cyan, H-2K^b is brown and dEV8 peptide is yellow. B. The “footprint” view showing the isolated CDR loops of 2C TCR as tubes over the surface rendering of K^b-dEV8. The 2C TCR contact surface on the K^b-dEV8 is drawn in blue for the V β footprint and red for the V α footprint. The dEV8 peptide is yellow. This figure was reproduced with permission.

The complete T cell antigen receptor showed a complex cell surface structure and includes the TCR $\alpha\beta$ heterodimer as well as the nonpolymorphic CD3 complex, which is formed by three distinct heterodimers, (CD3 $\delta\epsilon$, CD3 $\gamma\epsilon$ and CD3 $\zeta\zeta$) (Borst, Coligan et al. 1984) (see Figure I.4). The stoichiometry and assembly of the TCR $\alpha\beta$ and CD3 complex was shown by elegant immunoprecipitation experiments (Call, Pyrdol et al. 2002). Briefly, it was shown that three basic transmembrane residues in the TCR $\alpha\beta$ heterodimer interact with six acidic transmembrane residues in the three distinct CD3 heterodimers. The TCR α transmembrane subunit has one lysine and one arginine residue, which interacts with two aspartic acid residues found on CD3 $\delta\epsilon$ and CD3 $\zeta\zeta$, respectively. Meanwhile, the TCR β transmembrane subunit has one lysine residue which interacts with one aspartic acid and one glutamic acid residue in CD3 $\gamma\epsilon$. The order of receptor assembly is as follows: the CD3 $\delta\epsilon$ heterodimer associates with the TCR α chain, the CD3 $\gamma\epsilon$ heterodimer associates with the TCR β chain, the CD3 $\zeta\zeta$ heterodimer associates with the TCR α chain (see Figure I.4) (Call, Pyrdol et al. 2002).

The complete T cell antigen receptor contains 10 immunoreceptor tyrosine activation motifs (iTAMs). The CD3 δ , CD3 γ and CD3 ϵ chains have a single iTAM while the CD3 ζ chain has three iTAMs. The role of the iTAMs in the CD3 complex was initially unclear because the CD3 chains alone have no effector function. However, it was later demonstrated that phosphorylation of iTAMs on the CD3 chains leads to recruitment of downstream adaptors which can propagate signals leading to T cell activation (Smith-Garvin, Koretzky et al. 2009).

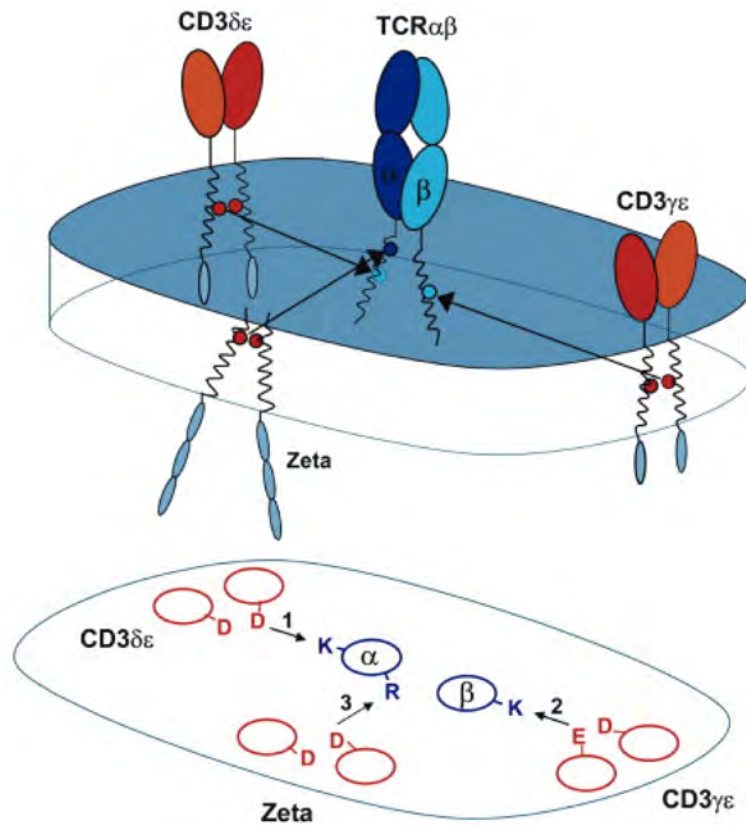


Figure I.4. Arrangement and Assembly of the T cell Antigen Receptor (Call, Pyrdol et al. 2002). The T cell antigen receptor consists of a single TCR $\alpha\beta$ heterodimer and three distinct CD3 heterodimers. Each of the three basic residues in the TCR $\alpha\beta$ transmembrane regions serves as a critical contact for one of the three CD3 heterodimers that associate with TCR $\alpha\beta$. The entire T cell antigen receptor contains 10 iTAM residues, which appear at the “tail” of the transmembrane region. The extracellular domains of TCR $\alpha\beta$ and CD3 are colored light/dark blue or light/dark orange, respectively. The intracellular iTAM residues are colored light blue. This figure was reproduced with permission.

1.D.2. The T cell Co-receptor CD8

T cells also express a co-receptor which recognizes antigen in a nonspecific manner by directly engaging MHC, without regard for the peptide presented. For CD8⁺ T cells, this co-receptor is CD8. Unlike TCR, CD8 co-receptors can be expressed as either CD8 $\alpha\beta$ heterodimers or CD8 $\alpha\alpha$ homodimers. CD8 $\alpha\beta$ heterodimers are expressed on the surface of TCR $\alpha\beta$ expressing T cells, while CD8 $\alpha\alpha$ homodimers are found on the surface of $\gamma\delta$ T cells and some NK cells (Poussier and Julius 1994). CD8 interacts with MHC class I in the highly conserved region of the $\alpha 3$ domain, distal to the antigen binding site that engages TCR (Figure I.5). The extracellular segments of both the CD8 α and CD8 β chains consist of a single immunoglobulin-like domain along with a stalk region that is highly glycosylated (Classon, Brown et al. 1992; Moody, Chui et al. 2001). The cytoplasmic tail of the CD8 α chain associates with the protein tyrosine kinase p56^{lck} and the binding of CD8 $\alpha\beta$ to the MHC class I was classically believed to initiate early signal transduction cascades leading to T cell activation (Kern, Teng et al. 1998). However, a recent report has shown that the kinase activity of p56^{lck} initiates recruitment of the CD8 co-receptor to the same peptide-MHC which is bound by TCR (Jiang, Huang et al. 2011). This report contradicts a previous theory, whereby CD8 engagement of peptide-MHC complexes precedes TCR engagement, which might increase the likelihood of an interaction between TCR and peptide-MHC.

In most cases, the importance of CD8 in T cell recognition and subsequent activation is supported by numerous reports (Potter, Rajan et al. 1989; Daniels and Jameson 2000; Dutoit, Guillaume et al. 2003; Wooldridge, van den Berg et al. 2005),

which have collectively shown that mutation of the CD8 binding site on the conserved MHC $\alpha 3$ domain abrogates TCR engagement of peptide-MHC ligands. Similar results have been shown for the CD4 co-receptor, albeit to a lesser extent (Doyle and Strominger 1987; Clayton, Sieh et al. 1989; Cammarota, Scheirle et al. 1992).

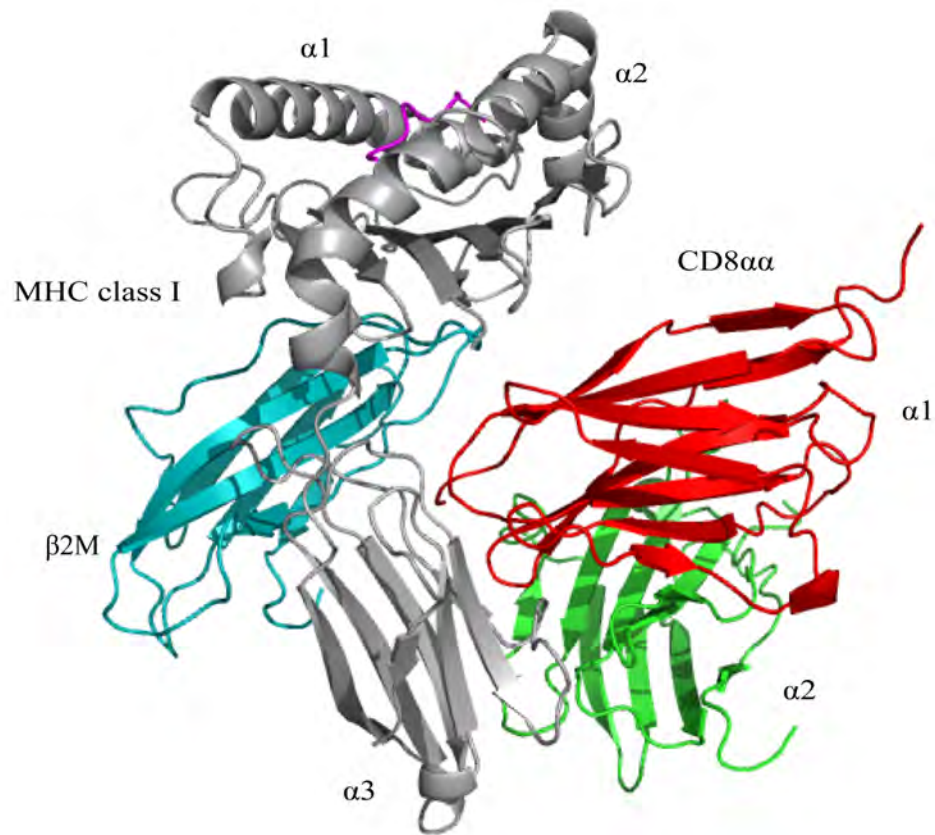


Figure I.5. Structure of MHC Class I in Complex with CD8αα co-receptor (Kern, Teng et al. 1998). Ribbon diagram of MHC class I molecule in complex with CD8αα (PDBID: 1BQH). CD8αα interacts with the MHC class I by making contacts with all six of its CDR-like loops to the conserved α3 domain of the MHC class I heavy chain. The MHC class I heavy chain is colored grey, the β2M is colored cyan, the CD8α1 chain is colored red and the CD8α2 chain is colored green.

1.D.3. Post Translation Modifications Alter T cell Recognition

Essentially all cell surface receptors involved in T cell recognition are glycoproteins. While modifications such as phosphorylation have been well characterized to play a role in T cell signaling, modifications such as glycosylation have been largely ignored. The main reason why glycobiology is less studied is partially due to glycan complexity. For example, each glycosylation site may have different patterns or numbers of the same glycan, which makes them almost impossible to monitor (Lowe 2001; Daniels, Hogquist et al. 2002). Regardless, the observation that carbohydrate binding proteins (i.e. phytohemagglutinin) can be used to artificially stimulate T cells by cross-linking cell surface glycoproteins indicates that glycan engagement can alter the immune response (Dustin and Chan 2000).

For T cell recognition, it has been shown that glycans might interfere with TCR and CD8 engagement of peptide-MHC complexes (Daniels, Hogquist et al. 2002). The mechanism for this inhibition is unclear, but because glycans can be as large as immunoglobulin domains, approximately 30Å (Rudd, Wormald et al. 1999), the inhibition has been attributed to steric hindrance created by the glycans on the plasma membrane. An alternate notion is that cell surface glycoproteins may interact with a group of glycan-binding proteins known as galectins, which has been suggested to inhibit recruitment of TCR or CD8 molecules to the immunological synapse (Demetriou, Granovsky et al. 2001).

To add to glycan complexity, individual glycosylation sites can also acquire the addition of sialic acids. The precise role of sialic acids in T cell recognition has been

difficult to address, but results have shown that the addition of sialic acids to the CD8 coreceptor inhibits CD8 co-engagement of the peptide-MHC and TCR complex (Daniels, Hogquist et al. 2002). Furthermore, it was found that increased sialylation of cell surface glycoproteins on more developed thymocytes corresponded with decreased engagement of peptide-MHC ligands (Daniels, Devine et al. 2001). This decrease in peptide-MHC engagement for the more mature thymocytes was attributed to decreased CD8 co-engagement and was reversible by removal of sialic acids from the cell surface glycoproteins (Daniels, Devine et al. 2001; Moody, Chui et al. 2001). The reduced CD8 co-engagement is likely due to sialic acid binding proteins, which bind to CD8 and prevents co-engagement, but other possibilities such as steric inhibition may also play a role.

I.E. T cell Differentiation

I.E.1. T cell Development

Development of T cells is an education process that transforms lymphoid progenitor cells into mature lymphocytes with effector function. Thymocytes, or immature T cells, originate from a common lymphoid progenitor that migrates into the thymus as early as day 11.5 in embryonic mice (Takahama 2006). These progenitors first form double negative (DN) thymocytes, which are cells that express neither the CD4 nor the CD8 co-receptor. DN thymocytes give rise to CD4⁺CD8⁺ double positive (DP) thymocytes, which migrate to the thymic cortex, where positive selection occurs. Positive selection enriches the thymocyte repertoire, which can react towards foreign

antigens. This process depends on interactions between the peptide-MHC molecules presented by cortical thymic epithelial cells and the TCRs expressed on the thymocytes. Only thymocytes that productively interact with cortical thymic epithelial cells are granted survival signals, while those that do not are targeted for apoptosis (Shortman, Egerton et al. 1990; Takahama 2006).

Following positive selection, recombination activating genes are turned off to prevent further TCR recombination (Brandle, Muller et al. 1992). DP thymocytes can differentiate into either CD8+ or CD4+ singly-positive thymocytes and undergo negative selection. Negative selection occurs in the boundary between the thymic cortex and thymic medulla with the targeted goal of eliminating any thymocytes expressing self-reactive TCRs (Kappler, Roehm et al. 1987). During negative selection, any thymocytes that react towards self-antigens presented by medullary thymic epithelial cells are eliminated. It has been estimated that less than 5% of all developing thymocytes survive both positive and negative selection (Takahama 2006). Although selection is an elegant process which eliminates self-reactive T cells while enriching for potentially useful T cells, selection alone is often insufficient to prevent autoreactivity. For this reason, various peripheral mechanisms have been suggested to account for either self-reactive TCRs which escape negative selection (Mueller 2010) or antigen diversity due to limited TCR pairings (Mason 1998).

1.E.2. T cell Activation

T cells are activated by a process which involves two distinct signals. The commonly known “signal one” is provided by engagement of the TCR to its cognate peptide-MHC ligand, presented on the surface of APCs. T cells also require a secondary signal, known as “signal two” which is provided by co-stimulatory molecules, also expressed on the surface of APCs. Expression of costimulatory molecules occurs after APC activation, which for dendritic cells (DCs) is achieved by Toll-like receptor signaling. Most pathogens contain a built-in adjuvant, such as lipopolysaccharide for gram negative bacteria, which is recognized by germline encoded Toll-like receptors expressed on DCs. Ligation of Toll-like receptors activates DCs and stimulates the surface expression of costimulatory molecules (Banchereau, Briere et al. 2000). DCs can also be induced to express costimulatory molecules by type I (α , β) interferon (IFN) (Siegal, Kadowaki et al. 1999; Biron 2001) or inflammatory molecules such as tumor necrosis factor alpha (TNF α) (Gallucci and Matzinger 2001). T cells are fully activated only in the presence of both signals. In the absence of costimulation, T cells enter an unresponsive state known as T cell anergy (Schwartz 2003). Thus, costimulation provides an additional level of control over T cell activation as self-antigens do not activate the germline encoded Toll-like receptors to express costimulatory molecules (Janeway 2001; Sprent and Surh 2002).

Naïve T cells do not possess the migratory properties to recognize antigens at the site of infection, thus, activation of naïve T cells only occurs in the secondary lymphoid organs. In order for naïve T cells to meet antigen, antigens must be transported from the site of infection to the spleen or lymph nodes, where antigen presentation occurs. The

two main routes of antigen transportation to the secondary lymphoid organs are the lymphatic system to reach the lymph nodes and the bloodstream to reach the spleen (Banchereau, Briere et al. 2000). For transportation of antigens to the lymph nodes, antigens are either phagocytosed by immature DCs, which process and transport antigens directly to the lymph nodes or transported in their native form through the lymphatics to the lymph nodes, where they are loaded onto lymph node-resident DCs (Sixt, Kanazawa et al. 2005; Clement, Cannizzo et al. 2010). A similar pathway exists for antigen transport to the spleen. There, antigens which are transported in the bloodstream to the spleen enter in soluble form and are phagocytosed and presented by immature DCs directly positioned in the spleen (Banchereau, Briere et al. 2000).

TCR ligation of peptide-MHC and costimulatory molecules activates a signal transduction cascade that ultimately leads to the activation of naïve T cells. As previously mentioned, the CD8 coreceptor is associated with a Src family kinase known as lymphocyte-specific protein tyrosine kinase ($p56^{Lck}$), which initiates the downstream signaling cascades via the signaling chains of the CD3 complex. Recruitment of zeta chain associated protein 70 (ZAP70) occurs, followed by activation of ZAP70 by $p56^{Lck}$. $p56^{Lck}$ and ZAP70 subsequently phosphorylate iTAM residues on many other molecules including linker for activated T cells (LAT), which subsequently activates other signaling cascade molecules that ultimately leads to T cell activation. A notable cytokine that's produced during activation is IL-2, which promotes the long term proliferation of activated T cells to ensure that pathogen clearance is achieved (Smith-Garvin, Koretzky et al. 2009).

1.E.3. Formation of T cell Memory

Multiple studies have shown that the T cell repertoire of memory CD8+ T cells is markedly similar to that found for naïve CD8+ T cells (Busch, Pilip et al. 1998; Sourdive, Murali-Krishna et al. 1998; Blattman, Sourdive et al. 2000), which suggests that memory T cells are derived from the effector pool. After pathogen clearance by effector T cells, a contraction phase occurs where the majority of the effector T cells die, with a few surviving members forming the memory compartment. The dying effector T cells have been found in the liver, which is regarded as the graveyard for dying effector T cells (Masopust, Vezyt et al. 2001), but dying effector T cells have also be found in the spleen where they are phagocytosed (Sprent and Surh 2002).

There are two different models for how effector T cells are transformed into long-living memory cells. In the “decreasing potential” model, effector T cells which arrive late at the secondary lymphoid organs are thought to receive less stimulation and are consequently less polarized, which allows these effector T cells to avoid the contraction phase (Moskophidis, Lechner et al. 1993; Sprent and Surh 2002). On the other hand, the “progressive differentiation” model states that T cells which receive more stimulation are better fit to survive contraction and transform into memory T cells (Lanzavecchia and Sallusto 2002). The latter has been supported by the observation that increased stimulation correlates with an increased memory T cell pool during viral infection (Quigley, Huang et al. 2007).

The cell surface markers that are generally used to phenotype memory T cells are different for humans and mice. The commonly used murine memory T cell markers are

low levels of CD62L expression and high levels of CD44 expression. However, two specific populations of memory T cells have been characterized based on their migratory properties. These subpopulations are known as “effector” memory T cells and “central” memory T cells (Sallusto, Lenig et al. 1999). The main difference between these two subsets of memory T cells is that effector memory cells can migrate to the site of infection and display immediate effector function. Effector memory cells have direct CTL activity, have rapid turnover and tend to express activation markers found on effector T cells (Zimmerman, Brduscha-Riem et al. 1996). On the other hand, central memory T cells behave more like naïve T cells, due to their resting-phenotype. Similar to naïve T cells, central memory cells home to the secondary lymphoid organs and have little or no effector function prior to antigen stimulation (Sallusto, Geginat et al. 2004). Although resembling naïve T cells, central memory cells express high levels of RNA, which suggests that these memory cells are in the G1 phase of cell cycle and maintained in a low activation state (Veiga-Fernandes, Walter et al. 2000).

I.F. T cell Cross-reactivity

Multispecific interactions have been found to occur for a variety of different proteins, ranging from enzymes (Hult and Berglund 2007) and DNA-binding proteins (Badis, Berger et al. 2009), to receptors involved in immune recognition, such as the TCR (Mariuzza 2006). In the specific case of TCR, multispecific TCR recognition of peptide-MHC complexes serves to amplify the effective TCR repertoire which can respond towards foreign antigens.

I.F.1. Mechanisms of T cell Cross-reactivity

In a general sense, it was thought that every antigen might be recognized by a unique T cell receptor. While the theoretical number of different TCR chain pairings is $\sim 10^{15}$ (Marrack and Kappler 1988), the actual number of different TCR clonotypes found in a naive mouse is closer to $\sim 10^6$ (Casrouge, Beaudoin et al. 2000), which is much lower than the number of possible antigens, which could theoretically approach 20^9 (20 amino acids in different 9mer combinations) or 5^{11} for CD8+ T cell epitopes (Mason 1998). Despite a disparity between the number of different TCR clonotypes and possible antigens, T cells from immunologically naïve hosts are not precluded from mounting functional responses towards a wide array of antigens. It has been suggested that the recognition of multiple antigens by a single T cell occurs, which is commonly referred to as T cell cross-reactivity (Mason 1998).

The simplest mechanism for multispecific interactions to occur between two interacting molecules is by utilizing different interaction sites. While this is possible for larger proteins, this is not the mode by which cross-reactive TCR recognition occurs. Instead, all TCRs recognize different peptides that are bound in the “peptide-binding groove”, that is formed in between the $\alpha 1$ and $\alpha 2$ helices of the MHC Class I molecule. Consequently, cross-reactive TCRs utilize overlapping interaction sites. To date, five different concepts of cross-reactive TCR recognition have been defined, which are illustrated in figure I.6 (Yin and Mariuzza 2009).

TCR cross-reactivity might rely on structural adjustments in the TCR, in the MHC or in the peptide, all of which facilitate the interaction between cross-reactive TCR and different peptide-MHC ligands. Structural modifications to the TCR molecule to accommodate different peptide-MHC ligands include: the induced fit mechanism, the differential TCR docking mechanism and the structural degeneracy mechanism. For the induced fit mechanism, a TCR may readjust its CDR3 loops to best accommodate cross-reactive antigens presented by the same MHC molecule (Mazza, Auphan-Anezin et al. 2007). Alternatively, a single TCR may globally reposition itself over two different peptide-MHC complexes, by shifting the TCR α and TCR β chains to form the majority of the peptide-MHC and TCR interactions that occur with either the MHC α 1 helix or the MHC α 2 helix (Differential TCR docking mechanism) (Colf, Bankovich et al. 2007). Alternatively, the absence of hydrogen bonding and salt bridges between TCR and peptide may allow for the majority of the contacts to occur between the TCR and the MHC, without regard for the peptide (Structural degeneracy mechanism) (Li, Huang et al. 2005).

Cross-reactive TCR engagement also occurs as a result of structural modifications to the peptide-MHC ligand. For the molecular mimicry mechanism, two different peptide-MHC complexes may structurally rearrange themselves to form two structurally similar interfaces with a single cross-reactive TCR (Macdonald, Chen et al. 2009). On the other hand, two structurally identical peptide-MHC complexes can undergo conformation changes in the peptide and the MHC molecules after TCR binding, which

leads to altered TCR engagement (antigen-dependent tuning of peptide-MHC flexibility mechanism) (Borbulevych, Piepenbrink et al. 2009).

An alternate explanation for cross-reactive T cell responses is the dual expression of two different TCRs, which has been found to occur in either the absence of allelic exclusion (Padovan, Casorati et al. 1993; Hardardottir, Baron et al. 1995; He, Janeway et al. 2002) or through TCR sharing between two different T cell clonotypes (Chaudhri, Quah et al. 2009). The function of the two distinct TCRs is unclear, but the general sense is that dual TCR expression occurs when one TCR does not recognize self or foreign antigens bound to self-MHC; therefore the expression of a second TCR allows these T cells to surpass selection (Hardardottir, Baron et al. 1995; He, Janeway et al. 2002). After selection, there has been some controversy as to the role of the non-selected TCR. Typically, allelic exclusion occurs to prevent the expression of two different TCR α chains (Niederberger, Holmberg et al. 2003). However, the “non-selected TCR” has been observed to mount responses in the periphery, which could lead to cross-reactive T cell responses (He, Janeway et al. 2002).

Most of the studies addressing the mechanisms of cross-reactive TCR engagement have evaluated some form of molecular mimicry, whereby structural homology between self and foreign epitopes leads to autoreactivity (Mazza, Auphan-Anezin et al. 2007; Macdonald, Chen et al. 2009; Borbulevych, Piepenbrink et al. 2011; Borbulevych, Santhanagopalan et al. 2011) (See Table I.1 for summary). For example, structural homology between self peptides and viral epitopes from vesicular stomatitis virus (Mazza, Auphan-Anezin et al. 2007) or human T lymphotropic virus (Borbulevych,

Piepenbrink et al. 2011) has been found to underlie cross-reactive TCR engagement. Furthermore, all of the reported studies have focused on the structural basis for cross-reactive TCR engagement, with little attention paid to functionally relevant T cell responses.

Only one known study has evaluated cross-reactive T cell epitopes between two distinct foreign pathogens (Borbulevych, Piepenbrink et al. 2009). In that study, the cross-reactive epitopes studied were from human T lymphotropic virus (LLFGYPVYV) and *Saccharomyces cerevisiae* (MLWGYLQYV) and share significant sequence homology, underlined at 6 of 9 positions. Therefore, the observed cross-reactive TCR recognition of similar epitopes in two distinct pathogens is not unexpected on the basis of sequence homology. The work presented in Chapter III will demonstrate a mechanism by which disparate epitopes from unrelated and pathogenic viruses are recognized by cross-reactive TCRs.

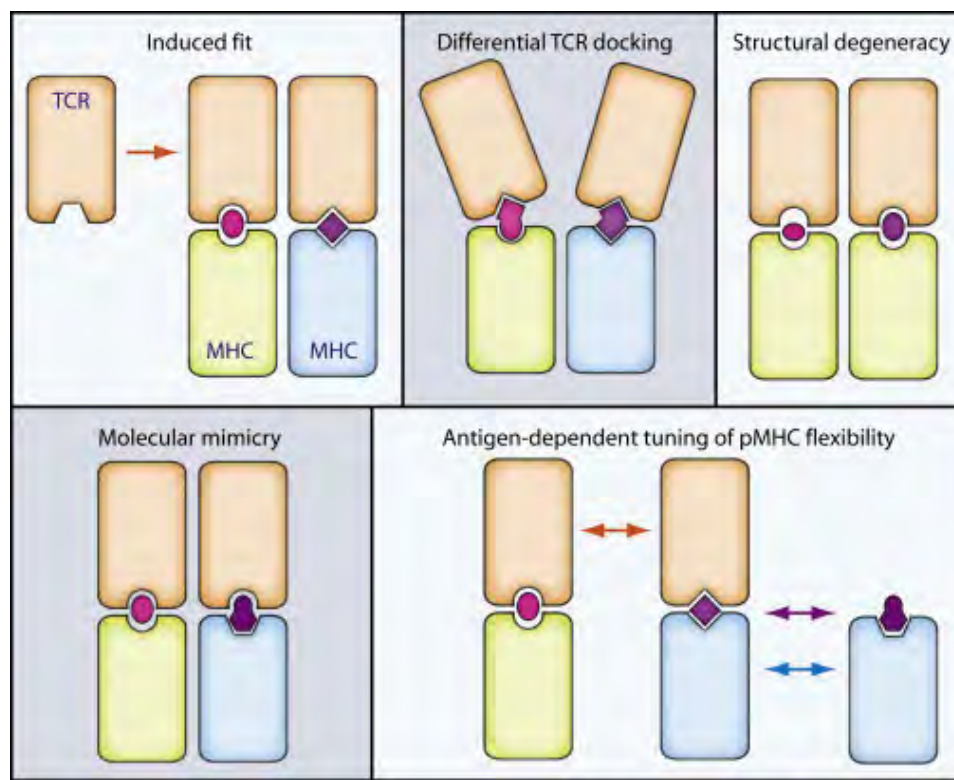


Figure I.6. Mechanisms for an Individual TCR to Cross-react with Different Peptide-MHC Ligands (Yin and Mariuzza 2009). The top row, from left to right: Cross-reactivity through an induced fit. A single TCR has a conformationally flexible binding site, which can accommodate different peptide-MHC ligands without changes to the docking orientation. Cross-reactivity through differential TCR docking. The same TCR binds different peptide-MHC ligands using different docking orientations. Cross-reactivity through structural degeneracy. Suboptimal contacts between peptide and TCR allows for the majority of contacts to occur between TCR and MHC. The bottom row, from left to right: Cross-reactivity through molecular mimicry. Different peptides in complex with MHC can form very similar interfaces with a cross-reactive TCR if the ligands are close structural mimics. Cross-reactivity through antigen-dependent tuning of peptide-MHC flexibility. Conformational dynamics in the peptide-MHC ligand allows for structural reorganization of the peptide, the MHC or the TCR molecules after TCR engagement. This figure was reproduced with permission.

Table I.1. Summary of some Cross-reactive CD8+ T cell Epitopes from Previous Publications.

Epitopes¹	Source	Reference
<u>LL</u> <u>FG</u> <u>YP</u> <u>VY</u> <u>V</u>	Tax from HTLV	(Borbulevych, Piepenbrink et al. 2009)
<u>ML</u> <u>WG</u> <u>YL</u> <u>QY</u> <u>V</u>	Tel1P from <i>S. Cerevisiae</i>	
<u>EE</u> <u>YL</u> <u>QA</u> <u>FT</u> <u>Y</u>	ATP binding cassette protein	(Macdonald, Chen et al. 2009)
<u>EE</u> <u>YL</u> <u>KA</u> <u>WT</u> <u>F</u>	Generated from randomized library	
<u>LL</u> <u>FG</u> <u>YP</u> <u>VY</u> <u>V</u>	Tax from HTLV	(Borbulevych, Piepenbrink et al. 2011)
<u>LG</u> <u>YG</u> <u>FN</u> <u>YI</u>	Neuronal self protein HuD	
<u>EA</u> <u>AG</u> <u>IG</u> <u>IL</u> <u>TV</u>	Overlapping tumor antigens from melanoma associated protein	(Borbulevych, Santhanagopalan et al. 2011)
<u>A</u> <u>AG</u> <u>IG</u> <u>IL</u> <u>TV</u>		
<u>SQ</u> <u>YY</u> <u>NS</u> <u>L</u>	Self-antigen	(Mazza, Auphan-Anezin et al. 2007)
<u>RG</u> <u>YV</u> <u>YQ</u> <u>GL</u>	VSV8 antigen	

¹Shared residues between the two epitopes in each study are underlined.

1.F.2. Cross-reactive T cell Responses between LCMV and VV

Cross-reactive T cells may recognize similar or different antigens from two different pathogens or two variants of the same pathogen. In mice, it is clear that cross-reactive CD8⁺ T cells play a major role during subsequent viral infections with consequences ranging from protective immunity (Selin, Varga et al. 1998; Walzl, Tafuro et al. 2000) to altered immunopathology (Chen, Fraire et al. 2003). This section will briefly review cross-reactive CD8⁺ T cell responses that occur between the unrelated viruses, lymphocytic choriomeningitis virus (LCMV) and vaccinia virus (VV), which is the model system under investigation in this thesis.

LCMV is an enveloped single-stranded RNA virus, which belongs to the arenavirus family. LCMV is a non-lytic virus that naturally infects rodents. Viral particles are propagated in many different tissue types, including the blood, liver, spleen, lymph nodes, lung, kidneys and brain. A common symptom of LCMV infection is encephalitis or inflammation of the brain. The peak of LCMV viral titers occur at four to five days post infection, and declines drastically as the result of strong T cell responses, which peaks at 8 days post infection (Buchmeier, Welsh et al. 1980).

LCMV contains a very small genome, which encodes only 4 proteins. The compact size of the LCMV genome has allowed for extensive characterization of T cell epitopes, which in turn, has made LCMV a commonly used virus for studying T cell responses. A notable characteristic of the LCMV-specific immune response is a large CD8⁺ T cell response. Acute LCMV infection of C57BL/6 mice elicits 28 known CD8⁺ T cell responses. Despite having 28 known epitopes, three immunodominant epitopes

(GP₃₃₋₄₁, GP₃₄₋₄₁, NP₃₉₆₋₄₀₄) account for the large majority of the LCMV-specific CD8⁺ T cell response (Kotturi, Peters et al. 2007; Kotturi, Scott et al. 2008).

An early indication that LCMV and VV might contain cross-reactive epitopes was determined when LCMV-immune mice challenged with VV showed altered immunopathology in the form of panniculitis or inflammation of the visceral fat (Selin, Varga et al. 1998). It was later shown that VV challenge of LCMV-immune hosts expanded three different epitope-specific responses from LCMV, all presented by H-2K^b: LCMV-NP₂₀₅₋₂₁₂, LCMV-GP₃₄₋₄₁ and LCMV-GP₁₁₈₋₁₂₅. On average, LCMV-NP₂₀₅₋₂₁₂ accounts for 50% of the LCMV-specific response upon VV challenge, with LCMV-GP₃₄₋₄₁ and LCMV-GP₁₁₈₋₁₂₅ specific responses each accounting for less than 25% (Kim, Cornberg et al. 2005). The particular LCMV epitope that expands after VV challenge depends on the responding T cell repertoires from the individual mice tested, which may be “private” or specific for any given mouse (Welsh, Che et al. 2010). Even genetically identical mice raised in similar environments have been found to contain different responding T cell repertoires (Bousso, Casrouge et al. 1998).

The observation that VV challenge of LCMV-immune mice expands LCMV-specific epitopes indicates the presence of a VV-specific epitope which is cross-reactive with LCMV. Screening the VV genome for a cross-reactive epitope homologous to LCMV-NP₂₀₅₋₂₁₂ revealed two candidate epitopes in VV-E7R₁₃₀₋₁₃₇ and VV-A11R₁₉₈₋₂₀₅ (Cornberg, Sheridan et al. 2007). In functional assays, VV-E7R₁₃₀₋₁₃₇-specific T cells were found to cross-react with other VV epitopes (Cornberg, Sheridan et al. 2007), but were never found to be cross-reactive with any epitopes from LCMV (Welsh, Che et al.

2010). However, the subdominant VV-A11R₁₉₈₋₂₀₅ epitope was found to be individually cross-reactive with LCMV-NP₂₀₅₋₂₁₂, LCMV-GP₃₄₋₄₁ and LCMV-GP₁₁₈₋₁₂₅ (Cornberg, Clute et al. 2010). Our recent study which utilized the cross-reactive T cell response between VV-A11R₁₉₈₋₂₀₅ and LCMV-GP₃₄₋₄₁ indicated that these two ligands are recognized by cross-reactive TCRs. The mechanism for this cross-reactive T cell response will be the focus of Chapter III.

Chapter II.

Bi-specific MHC heterodimers for Characterization of Cross-reactive T Cells

II.A. Abstract

T cell cross-reactivity describes the phenomenon whereby a single T cell can recognize two or more different peptide antigens presented in complex with MHC proteins. Cross-reactive T cells previously have been characterized at the population level by cytokine secretion and MHC tetramer staining assays, but single-cell analysis is difficult or impossible using these methods. In this study, we describe development of a novel peptide-MHC heterodimer specific for cross-reactive T cells. MHC-peptide monomers were independently conjugated to hydrazide or aldehyde-containing cross-linkers using thiol-maleimide coupling at cysteine residues introduced into recombinant MHC heavy chain proteins. Hydrazone formation provided bi-specific MHC heterodimers carrying two different peptides. Using this approach we prepared heterodimers of the murine class I MHC protein H-2K^b carrying peptides from lymphocytic choriomeningitis virus (LCMV) and vaccinia virus (VV), and used these to identify cross-reactive CD8⁺ T cells recognizing both LCMV and vaccinia virus antigens. A similar strategy could be used to develop reagents to analyze cross-reactive T cell responses in humans.

II.B. Introduction

The cellular immune response to foreign antigens depends on T cell receptor (TCR) recognition of short peptides bound to cell-surface Major Histocompatibility Complex (MHC) proteins. For a CD8⁺ T cell, antigen specificity is determined by the interaction of TCR with 8-10mer peptides presented by class I MHC proteins (Garboczi, Hung et al. 1992). During T cell development, TCR genes are assembled by somatic recombination of V, D, J, and C gene fragments, with additional diversity introduced by nucleotide addition at the junctions, resulting in a vast repertoire of clonally distributed TCR proteins, with hypervariable regions concentrated in the TCR loops that contact MHC and bound peptide antigen. Despite the diversity of TCR sequences, the diversity of foreign antigens is equally large or larger, and individual TCR are able to recognize multiple peptide sequences. During the negative selection phase of T cell development, autoreactive T cells capable of binding self MHC-peptide complexes at high affinity are deleted, and it has been suggested that negative selection removes so many TCR sequences that a high level of TCR cross-reactivity is required for the immune system to be able to recognize a sufficiently large set of foreign peptides (Mason 1998). T cell cross-reactivity has been observed in many systems (Udaka, Wiesmuller et al. 1996; Boen, Crownover et al. 2000; Dai, Huseby et al. 2008; Cornberg, Clute et al. 2010) and the structural basis for the phenomenon is beginning to be clarified (Borbulevych, Piepenbrink et al. 2009; Macdonald, Chen et al. 2009). T cell cross-reactivity appears to provide a molecular basis for T cell heterologous immunity, in which exposure to one pathogen provides protection against another (Cornberg, Sheridan et al. 2007). For

example, prior infection by lymphocytic choriomeningitis virus (LCMV) protects mice from a lethal dose of vaccinia virus (VV), with LCMV-immune mice showing alterations in their T cell response to VV infection due to LCMV-specific T cells cross-reacting with VV (Selin, Varga et al. 1998; Chen, Fraire et al. 2001). Similar patterns of T cell cross-reactivity have been suggested to underlie protective heterologous immunity between influenza A virus, Epstein Barr virus (EBV) (Clute, Watkin et al. 2005), and hepatitis C virus (Wedemeyer, Mizukoshi et al. 2001), and also immunopathology following sequential infection with Dengue virus subtypes (Rothman 2009). T cell cross-reactivity in these systems has been difficult to study, in part because reagents are not available for isolation and characterization of the cross-reactive T cells.

MHC tetramer staining is a very effective method for isolating and characterizing antigen-specific T cell populations (Altman, Moss et al. 1996). In this technique, biotin-labeled recombinant MHC molecules loaded with specific antigenic peptides are oligomerized using fluorescent streptavidin, to form highly specific reagents for analysis of antigen-specific T cells in mixed populations using flow cytometry. The use of oligomeric species is necessary because the MHC-TCR interaction is characterized by low affinity and rapid dissociation kinetics (Altman and Davis 2003), which precludes use of labeled MHC-monomers as specific staining reagents (Stone and Stern 2006). MHC tetramers conventionally are used in T cell staining protocols, mostly because of the ease of introducing biotin labels into recombinant proteins and the availability of a wide variety of fluorescent streptavidin conjugates (Altman, Moss et al. 1996). In addition to MHC tetramers, other oligomeric forms of MHC proteins including dimers,

trimers, and higher order oligomers are available and also have been used as effective staining reagents (Cochran, Cameron et al. 2001; Fahmy, Bieler et al. 2002). Antigen-specific analysis and isolation of T cells using MHC tetramers and similar reagents is a mainstay of current immunological practice, and for example has been used to characterize the fine specificity of the T cell response to VV and LCMV (Chen, Fraire et al. 2001; Kim, Cornberg et al. 2005; Cornberg, Clute et al. 2010). However, MHC-based staining reagents currently are available only as homo-oligomers with identical MHC-peptide components, and as such have not been used extensively to characterize T cell cross-reactivity. In principle two MHC tetramers could be used in co-staining experiments to evaluate the ability of a particular T cell to cross-react with different MHC-peptide complexes, but in practice competition between the two tetramers severely limits this approach (Cornberg, Clute et al. 2010). As an alternate approach to the specific detection and analysis of cross-reactive T cells, we describe here the development of novel bi-specific MHC-peptide dimers, and their use in characterization of cross-reactive T cells by flow cytometry. We employed thiol-maleimide and hydrazine-carbonyl chemistries (Kitagawa and Aikawa 1976; King, Zhao et al. 1986) to functionalize and then cross-link specific peptide complexes of the murine class I MHC molecule H-2K^b, and used fluorescent versions of these MHC heterodimers to specifically stain CD8⁺ T cells cross-reactive towards LCMV and VV. A previous strategy for production of class II MHC heterodimers has been reported (Krogsgaard, Li et al. 2005), but that strategy relies on sequential differential affinity purification for

isolation of heterodimers after non-specific cross-linking, and was not used for T cell staining or characterization of T cells in mixed populations.

II.B. Materials and Methods

II.B.1. Production of Class I H-2K^b Complexes

Extracellular domains of the murine MHC class I H-2K^b heavy chain carrying a C121R mutation and a non-native C-terminal cysteine introduced at position 282 (Stone and Stern 2006), and full length human light chain β_2 – microglobulin, were expressed separately as inclusion bodies in *Escherichia coli* and were folded *in vitro* by dilution in the presence of excess peptide, as previously described for human class I MHCs (Garboczi, Hung et al. 1992). Synthetic peptides purified by reverse phase-HPLC were purchased from 21st Century Biochemicals. Folded H-2K^b monomers were purified by anion exchange chromatography on Poros HQ columns (Roche) using a gradient of NaCl from 0-0.5M in 20 mM Tris buffer (pH 8.0). The concentration of each H-2K^b monomer was calculated by absorbance spectroscopy after anion exchange chromatography using $\epsilon_{280} = 74955 \text{ cm}^{-1} M^{-1}$ for H-2K^b heavy chain, $\epsilon_{280} = 20003 \text{ cm}^{-1} M^{-1}$ for β_2 – microglobulin light chain and varied ϵ_{280} for peptides depending on sequence. Purified H-2K^b monomers were adjusted to a concentration of 10-20 mg/mL using regenerated cellulose filters (Amicon) and stored in 5 mM DTT to prevent disulfide-linked species.

II.B.2. Cross-linking of Soluble MHC Class I H-2K^b Complexes

Reduced H-2K^b monomers were purified by size exclusion chromatography using NAP-5 columns (GE healthcare) to remove DTT prior to thiol modification. H-2K^b monomers were reacted with heterobifunctional cross-linkers MTFB (maleimido trioxa formyl benzaldehyde) or MHPH (3-N-maleimido-6-hydraziniumpyridine hydrochloride)

in a 6-fold molar excess for 3 hours in 100 mM NaH₂PO₄, 150 mM NaCl, pH 6.0 buffer (Solulink). Cross-linker-modified H-2K^b monomers were purified away from free cross-linker by size exclusion chromatography using a Superdex 200 column (GE healthcare). MHPH-modified H-2K^b monomers and MTFB-modified H-2K^b monomers were mixed together in a 1:1 molar ratio. The concentration of the reaction mixture (containing MHPH modified H-2K^b monomer and MTFB modified H-2K^b monomer) was adjusted to 1-2 mg/mL using a regenerated cellulose filter (Amicon) and incubated for 20 hours at room temperature in the presence of 5 mM aniline (Acros Organics), which was found to catalyze hydrazone formation (Dirksen, Dirksen et al. 2006). Chemically cross-linked H-2K^b dimers were purified away from H-2K^b monomers by size exclusion chromatography using a Superdex 200 column (GE healthcare). Purified, unlabeled H-2K^b dimers were stored at 4°C at a concentration of ~1 μM for upwards of a month.

II.B.3. Alexa 647 Labeling of H-2K^b Monomers, Cross-linked MHC Dimers, and Tetramers

H-2K^b monomers were purified by size exclusion chromatography using NAP-5 columns (GE healthcare) to remove DTT prior to thiol modification. Reduced H-2K^b monomers were reacted with a 5-fold molar excess of Alexa 647 maleimide (Invitrogen) for 2 hours at room temperature. Alexa 647 labeled H-2K^b monomers were purified by size exclusion chromatography using a Superdex 200 column (GE healthcare). H-2K^b homodimers and heterodimers, prepared as described above, were adjusted to a concentration of greater than 10 μM and labeled with a 20-fold molar excess of Alexa

647 succinimidyl ester (Invitrogen). The labeling reaction was quenched using a 50-fold molar excess of ethanolamine (Sigma), and H-2K^b dimers were re-purified by size exclusion chromatography using a Superdex 200 column (GE healthcare). Reaction yield and labeling efficiency were determined by absorbance spectroscopy after gel filtration purification, using $\epsilon_{280} = 265000 \text{ cm}^{-1} \text{ M}^{-1}$ for Alexa 647 succinimidyl ester and the above mentioned ϵ_{280} for H-2K^b heavy chain, β_2 -microglobulin light chain and peptides. All of the H-2K^b dimers were labeled with approximately two Alexa 647 per H-2K^b dimer with the exception of the A11R-A11R-H-2K^b homodimer which was labeled with approximately four Alexa 647 per dimer. For preparation of Alexa 647-labelled streptavidin-linked H-2K^b tetramers, H-2K^b monomers first were purified by size exclusion chromatography using NAP-5 columns (GE healthcare) to remove DTT prior to thiol modification, and then were biotinylated by reacting with a 5-fold molar excess of biotin maleimide (Pierce) for 2 hours at room temperature and subsequently re-purified by size exclusion chromatography using a Superdex 200 column (GE healthcare). Biotinylation yield was determined by adding a 2-fold molar excess of streptavidin to the biotinylated H-2K^b monomers with analysis by 12% SDS-PAGE. The biotinylated H-2K^b monomers were subsequently oligomerized by stepwise addition of Alexa 647 streptavidin (Invitrogen) to the biotinylated H-2K^b to a final molar concentration of 1:6.

II.B.4. Mass Spectroscopy

Alexa 647-labeled H-2K^b tetramers/dimers/monomers were checked for the presence of intact peptide by Matrix-Assisted Laser Desorption/Ionization (MALDI).

Alexa 647-labeled H-2K^b complexes were purified by size exclusion chromatography using a Superdex 200 column (GE healthcare) and purified fractions were mixed with UV absorbing matrix (alpha-cyano-4-hydroxy-cinnamic acid) prior to laser desorption, ionization and detection of ionized species. The sample was analyzed on a Waters MALDI LR spectrometer.

II.B.5. Isolation of Antigen-Specific CTL

LCMV (Armstrong strain), an RNA virus in the Old World arenavirus family, was propagated in BHK-21 baby hamster kidney cells as previously described (Selin, Nahill et al. 1994). BL/6 mice were infected intraperitoneally (i.p.) with a non-lethal dose of 5×10^4 PFU of LCMV as previously described (Selin, Nahill et al. 1994). Mice were considered immune at greater than 6 weeks after infection (Cornberg, Sheridan et al. 2007). Splenocytes from LCMV-immune mice were co-cultured with mouse RMA cells that were pulsed with 1 μ M GP34 peptide, washed and then γ -irradiated (3000 rads) as previously described (Cornberg, Sheridan et al. 2007). RMA is a K^b-positive, Rauscher virus-induced, T-lymphoma cell line of BL/6 origin. Briefly, the co-culture of splenocytes and GP34-pulsed RMA cells were grown in RPMI supplemented with 100 U/ml penicillin G, 100 μ g/ml streptomycin sulfate, 2 mM L-glutamine, 10 mM HEPES, 1 mM sodium pyruvate, 0.1 mM MEM nonessential amino acids, 0.05 mM β -mercaptoethanol, and 10% FBS for 5 days at 37°C at 5% CO₂. Following this initial culture period, cells were harvested and stimulated with GP34 peptide-pulsed RMA cells in the presence of 10% BD T-Stim (BD Biosciences), an IL-2 culture supplement.

LCMV-GP34 peptide-pulsed RMA stimulation was repeated every 4 to 5 days. After 20 to 25 days of stimulation (four or five stimulations), T-cell lines were characterized by intracellular cytokine staining or MHC staining with the panel of MHC class I H-2K^b monomers/dimers/tetramers.

II.B.6. Cell Surface and MHC Staining by Flow Cytometry

Cell suspensions were incubated in staining buffer (phosphate-buffered saline containing 1% FBS and 0.2% sodium azide) containing anti-mouse CD16/CD32 (Fc-block, clone 2.4G2). Cells were washed once with staining buffer and then stained with H-2K^b monomers/dimers/tetramers for 90 min. Thereafter, cells were washed twice with staining buffer and fixed in Cytofix (BD Pharmingen). Samples were analyzed using a Becton Dickinson LSRII flow cytometer (BD Biosciences) and FlowJo software (Tree Star).

II.B.7. Intracellular Cytokine Staining (ICS)

A suspension of 10^6 cells was stimulated with 1 μ M synthetic peptide or a medium only control. Stimulations were performed for 5 h at 37°C in a total volume of 200 μ l RPMI medium supplemented with 10% FBS, 10 U/ml of human recombinant interleukin-2 (IL-2), and 0.2 μ M of brefeldin A (GolgiPlug; BD Pharmingen). After incubation, cell-surface antibody staining with anti-CD8 α (clone 53-6.7), and anti-CD44 (clone IM7) was performed. Thereafter, cells were washed twice with staining buffer, and then fixed and permeabilized (Cytofix/Cytoperm; BD Pharmingen). Intracellular-

cytokine-producing cells were detected with PE-labeled anti-mouse interferon-gamma (IFN- γ , clone XMG1.2) and APC-labeled anti-mouse tumor necrosis factor alpha (TNF- α , clone MP6-XT22) monoclonal antibodies. Antibodies were purchased from BD Pharmingen. The samples were analyzed as described above for cell surface staining.

II.C. Results

II.C.1. Isolation and Characterization of a Cross-reactive CD8+ T Cell Line

To evaluate the utility of bispecific MHC heterodimers in analysis of T cell cross-reactivity, we made use of a previously described system of heterologous immunity, in which infection of mice with the old-world arenavirus LCMV confers partial T cell immunity to infection with the poxvirus VV (Kim, Cornberg et al. 2005). Some T cells responding to the LCMV peptide GP34 (AVYNFATM) can cross-react with VV peptide A11R (AIVNYANL) (Cornberg, Clute et al. 2010). The GP34 and A11R peptides have side chains that are identical at three of the eight positions (underlined in sequences above), and are conservatively substituted at three other positions. A crystal structure is available for the H-2K^b-GP₃₄₋₄₁ complex (Achour, Michaelsson et al. 2002), and shows that the bound GP34 peptide places peptide side chains at the P2(V), P5(F), and P8(M) positions into pockets in the K^b binding site, with the intervening peptide side chains available for TCR interaction (Achour, Michaelsson et al. 2002). T cells recognizing this peptide form a substantial component of the overall K^b-restricted response to LCMV (Puglielli, Zajac et al. 2001). The A11R peptide conforms to the K^b-binding motif (Achour, Michaelsson et al. 2002), and would be expected to bind similarly. No structural information is available for the K^b-A11R complex, but the peptide is known to bind to K^b (Cornberg, Sheridan et al. 2007), forming a subdominant epitope that persists in the K^b-restricted response to VV (Cornberg, Clute et al. 2010). These peptides, together with two unrelated K^b-binding LCMV-derived peptides NP205 and GP118, and

control tight-binding designed peptide SIY (Udaka, Wiesmuller et al. 1996) (Table II.1), were used in the experiments reported below.

T cell cross-reactivity in this system was addressed first by intracellular cytokine staining (ICS) (Figure II.1A). BL/6 mice were infected with LCMV and allowed to recover for 6 weeks. Splenocytes from the LCMV-immune mice were stimulated *in vitro* with K^b-expressing RMA cells pre-pulsed with LCMV-GP34 peptide, in order to expand the population of T cells that respond to this peptide, and were rested for 3-4 days prior to experimentation. After expansion, intracellular cytokine staining experiments (Figure II.1A) showed that the majority (56.3%) of the CD8⁺, CD44⁺ T cells secreted both TNF α (X axis) and IFN γ (Y axis) in response to the GP34 peptide. The same cells were tested for their response to other peptides. In response to VV-A11R peptide, 31.5% of T cells secreted both IFN γ and TNF α . Thus, at least a portion of the LCMV-GP34 specific T cells must be cross-reactive for VV-A11R. Similarly, if only the cells secreting TNF α are considered, 34.6% were positive in response to VV-A11R. Because nearly all (96.3%) were positive in response to LCMV-GP34, a majority of the 34.6% positive to VV-A11R must also cross-react with LCMV-GP34. The T cell population showed no reactivity against two other peptide-epitopes from LCMV, GP118 and NP205 (Figure II.1A).

Table II.1. Relevant Epitopes from VV and LCMV used for the Bi-specific MHC Heterodimer work presented in Chapter II

Source	Protein	Abbreviation	Sequence
VV	Nonstructural protein A11R ₁₉₈₋₂₀₆	A11R	AIVNYANL
LCMV	Glycoprotein ₃₄₋₄₁	GP34	AVYNFATM ^a
LCMV	Nucleoprotein ₂₀₅₋₂₁₂	NP205	YTVKYPNL
LCMV	Glycoprotein ₁₁₈₋₁₂₅	GP118	ISHNFSNL
Control	(designed sequence)	SIY	SIYRYYGL

^aThis peptide carries a C-terminal Met->Cys mutation relative to the native LCMV sequence. The substitution has been used in previous studies (Achour, Michaelsson et al. 2002; Khanolkar, Fuller et al. 2004) and does not have a significant impact on interaction with MHC or T cell receptors.

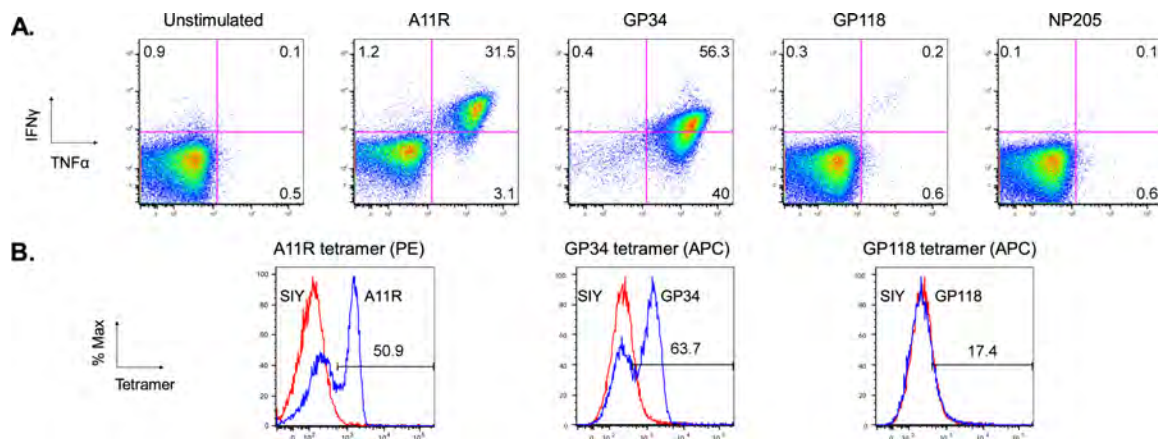


Figure II.1. CD8⁺ T Cells Specific for VV-A11R and LCMV-GP34. A. CD8⁺ T cell response against VV-A11R and LCMV-GP34 was measured by intracellular IFN γ (y axis) and TNF α (x axis) staining in response to 1 μ M of the indicated peptides. T cells from an LCMV-immune mouse were isolated and expanded *in vitro* using LCMV-GP34 peptide, and then were analyzed for cytokine secretion in response to K^b-expressing cells pulsed with VV-A11R or LCMV-GP34 peptides, using an intracellular cytokine staining assay, with the results presented as dot plots. B. Visualization of CD8⁺ T cell response against VV-A11R and LCMV-GP34 by peptide-K^b tetramer staining using 300 nM tetramer. The T cell line from panel A was used. T cells were stained with R-phycoerythrin (PE) or allophycocyanin (APC) labeled streptavidin-based K^b tetramers folded with VV-A11R, LCMV-GP34, LCMV-GP118, or control SIY peptides. The indicated tetramer stain (blue traces) was overlaid with control-SIY tetramer stain (red traces), with results presented as histograms.

MHC tetramer staining similarly demonstrates that a portion of the T cell population can engage both VV-A11R and LCMV-GP34 peptide-epitopes (Figure II.1B). T cells were stained with fluorescently labeled streptavidin-linked tetramers carrying VV or LCMV peptides bound to biotinylated H-2K^b, or with control tetramers carrying an unrelated SIY peptide (SIYRYYGL). The SIY peptide is a self-antigen not expected to induce T cell responses in K^b+ mice (Udaka, Wiesmuller et al. 1996). In Figure II.1b, cognate tetramer staining (blue traces) is overlaid with control-SIY tetramer staining (red traces). Staining with A11R tetramer and GP34 tetramer clearly identifies in both cases positive and negative populations, with the negative staining population overlapping with the control tetramer stain. The fraction of cells staining positive for the VV-A11R tetramer is 50.9% and the fraction staining positive for LCMV-GP34 is 63.7%, again indicating that at least some of the T cells cross-react with both VV-A11R and LCMV-GP34 peptide complexes. The specificity of the MHC tetramers is further confirmed by the lack of staining for the related LCMV-GP118 tetramer, which completely overlaps with the control-SIY tetramer staining (Figure II.1B).

II.C.2. Competition between MHC Tetramers in Conventional Staining Experiments

In principle, cross-reactive T cell populations could be identified by co-staining with two differently-labeled tetramers, but in practice competition between the two MHC tetramers greatly complicates this approach. We evaluated such tetramer cross-competition using the VV-A11R and LCMV-GP34 cross-reactive cell line. Double MHC tetramer staining experiments were performed using various mixtures of cognate MHC

tetramers (VV-A11R and LCMV-GP34) and noncognate MHC tetramers (LCMV-GP118, control-SIY). In each experiment one MHC-tetramer was prepared using streptavidin coupled to R-phycoerythrin (PE), with another prepared using streptavidin coupled to allophycocyanin (APC), so that binding of both tetramers could be monitored simultaneously (Figure II.2). Prior to coupling to streptavidin, each MHC-peptide complex was evaluated by an SDS-PAGE mobility-shift assay (Figure II.3) to ensure essentially complete biotinylation. When cognate VV-A11R-PE tetramer was mixed with non-cognate LCMV-GP118-APC tetramer or with the control-SIY-APC tetramer, the T cell staining percentages and intensities were similar to staining experiments performed with VV-A11R-PE tetramer alone. For example, the VV-A11R-PE tetramer in the presence of non-cognate LCMV-GP118-APC stained 52.8% of the cells (Figure II.2A), as compared to 50.9% for the VV-A11R-PE tetramer alone (Figure II.1B), or 50.5% for VV-A11R-PE in the presence of control SIY-APC tetramer (Figure II.2B). Similarly, staining of the cross-reactive cell population by the cognate LCMV-GP34-APC tetramer, which stained 63.7% of the cells (Figure II.1B), was not greatly altered in the presence of the non-cognate LCMV-GP118-PE tetramer, which stained 59.9% (Figure II.2C). However, staining of the LCMV-GP34-APC tetramer was dramatically reduced in the presence of the cognate VV-A11R-PE tetramer, with only 15.5% of the cells staining positively (Figure II.2E). For the VV-A11R-PE tetramer, the presence of the LCMV-GP34-APC tetramer had a much smaller effect, with the reduction in staining barely discernable (48.7% positive, Figure II.2E). The fluorescence intensity changes followed the same pattern, with the VV-A11R-PE tetramer exhibiting mean fluorescence

intensity (MFI) of 843 in single tetramer stain, 825 and 793 in double tetramer stain with non-cognate tetramers LCMV-GP118-APC and SIY-APC, respectively, and 727 in a double tetramer stain with cognate LCMV-GP34-APC. LCMV-GP34-APC MFI was 1268 as a single tetramer, 1082 in the presence of non-cognate SIY-PE, and decreased substantially to 551 in the presence of cognate VV-A11R-PE. Overall, the presence of cognate tetramer causes a shift in the LCMV-GP34-APC staining intensity, so that the double positive population (upper right quadrant) now significantly overlaps with the singly positive VV-A11R-PE single positive population (upper left quadrant), with only 12.5% of the cells clearly identified as positive for both tetramers (Figure II.2E). Presumably the stronger competition by VV-A11R-PE tetramers as compared to LCMV-GP34-APC tetramers is due to stronger binding of K^b-VV-A11R as compared to K^b-LCMV-GP34 to TCR on most of the cells in the cross-reactive population. In summary, both the LCMV-GP34-APC tetramer and VV-A11R-PE tetramer can engage TCR to stain cells. However, in double staining experiments with LCMV-GP34 and VV-A11R, the tetramers compete with each other. This competition between MHC tetramers for binding to cross-reactive receptors on T cells interferes with the use of tetramer staining in distinguishing cross-reactive from mono-specific T cells, and seriously complicates the use of MHC tetramers in investigation of heterologous immunity.

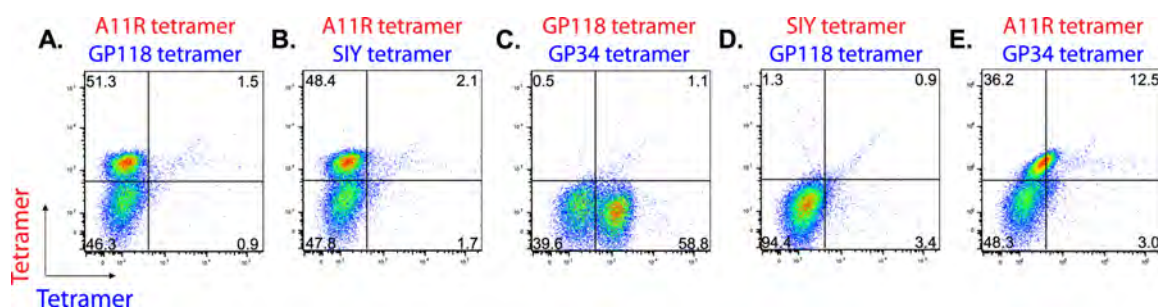


Figure II.2. Cross-reactive T Cells Engage Cognate Peptide-MHC Tetramers in a Manner which Reveals that there Exists Cross-reactive TCR on these Cells.

Visualization of VV-A11R and LCMV-GP34 specific T cells by double MHC tetramer staining at 300 nM. Double MHC tetramer staining experiments were set up using a PE-labeled peptide-K^b tetramer and a APC-labeled peptide-K^b tetramer as follows. *A.* A11R tetramer (PE) and GP118 tetramer (APC); *B.* A11R tetramer (PE) and SIY tetramer (APC); *C.* GP118 tetramer (PE) and GP34 tetramer (APC); *D.* SIY tetramer (PE) and GP118 tetramer (APC); and *E.* A11R tetramer (PE) and GP34 tetramer (APC). *F.* Overlay of data shown in panels *B.* (in red) and *E.* (in blue) to facilitate comparison.

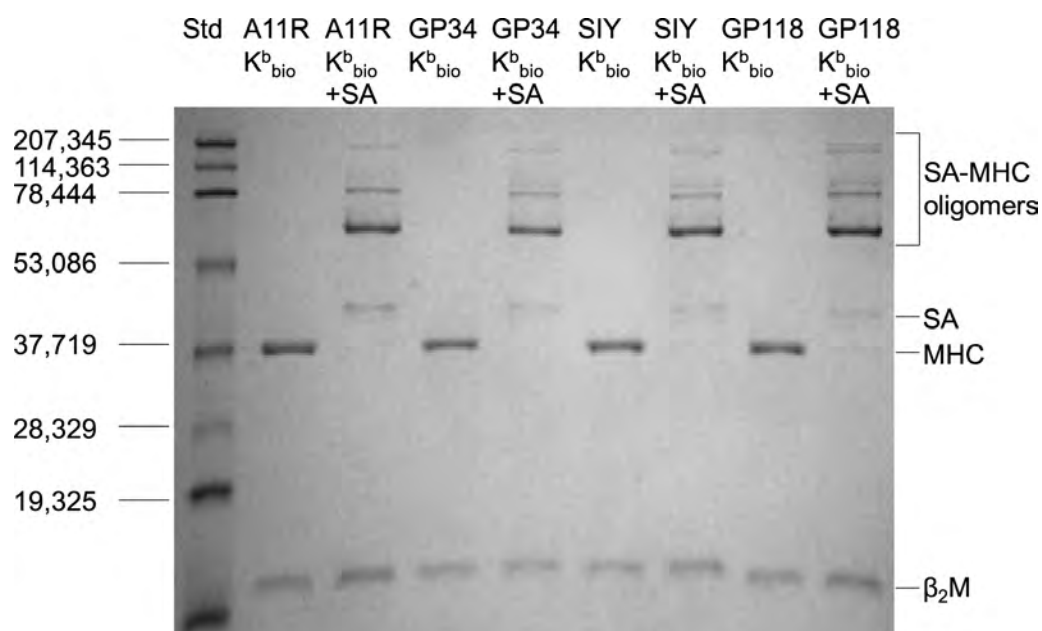


Figure II.3. Comparable Biotinylation Levels for the Different Peptide-MHC Monomers Used for Tetramer Staining. 12% SDS-PAGE analysis of pep-K^b_{bio} monomers in the presence of streptavidin (SA) under reducing conditions. MHC oligomers are formed to a similar yield among the different peptide-K^b_{bio} monomers upon addition of SA. Molecular weight markers are indicated on the left.

II.C.3. Construction of Heterodimeric MHC-based Staining Reagents by Keto-Hydrazide Coupling

Since cross-reactive T cell populations can be difficult or impossible to identify by MHC tetramer co-staining experiments due to competition between the tetramers, we investigated the possibility of developing reagents that would be individually specific for the cross-reactive population of interest. One such reagent would be a bi-specific, MHC heterodimer carrying two different MHC-peptide complexes. MHC homodimers, prepared as fusion proteins using immunoglobulin Fc domains (Fahmy, Bieler et al. 2002) or by cysteine-mediated coupling (Cochran, Cameron et al. 2001), already have been developed for use as staining reagents, and can be used similarly to MHC (homo)tetramers, although with somewhat lowered binding avidity (Stone and Stern 2006). If MHC heterodimers were available, they would be expected to exhibit specific binding only to T cells carrying receptors able to bind to both component MHC-peptide complexes, as the affinity of monomeric MHC-peptide engagement by T cell receptors ($\sim 10\mu\text{M}$, (Cole, Pumphrey et al. 2007)) generally is too low to survive typical washing protocols (unpublished data).

Our strategy for production of a novel, bi-specific H-2K^b heterodimer is shown in Figure II.4. This strategy takes advantage of heterobifunctional cross-linkers, MTFB and MHPH, and previously developed H-2K^b proteins carrying C-terminal cysteine residues (Stone and Stern 2006). MTFB and MHPH each contain a maleimide moiety, which can be used to couple the cross-linkers onto thiols, such as unpaired cysteine residues introduced into the membrane-proximal domains of MHC proteins (Cochran, Cameron et

al. 2001). Opposite the maleimide group is an aldehyde or hydrazine, which can be used in cross-linking to form the desired hydrazone-linked dimers (King, Zhao et al. 1986; Dirksen, Dirksen et al. 2006). Both maleimide-thiol coupling (Kitagawa and Aikawa 1976) and aldehyde-hydrazine cross-linking reactions can be carried out under relatively mild conditions appropriate for maintaining MHC peptide binding and native structure (Figure II.5).

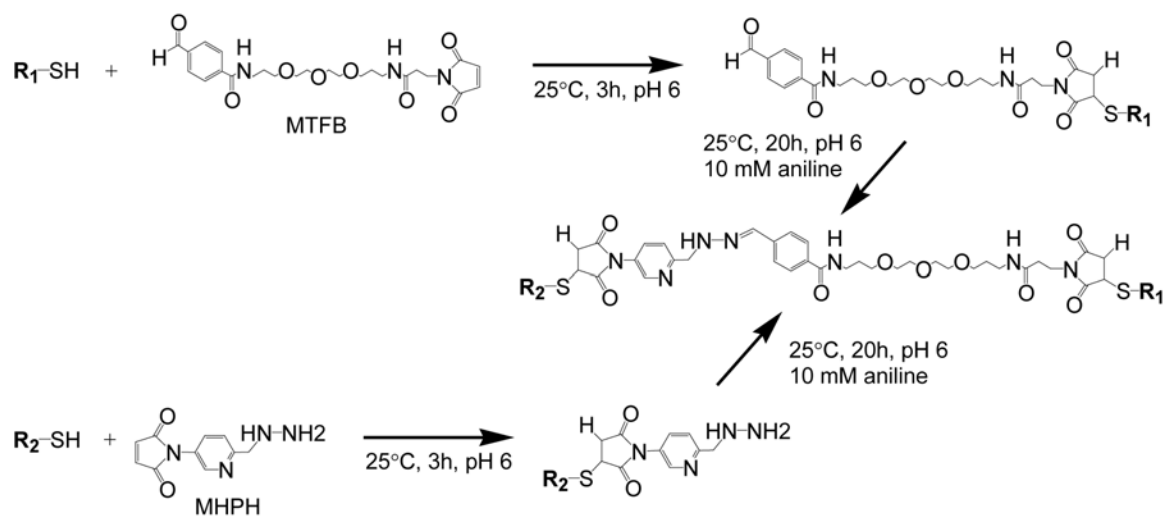


Figure II.4. Chemical Reaction Scheme of Heterobifunctional Cross-linkers MHPH and MTFB. Peptide- K^b monomers (R_1 , R_2) containing a free thiol at the C-terminus of the class I heavy chain (position 282) were reacted with heterobifunctional linkers, maleimido trioxa formyl benzaldehyde (MTFB) or 3-N-maleimido-6-hydraziniumpyridine hydrochloride (MHPH) through their maleimide moieties. The hydrazine on the MHPH modified peptide- K^b monomer subsequently cross-links with the benzaldehyde on the MTFB modified peptide- K^b monomer (when mixed in a 1:1 molar ratio) to generate a hydrazone cross-linked peptide- K^b dimer.

In independent tubes, H-2K^b monomers containing a C-terminal cysteine (P282C) were conjugated with MHPH and MTFB heterobifunctional linkers via their respective maleimides. The MHPH and MTFB H-2K^b modified monomers (R1, R2) were isolated by gel filtration and subsequently cross-linked through their aldehyde (MTFB) or hydrazine (MHPH) moieties to form a hydrazone-bonded, bi-specific H-2K^b heterodimer (Figure II.4). The extent of dimerization of the MHPH-modified A11R-H-2K^b monomer with the MTFB-modified GP34-H-2K^b monomer was approximately 40% as evaluated by analytical size exclusion chromatography (“Dimer reaction mix” trace, Figure II.5A). The hydrazone-linked A11R-H-2K^b, GP34-H-2K^b heterodimer was isolated by gel filtration and labeled with the amine-reactive fluorescent dye Alexa647-succinimidyl ester, to a ratio of approximately ~2 dye per MHC molecule. Importantly, after Alexa 647 succinimidyl ester labeling, the purified, labeled MHC heterodimer exhibited the expected apparent molecular weight, as did the unlabeled dimer in the reaction mixture, with no evidence of appreciable aggregation or dissociation (Figure II.5A). Furthermore, neither MHPH-modified A11R-H-2K^b monomer nor MTFB-modified GP34-H-2K^b monomer exhibited appreciable homo-dimerization, which potentially would interfere with specific staining of cross-reactive cells (Figure II.5A). Because no cross-linking is observed in the absence of either MHPH or MTFB, it appears that the heterobifunctional cross-linking reaction is quite specific.

Reducing SDS-PAGE analysis also was used to characterize the maleimide coupling and hydrazone cross-linking reactions (Figure II.5B). MHPH and MTFB coupling reactions do not compromise the purity of the H-2K^b heavy chain through

cleavage or degradation, as judged by SDS-PAGE, and the MHPH-modified A11R-H-2K^b and MTFP-modified GP34-H-2K^b appear to be essentially completely homogenous (the small β 2m subunit and peptide components of the MHC-peptide complexes migrate with the dye front and are not visible by this analysis) (Figure II.5B). Analysis of the A11R-GP34-H-2K^b heterodimer reaction mixture shows that slightly less than half of the total monomers react to form the desired heterodimer, confirming the results from size exclusion chromatography. Reducing SDS-PAGE also reveals that A11R-GP34-H-2K^b heterodimer is covalently linked and not formed as a consequence of disulfide bonding or non-covalent interaction, because no appearance of a monomeric species (around 37,000 daltons) is observed for the Alexa 647-labeled, A11R-GP34-H-2K^b heterodimer after boiling and reduction (Figure II.5B). Finally, Alexa 647-labelled MHC monomers also exhibited no tendency to form disulfide-linked dimers (Figure II.7).

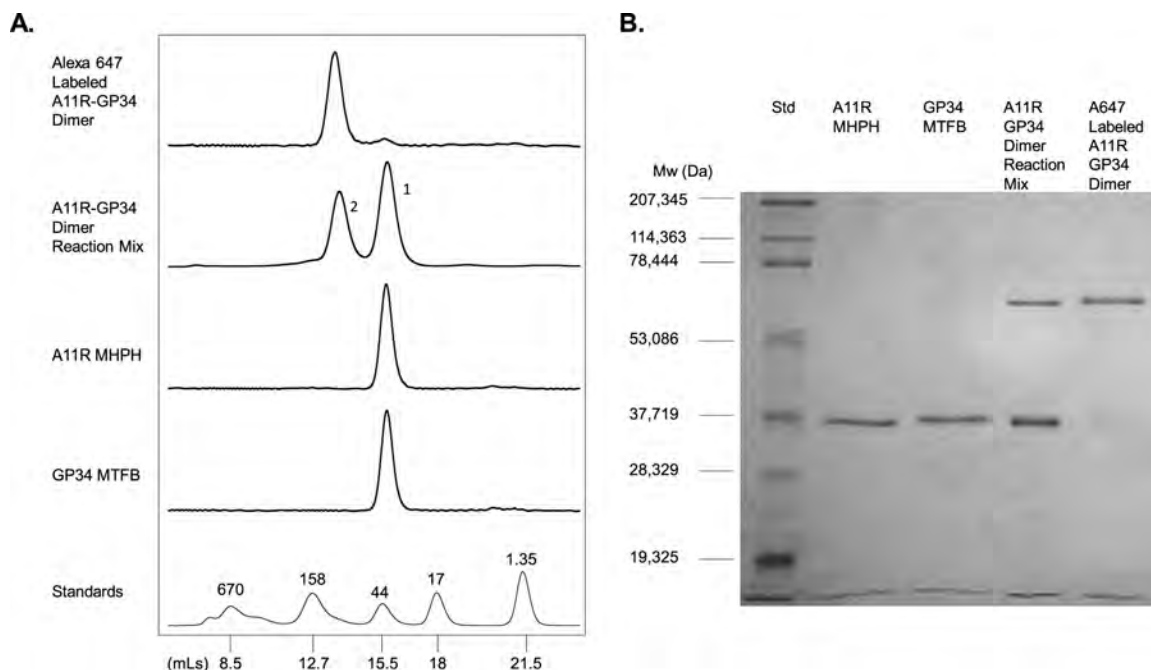


Figure II.5. Heterobifunctional Cross-linking of Peptide-K^b Monomers. K^b monomers modified with MTFB (GP34 MTFB) or MHPH (A11R MHPH), cross-linked K^b heterodimer reaction mixture (GP34-K^b MTFB and A11R-K^b MHPH) and Alexa 647 labeled, cross-linked K^b heterodimer (A647 labeled A11R-GP34 dimer) were analyzed by size exclusion chromatography and 12% SDS-PAGE. The MTFB-MHPH chemistry is specific because the A11R MHPH K^b monomer and GP34 MTFB K^b monomers do not form cross-linked K^b dimers independently. Additionally, Alexa 647 succinimidyl ester labeling does not alter the hydrodynamic radius or purity of the cross-linked K^b dimer. *A.* In the A11R-GP34 dimer reaction mix, cross-linked K^b dimer with a retention volume ~14 mL was purified from K^b modified monomers (retention volume ~15.5 mL) by size exclusion chromatography using a Superdex 200 column. The molecular weight standards are indicated along with the approximate retention volumes. *B.* Reducing SDS-PAGE confirms the purity of the modified K^b monomers and cross-linked K^b dimers. Proteolysis is not observed after modification (GP34 MTFB, A11R MHPH) or cross-linking (A11R-GP34 dimer reaction mix). Molecular mass markers are indicated on the left. All of the Alexa 647-labeled, H-2K^b dimers used in this study were analyzed by matrix-assisted laser desorption/ionization (MALDI) mass spectroscopy to confirm that the peptide antigens are present in unmodified form in the MHC complexes (Figure II.6). In the A11R-H-2K^b monomer and A11R-H-2K^b homodimer, a peak at 899 daltons, corresponding to the molecular weight of A11R peptide, was observed, and in the GP34-H-2K^b monomer and GP34-H-2K^b homodimer, a peak at 938 daltons, corresponding to the molecular weight of GP34 peptide, was observed. For the A11R-GP34-H-2K^b heterodimer, peaks at both 899 daltons (A11R peptide) and 938 daltons (GP34 peptide) were observed.

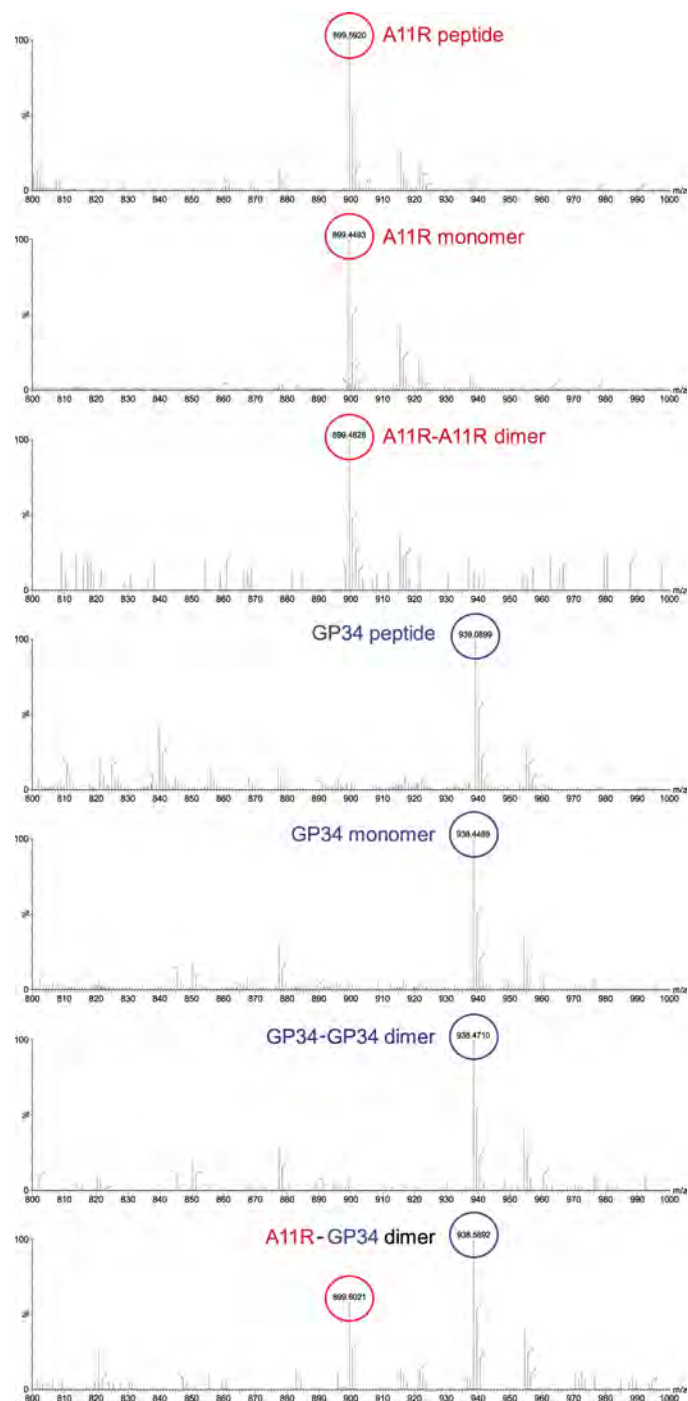


Figure II.6. Peptides are not Modified after Heterobifunctional Cross-linking and Labeling. Mass spectroscopy using Matrix-Assisted Laser Desorption/Ionization (MALDI) of peptide (control) and peptide-Kb monomers and dimers shows that the peptide is intact in its native, unmodified form after heterobifunctional cross-linking and Alexa 647 labeling.

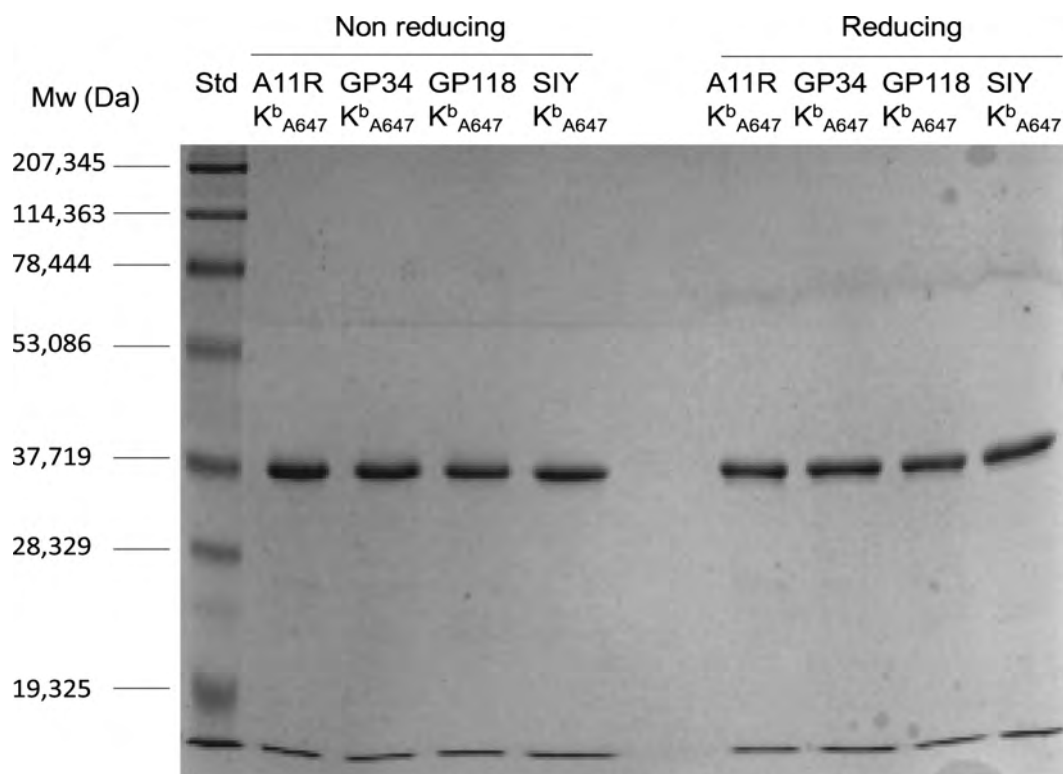


Figure II.7. Binding of Alexa 647 Labeled Monomers cannot be Attributed to the Formation of Disulfide Linked Dimers. The presence of disulfide linked species was not detected in the Alexa 647 labeled peptide-K^b monomers used to stain CD8⁺ T cells. Labeled monomers were analyzed by SDS-12% SDS PAGE under non-reducing conditions (lanes 2-5) and reducing (lanes 7-10) conditions. No disulfide-linked K^b dimers were apparent. Molecular mass markers are indicated on the left.

II.C.4. Identification of Cross-reactive TCR on T cells using MHC Heterodimers

The previously characterized VV-A11R, LCMV-GP34 cross-reactive T cells (Figure II.2) were re-stimulated with LCMV-GP34 peptide-pulsed targets prior to use to maintain the cells during *in vitro* culture. To ensure that the T cells did not change specificity from VV-A11R and LCMV-GP34 after re-stimulation, MHC tetramer staining was performed on the re-stimulated line (Figure II.8A). The cells exhibited strong staining with A11R tetramer (88.5%) and GP34 tetramer (80.9%), and little staining with LCMV-GP118 tetramer (2.0%) or control-SIY tetramer (3.7%), both of which overlap almost completely with the unstained population (Figure II.8A, red curves). This confirms that the specificity of the T cells did not change upon re-stimulation with peptide-pulsed targets, although the percentage of VV-A11R and LCMV-GP34 tetramer positive cells increased as expected because of preferential expansion of the specific population.

In order to attribute H-2K^b heterodimer binding to cross-reactive T cell receptors, it was necessary to ensure that H-2K^b monomers do not exhibit appreciable binding under our experimental conditions. For this reason, binding of all H-2K^b monomers was tested on VV-A11R, LCMV-GP34 specific T cells (Figure II.8B). No binding of any of the H-2K^b monomers (VV-A11R, LCMV-GP34, LCMV-GP118, control-SIY) was observed above the unstained background. Thus, as expected, MHC-peptide binding to T cells requires more than a single cognate MHC-TCR and MHC-CD8 interaction.

Our MHPH-MTFB cross-linking strategy generates a novel MHC-MHC linkage, and we wanted to ensure that the hydrazone linked H-2K^b dimers could engage T cells

with sufficient affinity and specificity for use in conventional staining protocols. For this purpose cognate (VV-A11R, LCMV-GP34) and noncognate (control-SIY) H-2K^b homodimers were made using the same MHPH-MTFB chemistry described above, and binding was tested on the re-stimulated VV-A11R, LCMV-GP34 cross-reactive T cells. As shown in Figure II.9, both cognate A11R-A11R-H-2K^b homodimer and GP34-GP34-H-2K^b homodimer stain the T cells, with MFI = 1093 and 395 respectively. (The increased staining intensity for the A11R-A11R-H-2K^b homodimer reflects the greater degree of Alexa 647 labeling, approximately twice that of the other H-2K^b dimers; see Methods for details). In contrast, the non-cognate SIY-SIY-H-2K^b homodimer control staining (MFI=199) is only slightly higher than the unstained background (MFI = 132). These results parallel the tetramer staining results (Figure II.8A) in terms of specificity and demonstrate that heterobifunctional cross-linking does not alter the ability of H-2K^b homodimers to engage TCRs.

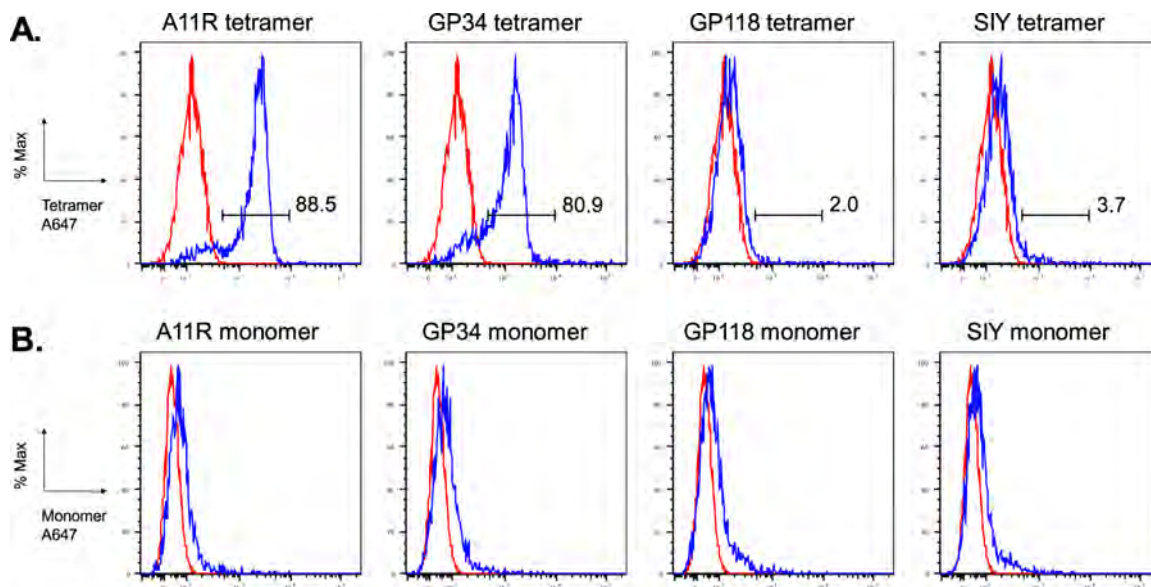


Figure II.8. MHC Tetramer and MHC Monomer Staining of Cross-reactive T Cells. *A.* T cells previously characterized by tetramer staining as specific for both VV-A11R and LCMV-GP34 maintained their specificity after additional restimulation with LCMV-GP34 peptide pulsed targets. After restimulation and passage *in vitro*, T cells were stained with the indicated streptavidin-based K^b tetramers at 300 nM (blue trace) shown overlaid with an unstained control (red trace). The MFI of the positive staining population is indicated in the upper right in each histogram. Positive staining with the VV-A11R tetramer and the LCMV-GP34 tetramer shows that the specificity of the T cells is maintained after passage. *B.* MHC monomers do not have sufficient affinity required for T cell staining. The T cell culture from panel A was stained with peptide-K^b monomers at 2 μ M as indicated. The indicated monomer stain (blue trace) was overlaid with the unstained control (red trace) in each histogram. Positive staining of T cells is not observed with any of the monomers.

Finally, we wanted to evaluate whether T cells which express cross-reactive TCR could be identified using the bi-specific, cognate H-2K^b heterodimer. As shown in Figure II.9B, the bi-specific, A11R-GP34-H-2K^b heterodimer is able to stain the cross-reactive T cell population (MFI = 377), with 32% positive as compared to 4.9% positive for the SIY-SIY homodimer (MFI = 199). The staining signal is clearly distinguishable from the unstained background, and the staining intensity is similar to that observed for the specific GP34-GP34-H-2K^b homodimer (MFI = 395) with 49% positive (Figure II.9B). To confirm that MHC heterodimer binding depends on MHC-TCR contacts with both cognate peptide-epitopes, we generated “control” H-2K^b heterodimers where one H-2K^b monomer is folded with a self-peptide (control-SIY) and the other with a cognate peptide (VV-A11R or LCMV-GP34), and compared staining of these reagents to the A11R-GP34-H-2K^b heterodimer of interest (Figure II.8B). These controls are necessary for two reasons. First, if either the VV-A11R monomer or LCMV-GP34 monomer undergoes unexpected dimerization, an artifactual H-2K^b “homodimer” would result and binding would be observed. Second, relative to the non-binding MHC monomers, the non-cognate MHC heterodimers carry an additional CD8-MHC contact as well as an additional non-specific pMHC-TCR contact, either or both of which potentially could provide sufficient binding affinity to allow significant staining under typical experimental conditions. However, significant staining by the non-cognate A11R-SIY-H-2K^b (MFI = 162) and SIY-GP34-H-2K^b (MFI = 215) control heterodimers was not observed, with 2.8% and 4.6% positive, respectively, values similar to those for the control SIY-SIY homodimer. Thus, staining of the cross-reactive T cell line by the A11R-GP34-H-2K^b

heterodimer requires bivalent engagement involving both MHC-peptide components, and reflects specific detection of cross-reactive T cells within the population.

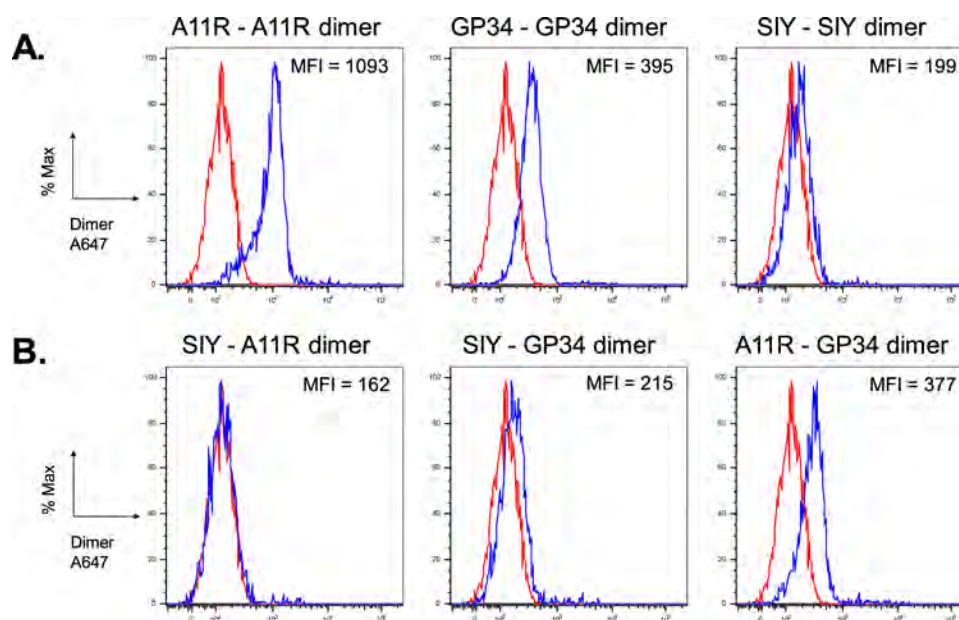


Figure II.9. MHC Heterodimer Staining of Cross-reactive T Cells. The T cell culture shown in Figure II.8 was stained with the indicated K^b -homodimers (A.) or K^b -heterodimers (B.) at 1 μ M. A. MHC homodimer staining demonstrates that the novel hydrazone linkage does not disturb MHC engagement of TCR and confirms that the T cells are cross-reactive for LCMV-GP34 and VV-A11R as seen in the tetramer staining experiment. B. Bi-specific MHC heterodimer (A11R-GP34- K^b) staining shows that cross-reactive T cells can be readily identified. All of the indicated MHC homodimers and heterodimers (blue trace), were overlaid with an unstained control (red trace). The MFI of the positive staining population is indicated in the upper right in each histogram.

II. D. Discussion

We developed a specific hetero-dimerization strategy to prepare hydrazone-linked MHC dimers carrying two different MHC-peptide complexes. As expected from previous work using other disulfide or Ig-linked MHC dimers, the avidity of such complexes was sufficient to allow for specific staining and flow cytometric analysis of T cell cultures. Unlike previous work, the heterodimers were specific for cross-reactive T cells, i.e. T cells able to bind to two different MHC-peptide complexes. Unlike dual-tetramer staining, the MHC heterodimer experiments do not suffer from cross-competition between their component MHC-peptide complexes. A cross-reactive T cell with significantly greater affinity for one of the two component MHC-peptide complexes was easily detected. We expect that such MHC heterodimers will find application in analysis of heterologous T cell responses induced by vaccination, infection, or autoimmune stimuli.

One potential pitfall in development of the heterobifunctional cross-linking strategy was the high reactivity of the hydrazine moiety in the MHPH cross-linker, such that the MHPH-modified H-2K^b monomers (and particularly Alexa 546-labeled MHPH-modified H-2K^b monomers) exhibited a propensity to self-react upon extended storage in higher concentrations in 4°C degrees (data not shown). For this reason, MHPH-modified H-2K^b monomers were kept at low concentrations after modification, and were promptly mixed with previously prepared MTFB-modified H-2K^b monomers, so that once conjugated the hydrazine moieties (MHPH) could preferably react with aldehyde moieties (MTFB) as compared to other more sluggish side reactions which may occur.

Our cross-linking results from Figure II.5 coupled with the results from mass spectroscopy (see Figure II.6), indicate that this method is effective in achieving the desired dual-specificity for the H-2K^b heterodimer. Another potential limitation of the heterobifunctional cross-linking strategy described here is that both thiols and amine groups are used for coupling (cross-linker conjugation and fluorescent labeling, respectively). Thus, the peptides used in heterobifunctional cross-linking of H-2K^b complexes should not have exposed side chains from cysteine residues (to prevent peptide-cross-linking) or lysine residues (to prevent direct labeling of peptide which might interfere with TCR interaction). In such cases the cysteine and/or lysine residues could be conservatively substituted to remove the reactive species. For example, substitution of the original cysteine at position 41 by methionine in the LCMV-GP₃₄₋₄₁ used in this study does not substantially impact T cell recognition (Achour, Michaelsson et al. 2002; Khanolkar, Fuller et al. 2004). Alternatively, a photo-exchangeable peptide strategy (Toebe, Coccoris et al. 2006) could be employed to allow for peptide loading after fluorescent labeling.

In this study we examined a polyclonal T cell line exhibiting cross-reactivity between two different viral antigens bound to the murine class I MHC H-2K^b, one derived from LCMV and one from VV. Such T cells are known to arise after natural infection with these viruses, and are believed to play a role in heterologous immune responses observed upon infection with one virus after prior exposure to the other (Kim, Cornberg et al. 2005). GP34-A11R cross-reactivity has been observed for T cell lines obtained by a variety of immunization/culture protocols (Cornberg, Sheridan et al. 2007;

Cornberg, Clute et al. 2010). The fraction of cross-reactive cells in the overall LCMV-responsive and VV-responsive populations varies between individual mice because of the “private” nature of the T cell response (Cornberg, Chen et al. 2006; Cornberg, Sheridan et al. 2007; Cornberg, Clute et al. 2010), and the fraction of cross-reactive T cells present after *in vitro* culture depends on the conditions used to expand the antigen-specific cell population (unpublished observations). The particular T cell line investigated here exhibited an unusually high degree of cross-reactivity, thus providing an opportunity to evaluate the novel MHC heterodimer staining strategy, and to characterize in detail the nature of the cross-reactive T cell population.

If MHC monomers bound to TCRs, it would be difficult to distinguish cross-reactive from singly-reactive T cell populations. In this system, we confirmed that binding of MHC monomers is not observed on the T cells bearing cross-reactive TCRs (Figure II. 8B). Furthermore, clear absence of observable binding by control MHC heterodimers carrying one cognate and one non-specific peptide demonstrates that both peptides need to be cognate in order for MHC heterodimer binding to be observed (Figure II.9B). This contrasts with an observation of binding of non-cognate MHC-tetramers to human peripheral blood T cells via CD8 interactions (Laugel, van den Berg et al. 2007), although in that study MHC oligomer staining was performed at higher concentrations and temperatures (Schott and Ploegh 2002). We cannot exclude the possibility that exceptionally tight-binding T cells, with MHC-TCR affinity significantly higher than those observed to date (Cole, Pumphrey et al. 2007), might be able to engage MHC-peptide monomers.

Cross-reactive T populations may represent one of three situations: 1) a mixture of two T cell sub-populations, each specific for a different antigen, but with no cross-reactivity at the single cell level, 2) a population of T cells expressing two distinct TCR as a result of incomplete allelic exclusion at the TCR α locus (Padovan, Casorati et al. 1995) or possibly TCR sharing (Chaudhri, Quah et al. 2009) (i.e. with cross-reactivity at the single cell but not single receptor level (Padovan, Casorati et al. 1993; Hardardottir, Baron et al. 1995; He, Janeway et al. 2002), or 3) a T cell population carrying T cell receptors that individually react with two (or more) different MHC-peptide complexes. Since monomeric engagement is not sufficient to observe binding of the MHC heterodimers (Figure II.8B and II.9B), individual T cells staining positively with the MHC heterodimers must express receptors for both of the component MHC-peptide complexes. Thus, we can rule out 1) as an explanation for the observed cross-reactivity of the LCMV-VV cross-reactive T cell population, i.e. the cross-reactivity is apparent at the single cell level, and not just at the population level. The MHC heterodimer staining experiment by itself cannot distinguish between cases 2) and 3), both of which have been proposed to be relevant in T cell responses to infectious agents (He, Janeway et al. 2002; Macdonald, Chen et al. 2009). However, our observation of competition between MHC tetramers in the (homo-)tetramer staining experiments indicates that, for most or all of the T cells in the LCMV-VV cross-reactive population, individual TCR able to bind H-2K^b-LCMV-GP34 also were able to bind H-2K^b-VV-A11R, i.e. case 3) the cross-reactivity is apparent at the single receptor level. We note however that this demonstration depends on the relative avidities of the two tetramers. For example, we could observe competition

of H-2K^b-LCMV-GP34-tetramers by the tighter-binding H-2K^b-VV-A11R, but not the reverse. Although it was clear from previous studies that the LCMV-VV cross-reactive T cell populations are present after subsequent infections with LCMV and VV (Kim, Cornberg et al. 2005; Cornberg, Sheridan et al. 2007), and cross-reactive T cells were observed in (BL/6 x TCR α KO) F1 mice, whose T cells express only a single TCR α chain and are not subject to allelic exclusion (Welsh, Kim et al. 2006), the present study confirms the idea that LCMV-VV cross-reactive T cell populations utilize T cell receptors individually cross-reactive with K^b-LCMV-GP34 and K^b-VV-A11R complexes.

T cells with receptors specific for class I MHC proteins like H-2K^b typically express the CD8 co-receptor, which binds to class I MHC in a peptide-antigen independent manner through an interaction outside the peptide binding site (Gao, Tormo et al. 1997; Kern, Hussey et al. 1999). The CD8-MHC interaction is substantially weaker (K_d for H-2K^b \sim 90 μ M (Moody, Xiong et al. 2001) than that of typical MHC-TCR interactions (\sim 10 μ M) (van der Merwe and Davis 2003), but nonetheless engagement of MHC by CD8, particularly multivalent engagement, could potentiate MHC dimer binding as it does MHC tetramer binding (Dutoit, Guillaume et al. 2003; Kerry, Buslepp et al. 2003; Nugent, Renteria et al. 2005) However, the clear absence of observable binding by control MHC heterodimers carrying one cognate and one non-specific peptide demonstrates that both peptides need to be cognate in order for MHC heterodimer binding to be observed (Figure II.9B). This contrasts with an observation of binding of non-cognate MHC-tetramers to human peripheral blood T cells via CD8 interactions (Laugel, van den Berg et al. 2007), although in that study MHC oligomer

staining was performed at higher concentrations and temperatures (Schott and Ploegh 2002).

In conclusion, the hetero-dimerization strategy developed here for the murine class I MHC molecule H-2K^b provides specific fluorescent MHC heterodimers composed of one MPPH-linked MHC-peptide monomer and one MTFB-linked MHC monomer carrying a different peptide, with no apparent perturbation of the MHC-peptide complex or its interaction with T cell receptors. Using H-2K^b heterodimer carrying peptides VV-A11R₁₉₈₋₂₀₅ and LCMV-GP₃₄₋₄₁, we showed that a unique subset of LCMV-VV cross-reactive T cells can be characterized. Double MHC tetramer staining on these cross-reactive T cells highlighted the problems with MHC tetramer cross-competition, but also revealed that these cross-reactive T cells express a single cross-reactive TCR able to bind to both VV-A11R₁₉₈₋₂₀₅ and LCMV-GP₃₄₋₄₁ peptides. Similar strategies could be used to develop human peptide-MHC reagents for quantifying T cell cross-reactivity during human viral infections. For example, cross-reactive influenza virus-specific T cells have been observed in EBV-induced infectious mononucleosis (Clute, Watkin et al. 2005) and implicated in hepatitis C virus-induced fulminating hepatitis (Wedemeyer, Mizukoshi et al. 2001) and they could be quantified by this method.

Chapter III:

Disparate Epitopes Mediating Protective Heterologous Immunity to Unrelated Viruses share Peptide-MHC Structural Features that are recognized by Cross-reactive T cells

Abstract

Closely related T cell peptide epitopes can, not surprisingly, be recognized by the same T cells and contribute to the immune response against pathogens encoding those epitopes. However, sometimes cross-reactive epitopes share little homology, and the degree of structural homology required for such disparate ligands to be recognized by cross-reactive TCR remains unclear. Here, we examined the mechanistic basis for cross-reactive T cell responses between two disparate epitopes from unrelated and pathogenic viruses, lymphocytic choriomeningitis virus (LCMV) and vaccinia virus (VV). Cross-reactive T cell responses were measured by IFN γ production and *in vivo* cytotoxicity, with TCR specificity checked by peptide-MHC tetramer binding. Our results show that the LCMV-cross-reactive T cell response towards VV is dominated by a shared asparagine residue at the P4 position, together with other shared structural elements conserved in the structures of K^b-VV-A11R and K^b-LCMV-GP34. Based on analysis of the K^b-VV-A11R and K^b-LCMV-GP34 crystal structures, which we report in this study, and previously reported K^b-OVA structures, we were able to predict and generate a LCMV-cross-reactive T cell response towards a variant of the OVA null peptide.

Combined, our results demonstrate that shared structural features formed by peptide-MHC complexes mediate cross-reactive T cell responses.

III.A. Introduction

Memory T cell populations generated against a previously encountered pathogen can alter the outcome of a subsequent exposure to an unrelated pathogen (Selin, Cornberg et al. 2004; Selin, Brehm et al. 2006; Welsh, Che et al. 2010). This phenomenon, known as heterologous immunity, has been well documented in humans and mice for both related and unrelated pathogens (Mathew, Kurane et al. 1998; Wedemeyer, Mizukoshi et al. 2001; Clute, Watkin et al. 2005; Urbani, Amadei et al. 2005; Cornberg, Clute et al. 2010; Chen, Cornberg et al. 2012). For example, cross-reactive T cells have been found to mediate heterologous immune responses between different serotypes of dengue virus (Spaulding, Kurane et al. 1999), between the closely related arenaviruses Pichinde and lymphocytic choriomeningitis virus (LCMV) (Chen, Cornberg et al. 2012), and between two completely unrelated viruses, LCMV and vaccinia virus (VV) (Cornberg, Sheridan et al. 2007; Cornberg, Clute et al. 2010). For LCMV and VV, previous exposure to LCMV results in either protective immunity or altered immunopathology in mice that are challenged with VV (Selin, Vergilis et al. 1996; Chen, Fraire et al. 2001). The demonstrated impact on the overall immune response for T cell crossreactivity highlights the importance of understanding the underlying mechanisms.

VV challenge of LCMV-immune mice results in proliferative T cell responses towards three previously characterized LCMV epitopes: LCMV-GP34, LCMV-GP118 and LCMV-NP205 (See Table III.1) (Kim, Cornberg et al. 2005). We previously showed that VV-A11R crossreacts *in vitro* with LCMV-GP34 in a cross-reactive T cell line (Shen, Brehm et al. 2010), with the cross-reactive response mediated through T cell

receptors (TCR) that could recognize both epitopes (Shen, Brehm et al. 2010). However, the underlying mechanism for this cross-reactive response was not studied. The sequence disparity between LCMV-GP34 (AVYNFATM) and VV-A11R (AIVNYANL), which share only three of eight residues, made it seemingly unlikely that structural mimicry could be the underlying mechanism.

There are two basic concepts by which cross-reactive T cells can recognize heterologous antigens. The simplest method is that cross-reactive T cells express T cell receptors that are individually cross-reactive towards two or more epitopes (Yin and Mariuzza 2009). Alternatively, it has been shown that cross-reactive T cell responses might be mediated by two different T cell receptors present on a single T cell. The dual expression of two different TCRs may occur through TCR sharing, where two clonotypically different T cells transfer cell surface TCRs amongst each other (Chaudhri, Quah et al. 2009) or in the absence of allelic exclusion, where the non-selected TCR α chain is retained on the cell surface (Hardardottir, Baron et al. 1995; He, Janeway et al. 2002).

For individually cross-reactive TCRs, structural similarities between different peptide-MHC ligands, either through structural reconfiguration of the peptide and/or the MHC, is one of a few reported mechanisms for cross-reactive T cell responses (Macdonald, Chen et al. 2009). However, the degree of structural homology required before TCR engagement remains unclear as many studies have been focused on peptide-epitopes which share greater than 50% sequence homology (Borbulevych, Piepenbrink et al. 2009; Macdonald, Chen et al. 2009; Borbulevych, Santhanagopalan et al. 2011).

Furthermore, most studies have focused on the cross-reactive TCR engagement of self epitopes that mimic foreign epitopes, leading to aberrant autoreactivity (Mazza, Auphan-Anezin et al. 2007; Macdonald, Chen et al. 2009; Borbulevych, Piepenbrink et al. 2011; Borbulevych, Santhanagopalan et al. 2011). Only one study has evaluated beneficial immune responses towards two distinct foreign pathogens (Borbulevych, Piepenbrink et al. 2009). In that particular study, the epitopes in question share greater than 50% homology, which makes the cross-reactive TCR engagement less surprising.

Structural rearrangements for cross-reactive TCR have also been shown as a mechanism for cross-reactive TCR engagement (Colf, Bankovich et al. 2007; Mazza, Auphan-Anezin et al. 2007). One example is the cross-reactive TCR BM3.3, which was found to modify its CDR loops to accommodate three different peptides, all presented by H-2K^b, using the same overall docking strategy (Mazza, Auphan-Anezin et al. 2007). Another example is the 2C TCR, which globally repositions itself over two different cross-reactive peptide-MHC ligands (Colf, Bankovich et al. 2007). The 2C TCR is able to accommodate a self-ligand and a foreign ligand by shifting its TCR α and TCR β chains (Colf, Bankovich et al. 2007).

To determine the mechanistic basis for the LCMV-VV cross-reactive T cell response, we compared the recognition determinants for LCMV-GP34 and VV-A11R using site-specific mutations at the predicted non-MHC binding residues in both epitopes. We studied the impact of these mutations by using a combination of intracellular cytokine staining (ICS), MHC tetramer staining and *in vivo* cytotoxicity assays. The studies were conducted on either acute LCMV-infected mice or GP34-A11R cross-

reactive T cell lines, which were derived from LCMV-immune mice and expanded *in vitro* with peptide-pulsed targets. In addition, we determined X-ray crystal structures of the K^b-LCMV-GP34 and K^b-VV-A11R peptide-MHC complexes recognized by cross-reactive T cells. Structural analysis revealed that the cross-reactive ligands are nearly identical structural mimics that share a conserved asparagine at P4 for both LCMV-GP34 and VV-A11R, corresponding with the requirement of the P4N for the LCMV-cross-reactive T cell response against VV. Using the functional and structural requirements for the cross-reactive T cell response, we were able to predict and generate a cross-reactive response towards a variant of the null OVA peptide. Together, our results highlight that shared structural features of the K^b-LCMV-GP34 and K^b-VV-A11R molecular surfaces underlie the LCMV-VV cross-reactive T cell response.

III.B. Materials and Methods

III.B.1. Production of Class I H-2K^b complexes

Extracellular domains of the murine MHC class I H-2K^b heavy chain and full length human light chain β_2 -microglobulin, were expressed separately as inclusion bodies in *Escherichia coli* and were folded *in vitro* by dilution in the presence of excess peptide, as previously described for human class I MHCs (1). Synthetic peptides purified by reverse phase-HPLC were purchased from 21st Century Biochemicals. Folded H-2K^b monomers were purified by anion exchange chromatography on Poros HQ columns (Roche) using a gradient of NaCl from 0-0.5M in 20 mM Tris buffer (pH 8.0). The concentration of each H-2K^b monomer was calculated by absorbance spectroscopy after anion exchange chromatography using $\epsilon_{280} = 74955 \text{ cm}^{-1} M^{-1}$ for H-2K^b heavy chain, $\epsilon_{280} = 20003 \text{ cm}^{-1} M^{-1}$ for β_2 -microglobulin light chain and varied ϵ_{280} for peptides depending on sequence. Purified H-2K^b monomers were adjusted to a concentration of 10-20 mg/mL using regenerated cellulose filters (Amicon) and stored at -80°C.

III.B.2. Isolation of Antigen-Specific CTL

LCMV (Armstrong strain), an RNA virus in the Old World arenavirus family, was propagated in BHK-21 baby hamster kidney cells as previously described (Selin, Nahill et al. 1994). C57BL/6 (B6) mice were infected intraperitoneally (i.p.) with a non-lethal dose of 5×10^4 PFU of LCMV as previously described (Selin, Nahill et al. 1994). Mice were considered immune at greater than 6 weeks after infection (Cornberg, Sheridan et al. 2007). Splenocytes from LCMV-immune mice were co-cultured with mouse RMA

cells that were pulsed with 1 μ M VV-A11R peptide, washed and then γ -irradiated (3000 rads) as previously described (Cornberg, Sheridan et al. 2007). RMA is a K^b-positive, Rauscher virus-induced, T-lymphoma cell line of B6 origin. Briefly, the co-culture of splenocytes and VV-A11R-pulsed RMA cells were grown in RPMI medium supplemented with 100 U/ml penicillin G, 100 μ g/ml streptomycin sulfate, 2 mM L-glutamine, 10 mM HEPES, 1 mM sodium pyruvate, 0.1 mM MEM nonessential amino acids, 0.05 mM β -mercaptoethanol, and 10% FBS for 5 days at 37°C at 5% CO₂. Following this initial culture period, cells were harvested and stimulated with GP34 peptide-pulsed RMA cells in the presence of 10% BD T-Stim (BD Biosciences), an IL-2 culture supplement. VV-A11R peptide-pulsed RMA stimulation was repeated every 4 to 5 days. After 30 to 35 days of stimulation (six or seven stimulations), T-cell lines were characterized by intracellular cytokine staining or MHC tetramer staining.

III.B.3. Cell Surface and MHC Staining by Flow Cytometry

Cell suspensions were passed through lympholyte M gradient (Cedarlane) to exclude dead cells and subsequently washed and incubated in staining buffer (phosphate-buffered saline containing 1% FBS and 0.2% sodium azide). Cell suspensions were incubated in staining buffer containing anti-mouse CD16/CD32 (Fc-block, clone 2.4G2). Cells were washed once with staining buffer and then stained with H-2K^b tetramers for 40 min followed by cell-surface antibody staining with anti-CD8 β (clone 53-6.8), anti-CD44 (clone IM7) and Live/Dead aqua exclusion dye (Invitrogen) for 20 min. Thereafter, cells were washed twice with staining buffer and fixed in Cytotfix (BD Pharmingen). Samples

were analyzed using a Becton Dickinson LSRII flow cytometer (BD Biosciences) and FlowJo software (Tree Star).

III.B.4. Intracellular Cytokine Staining (ICS)

A suspension of 10^6 cells was stimulated with 1 μ M synthetic peptide or a medium only control. Stimulations were performed for 5 h at 37°C in a total volume of 200 μ l RPMI medium supplemented with 10% FBS, 10 U/ml of human recombinant interleukin-2 (IL-2), and 0.2 μ M of brefeldin A (GolgiPlug; BD Pharmingen). After incubation, cell-surface antibody staining with anti-CD8 β (clone 53-6.8), anti-CD44 (clone IM7), and Live/Dead aqua (Invitrogen) was performed. Thereafter, cells were washed twice with staining buffer, and then fixed and permeabilized (Cytofix/Cytoperm; BD Pharmingen). Intracellular-cytokine-producing cells were detected with PE-labeled anti-mouse interferon-gamma (IFN- γ , clone XMG1.2) and APC-labeled anti-mouse tumor necrosis factor alpha (TNF- α , clone MP6-XT22) monoclonal antibodies. Antibodies were purchased from BD Pharmingen. The samples were analyzed as described above for cell surface staining.

III.B.5. In vivo CTL assay

RBC-lysed, single-cell spleen suspensions from naive B6 mice were pulsed at 10^7 cells/ml with 1 μ M peptide RPMI containing 10% FBS for 45 min at 37°C. For a four peak CTL assay (Figure III.1B), each peptide-pulsed spleen cell population was labeled with a dilution of carboxyfluorescein succinimidyl ester (CFSE, Invitrogen) at 5 μ M,

2.5 μ M, 1.25nM and 0.63nM along with 0.5 μ M of 7-hydroxy-9H-(1,3-dichloro-9,9-dimethylacridin-2-one) (DDAO, Invitrogen) at a cell density of 2×10^7 cells/ml in HBSS. Labeling was stopped by addition of excess HBSS. For an eight peak CTL assay (Figure III.3E), 1 μ M of Violet (Invitrogen) was used in addition to the CFSE and DDAO. One million cells of each peptide-pulsed population were mixed together, and 500 μ L was injected i.v. into LCMV infected and uninfected syngeneic mice.

III.B.6. Crystallization and Data Collection

H-2K^b complexes were crystallized in 14-16% PEG 8K, 0.1 M Na cacodylate, 0.2 M magnesium acetate at 4°C. Typically, 1 μ l of a 10 mg/ml protein solution in 10 mM Tris Cl (pH 7.0) was mixed with equal volumes of the crystallization reservoir. Crystals were transferred to a reservoir solution containing 30% glycerol and flash frozen using liquid nitrogen. X-ray diffraction data were collected as 1° oscillations at 100 K with 1.08 Å radiation at beamline X29A in the National Synchrotron Light Source. Data were processed and scaled using HKL2000 (Minor, Cymborowski et al. 2006). Data collection and refinement statistics are shown in Table 1.

III.B.7. Structure Determination and Refinement

Phases were estimated by molecular replacement using PHASER (McCoy, Grosse-Kunstleve et al. 2007) with PDB ID# 1S7R, peptide GNYSFYAL removed) as a search model. To validate the molecular replacement solution, composite omit maps (CNS) (Brunger 2007) were generated and inspected using COOT (Emsley and Cowtan 2004).

During refinement, the peptide was omitted to reduce model bias. The peptide was later built into the observed electron density, which was unambiguous within the peptide binding groove. Crystallographic rigid body, positional, B-factor, and TLS refinement was performed in PHENIX (Adams, Afonine et al. 2010). Ramachandran statistics showed all residues in the allowed regions. Diffraction data and coordinates were deposited into the Protein Data Bank (PDB ID# 3TID and 3TIE) (Moskophidis, Lechner et al. 1993).

III.C. Results

III.C.1. VV-A11R and LCMV-GP34 are Cross-reactive CD8+ T cell Epitopes Elicited by LCMV Infection

Previous work indicated that VV challenge of LCMV-immune mice stimulates expansion of T cell populations recognizing LCMV-GP34 (Cornberg, Clute et al. 2010). To show that these cross-reactive T cell responses were elicited in mice infected with only LCMV, we infected B6 mice with LCMV for 8 days, and at the peak of the infection performed an *ex vivo* intracellular cytokine staining (ICS) assay for cross-reactive VV-A11R T cell responses in immunized as compared to control naïve B6 mice. The results from a representative LCMV-infected mouse show an IFN γ response to the cross-reactive VV-A11R peptide at ~1% of total CD8 T cells, with only background levels of VV-A11R cross-reactivity observed in a representative naïve mouse (Figure III.1A). A T cell response to the control-SIY peptide was not observed, and the response to cognate LCMV-GP34 was observed at ~5% of total CD8 T cells (Figure III.1A). See Table III.1 for relevant epitopes.

Table III.1. Relevant Epitopes from VV and LCMV used for the study on GP34-A11R Cross-reactive T cell Responses presented in Chapter III

Source	Protein	Abbreviation	Sequence
VV	Nonstructural protein A11R ₁₉₈₋₂₀₆	A11R	AIVNYANL
VV	E7R ₁₃₀₋₁₃₇	E7R	STNLFNNL
LCMV	Glycoprotein ₃₄₋₄₁	GP34	AVYNFATM ^a
LCMV	Nucleoprotein ₂₀₅₋₂₁₂	NP205	YTVKYPNL
-	Designed sequence	SIY	SIYRYYGL
-	Ovalbumin ₂₅₇₋₂₆₄	OVA	SIINFEKL
-	Designed sequence	OVA-AA	SIINFAAL
-	Designed sequence	OVA-AT	SIINFATL

^aThis peptide carries a C-terminal Met -> Cys mutation relative to the native LCMV sequence. The substitution has been used in previous studies (Achour, Michaelsson et al. 2002; Khanolkar, Fuller et al. 2004) and does not have a significant impact on interaction with MHC or T cell receptors.

To determine if VV-A11R is recognized *in vivo* in acute LCMV-infected mice, we set up an *in vivo* cytotoxicity assay using uninfected mice as controls. Briefly, splenocytes from syngeneic B6 mice were isolated, peptide-pulsed and then fluorescently-labeled with different dilutions of carboxyfluorescein succinimidyl ester (CFSE) and a constant concentration of 7-hydroxy-9H-(1,3-dichloro-9,9-dimethylacridin-2-one) (DDAO) to monitor the target cell populations. The peptide-pulsed, DDAO- and CFSE-double labeled target populations were then injected intravenously into either acute LCMV-infected mice or uninfected controls. The cytolytic response was monitored by flow cytometry 3 hours after injection. Flow cytometry data from a representative mouse is shown in Figure III.1B, with percent specific lysis calculated for 5 mice plotted in Figure III.1C. The results show that cells from LCMV-infected mice can specifically lyse both VV-A11R and LCMV-GP34 peptide-pulsed targets *in vivo* (Figure III.1B). Killing was not observed in naïve mice, and background killing levels were observed with the non-cross-reactive peptide VV-E7R (Figure III.1B). These data clearly show that LCMV infection generates a specific T cell population which is cross-reactive *in vivo* against VV-A11R.

To study the cross-reactive T cell response specifically between VV-A11R and LCMV-GP34, we generated cross-reactive T cell lines, which were tested for TCR specificity using an ICS assay. From an LCMV-immune mouse, we generated a VV-cross-reactive T cell line (TCL), which was cross-reactive for LCMV-GP34 and VV-A11R (TCL #1). We also generated non-cross-reactive TCL, also from an LCMV-immune mouse, responding to VV-A11R only (TCL #2) for use as a control. We

performed ICS assays to show specific crossreactivity between VV-A11R and LCMV-GP34. For the ICS assay, the peptides utilized were VV-A11R, LCMV-GP34 and the control peptides SIY and OVA. The results indicate that nearly the entire (97%) memory CD8⁺ T cell population in the cross-reactive TCL #1 produces IFN γ in response to the VV-A11R peptide (Figure III.1D). In response to the LCMV-GP34 peptide, 23% of these T cells produce IFN γ , which was not observed in the VV-A11R singly-reactive TCL #2. Because essentially the entire T cell population in TCL #1 reacts against VV-A11R, any T cells that are reactive against VV-A11R must therefore also be cross-reactive against LCMV-GP34.

To test for the presence of cross-reactive TCRs, we designed a MHC tetramer competition experiment using the GP34-A11R cross-reactive TCL (TCL #1) and used the A11R singly-reactive TCL (TCL #2) as a control. For the MHC tetramer competition assay, we utilized a fixed concentration of 125 nM LCMV-GP34 tetramer and 2-fold dilutions of VV-A11R tetramer ranging from 125 nM down to 8 nM (Figure III.1E,F). We reasoned that if cross-reactive TCRs are present in the cross-reactive TCL, the binding of the VV-A11R tetramer would alter the binding of the LCMV-GP34 tetramer, due to tetramer competition for the same pool of cross-reactive TCRs. However, if two non-cross-reactive TCRs are present, the binding of LCMV-GP34 tetramer and the VV-A11R tetramer would be mutually exclusive, due to two different populations of cell surface TCRs. In this experiment, the LCMV-GP34 tetramer was prepared using streptavidin coupled to R-phycoerythrin (PE) with the VV-A11R tetramer prepared using streptavidin coupled to allophycocyanin (APC) so that binding of both tetramers could be

monitored simultaneously. The overall MHC tetramer binding MFI for APC-A11R (A11R+) versus PE-GP34 (GP34+) is plotted in Figure III.E. The arrows represent two representative FACs plots for 8 nM APC-A11R or 125 nM APC-A11R versus the fixed amount of 125 nM PE-GP34 (shown in Figure III.1F). With increasing concentrations of the APC-A11R tetramer, specific GP34 tetramer staining of the cross-reactive TCL (#1) decreased (Figure III.1E, top panel), whereas the specific GP34 tetramer staining was not observed at any concentration of APC-A11R tetramer (Figure III.1E, bottom panel). This demonstrates the presence of cross-reactive TCRs on the cross-reactive TCL (#1) which dually recognizes VV-A11R and LCMV-GP34.

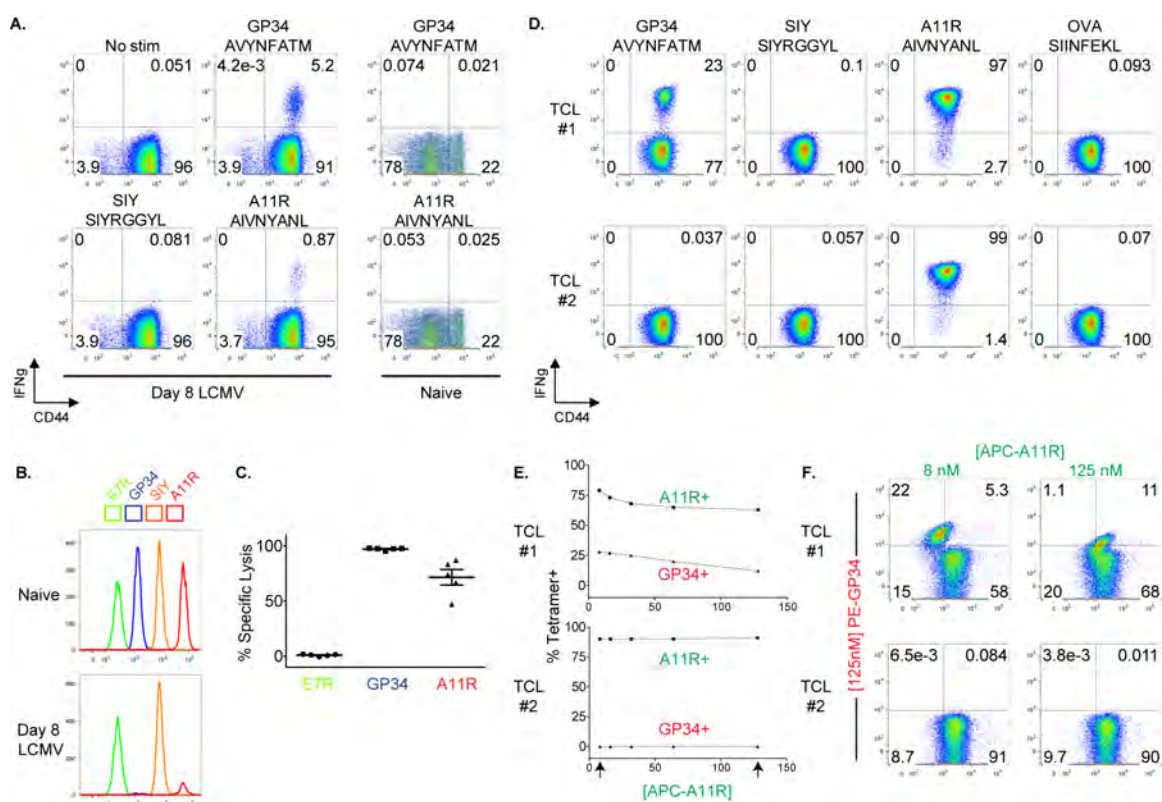


Figure III.1. VV-A11R and LCMV-GP34 are Cross-reactive CD8⁺ T cell Epitopes Elicited by LCMV Infection. *A.* CD8⁺ T cells from acute day 8 LCMV-infected mice (n=15) and uninfected mice (n=3) were isolated and analyzed for IFN γ production using an ICS assay, with results from a representative mouse presented as dot plots. *B+C.* A four peak *in vivo* cytotoxicity assay was set up using two different fluorophores as described in the materials and methods. Briefly, naïve B6 splenocytes were peptide-pulsed and then labeled with a dilution of CFSE and DDAO. Peptide-pulsed, and CFSE and DDAO double-labeled cells were injected (*i.v.*) into uninfected (naïve, n=3) or LCMV-infected (D8 LCMV, n=5) mice. Three hours after transfer, spleens were harvested and analyzed by flow cytometry. Plots from a representative infected and naïve mouse are shown in *b*. Percent specific lysis was calculated based on the “SIY” peptide-pulsed population and plotted in *c*. *D.* Splenocytes from an LCMV-immune mouse were isolated and expanded *in vitro* using VV-A11R peptide-pulsed targets to generate a GP34-A11R cross-reactive T cell line (TCL #1) and an A11R singly-reactive T cell line (TCL #2). T cell lines were analyzed for IFN γ production in response to the indicated peptides, with the results presented as dot plots. The results are representative of three different T cell lines. *E+F.* The T cell lines from panel *d* were stained with R-PE or APC-labeled streptavidin-based K^b tetramers folded with VV-A11R or LCMV-GP34 peptides. Double MHC tetramer staining experiments were set up using a PE-labeled LCMV-GP34-K^b tetramer and an APC-labeled VV-A11R-K^b tetramer. The VV-A11R

tetramers were used at concentrations starting at 125 nM titrated down two-fold to 8 nM while the LCMV-GP34 tetramer concentration was maintained constant at 125 nM. The percent tetramer positive for every concentration is plotted in f.

III.C.2. Recognition Determinants for the Cross-reactive T cells

To further characterize the cross-reactive T cell responses between LCMV-GP34 and VV-A11R, we compared the recognition determinants for LCMV-GP34 and VV-A11R individually. We reasoned that a comparison of the important TCR contact residues for both epitopes would highlight similarities and differences in recognition determinants, which might hint at the mode(s) of TCR engagement. Alanine substitutions were generated at the predicted non-MHC binding residues (underlined) in LCMV-GP34 (AVYNFATM) and VV-A11R (AIVNYANL). Peptide binding to MHC class I H-2K^b depends on the peptide positions 5 (P5) and 8 (P8) as primary anchors, and peptide positions 2 (P2) and 3 (P3) as secondary anchors (Fremont, Matsumura et al. 1992; Matsumura, Fremont et al. 1992). We modified the other positions and included the P3 secondary anchor position, in order to test the potential TCR contact residues. Residues with alanines present already were mutated to either glycine for a conservative substitution or to lysine for a non-conservative substitution. The substituted peptides were first tested for binding to K^b by using an RMA-S stabilization assay, and the EC₅₀ values for peptide binding were plotted (Figure III.2). We observed that the substituted LCMV-GP34 and VV-A11R peptides do not bind significantly different from the WT peptides (Figure III.2), with the exception of the P3A variants, which were not utilized further.

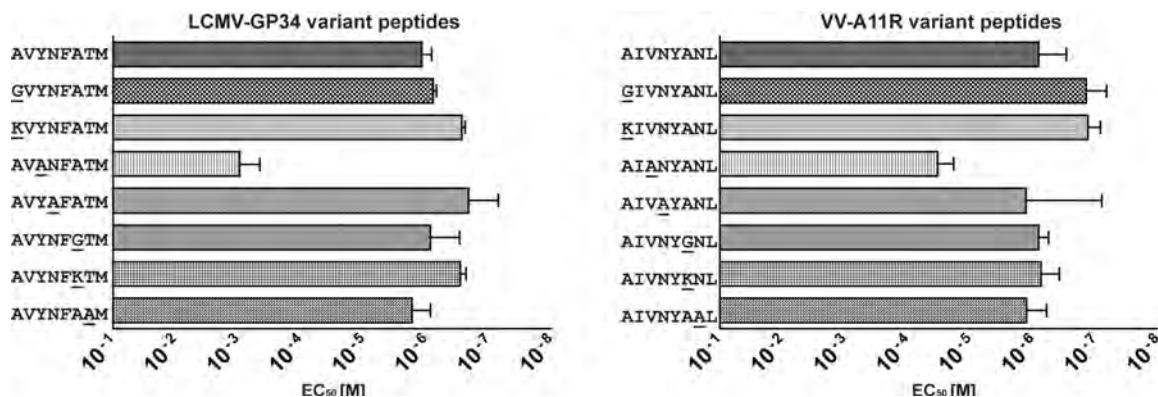


Figure III.2. Mutated Peptides from LCMV-GP34 and VV-A11R Bind to H-2K^b with Similar Affinities with the Exception of the P3A variants. An RMA-S stabilization assay was utilized to measure relative binding affinity of WT and variant peptides from LCMV-GP34 and VV-A11R. EC₅₀ values were calculated for each peptide titration series (n=3) and represented as bar graphs.

Next, we performed an ICS assay to test the substituted peptides from LCMV-GP34 and VV-A11R for reactivity with T cells from acutely LCMV-infected mice. Flow cytometry data from a representative mouse are shown for the LCMV-GP34 and VV-A11R peptide variants in Figure III.3A and Figure III.3B, respectively. Relative T cell responses, which are the proportion of IFN γ responses to WT GP34 or A11R controls, from 15 mice are shown in Figure III.3C and Figure III.3D, for the LCMV-GP34 and VV-A11R peptide variants, respectively. Substitutions in LCMV-GP34 at the P4N, the P6A and the P7T residues resulted in loss of IFN γ production (Figure III.3A,D). For LCMV-GP34 P6A, substitution by lysine (P6K) blocked T cell recognition but substitution by glycine (P6G) did not, which suggests that the P6A side chain is not a direct TCR contact (Figure III.3B,D). As for the cross-reactive ligand VV-A11R, a different pattern was observed, where substitution at the P1, P4 and P6 but not P7 positions resulted in loss of IFN γ production (Figure III.3C,E). For VV-A11R P1A, substitution by lysine (P1K) but not glycine (P1G) reduced T cell recognition, suggesting that for this peptide the P1A side chain is not directly involved in T cell recognition (Figure III.3C,E). For LCMV-GP34, substitutions at this position had no effect. For the VV-A11R P4N, substitution by alanine (P4A) blocked recognition, as it did for LCMV-GP34. The shared recognition determinant at P4 suggests that cross-reactive TCRs utilize this residue for T cell responses. At P6, both VV-A11R P6G and P6K substitution resulted in decreased IFN γ production, differently from LCMV-GP34 where the P6G mutation had no effect. Finally, the VV-A11R P7 residue was not important for IFN γ production on average, but there was a broad range of reactivity amongst the different

mice tested. In summary, cognate recognition of LCMV-GP34 is dependent on P4N and P7T whereas cross-reactive recognition of VV-A11R depends mainly on P4N.

To determine whether the P4 and the P7 residues are required for the cross-reactive recognition of VV-A11R *in vivo*, we performed a dual label *in vivo* cytotoxicity assay as described in the methods, utilizing dilutions of CFSE and DDAO for target cells pulsed with the GP34 variants or dilutions of CFSE and Celltrace violet for cells pulsed with the A11R variants (Figure III.3E,F). Flow cytometry data from a representative naïve mouse and LCMV-infected mouse is shown in Figure III.3E, with percent specific lysis calculated for 7 LCMV-infected mice plotted in Figure III.3F. We asked if CD8⁺ T cells from acute LCMV-infected mice could specifically lyse WT, P4A and P7A variants of LCMV-GP34 and VV-A11R, using the non-cross-reactive peptides OVA and SIY as controls. The P4A substitution in VV-A11R resulted in a log reduction in percent specific lysis (Figure III.3F), showing that T cells which crossreact with VV-A11R from LCMV-infected mice require the P4N in VV-A11R for specific lysis *in vivo*. These functional data demonstrate that P4N is a major recognition determinant that is required for the polyclonal LCMV-cross-reactive T cell response against VV-A11R. To confirm that cross-reactive T cell responses towards VV-A11R are not unique to one T cell clone, we evaluated the T cell receptor repertoire from LCMV-infected mice that respond towards VV-A11R (Figure III.4). A polyclonal response including at least six different TCR β genes was observed, which indicates that the polyclonal, cross-reactive T responses towards VV-A11R require the P4N as a major recognition determinant.

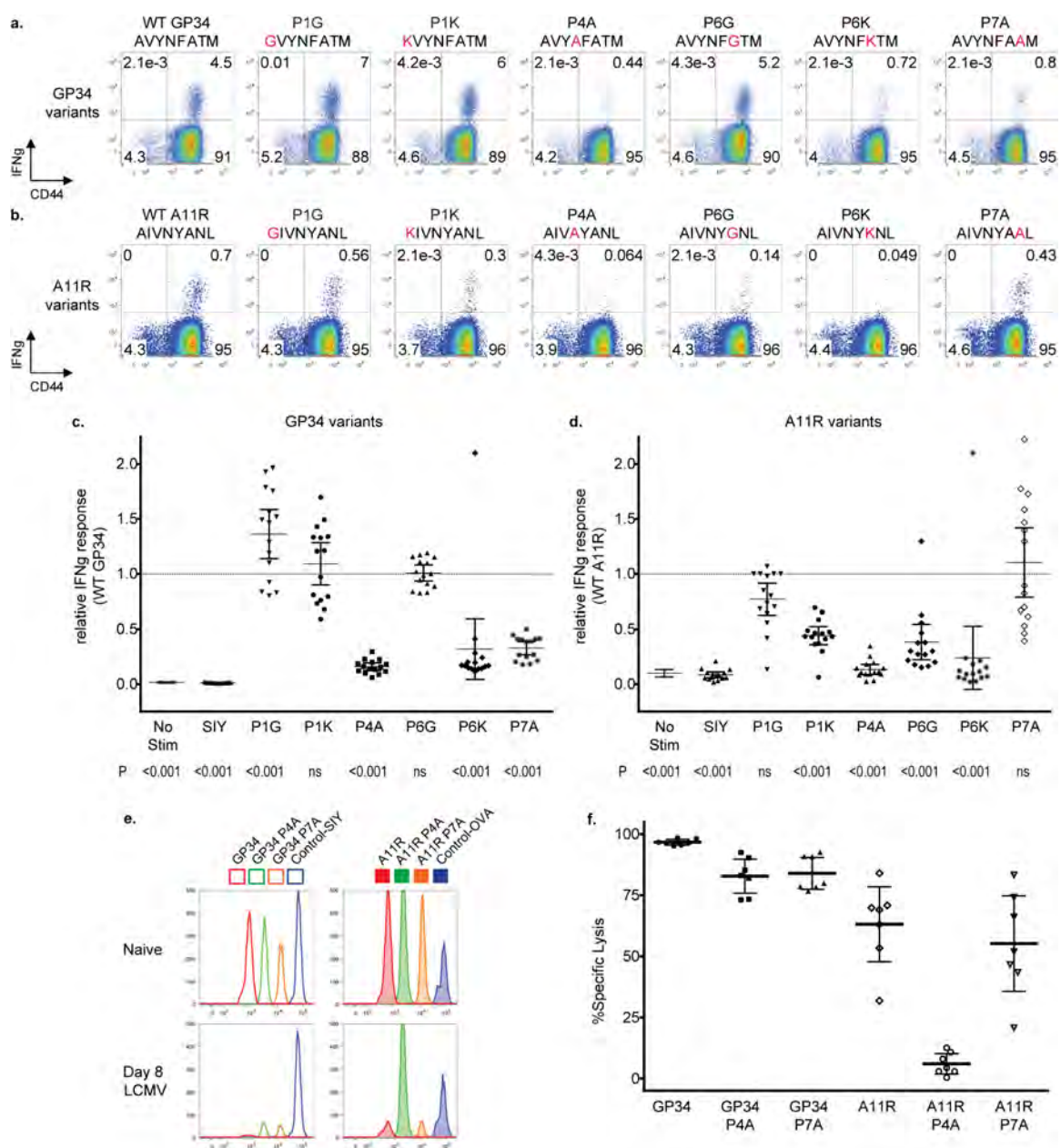


Figure III.3. Recognition Determinants for Cross-reactive T cells. Recognition determinants for CD8⁺ T cell responses against VV-A11R and LCMV-GP34 were mapped by mutational analysis. Non-H-2K^b binding residues from LCMV-GP34 and VV-A11R, which include p1, p4, p6 and p7, were mutated to alanine, with alanine residues mutated to either glycine or lysine. *A+B*. CD8⁺ T cells from acute LCMV-infected mice were tested for IFN γ production in response to 1 μ M of the indicated peptides with representative results from a single mouse shown as dot plots (n=15). *C+D*. IFN γ production results from acute LCMV-infected mice (n=15) were normalized

to WT LCMV-GP34 for the LCMV-GP34 variants or WT VV-A11R for the VV-A11R variants. *E+F*. To test the necessary contact residues at p4 and p7 *in vivo*, an eight peak cytotoxic T lymphocyte assay was set up like previously described in Figure III.1. Briefly, the 8 peak assay was split into two simultaneous four peak assays using dilutions of either CFSE vs. DDAO or CFSE vs. violet as described in the Materials and Methods. Target cell populations were injected (i.v.) into acute LCMV-infected mice (n=7) or uninfected mice (n=3). Percent specific lysis in panel f was calculated based on either the “SIY” peptide-pulsed population or the “OVA” peptide-pulsed population.

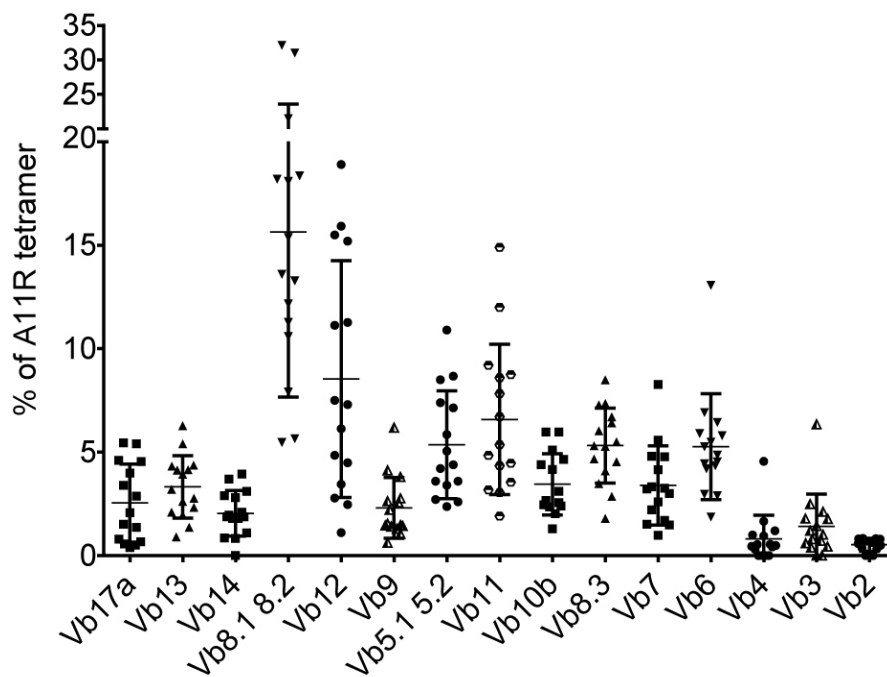


Figure III.4. Acute LCMV-infected mice have a Polyclonal Cross-reactive T cell Response towards VV-A11R. CD8⁺ T cells from acute LCMV-infected mice (n=15) were stained with VV-A11R tetramer and TCR Vβ antibodies. The percentage of TCR Vβ utilized for the recognition of VV-A11R tetramer is plotted.

Although a clear role for the P4N in LCMV-cross-reactive T cell responses against VV-A11R was observed *in vivo*, the experiments reported in Figure III.3 used highly polyclonal populations, making it difficult to evaluate the contribution of cross-reactive TCRs relative to recognition by different T cell populations. Therefore, we tested for the P4N dependence on cross-reactive T cell lines that have narrowed T cell receptor repertoires due to repeated *in vitro* expansion (results from previous *in vitro* expanded TCLs, see Figure III.5). We performed ICS assays followed by tetramer staining assays using the P4A and P7A variants of both LCMV-GP34 and VV-A11R. For both assays, we tested the variant peptides on an LCMV-GP34 and VV-A11R cross-reactive T cell line (TCL #3) and used a VV-A11R singly-reactive T cell line (TCL #2) as a control. The results of the ICS assay show that for the cross-reactive TCL #3, IFN γ production in response to LCMV-GP34 was dependent on both P4N and P7T, while recognition of the VV-A11R was dependent only on P4N (Figure III.6A), consistent with the *in vivo* results. In contrast, for the VV-A11R singly-reactive T cell line (TCL #2), recognition of VV-A11R was dependent on both P4N and P7N.

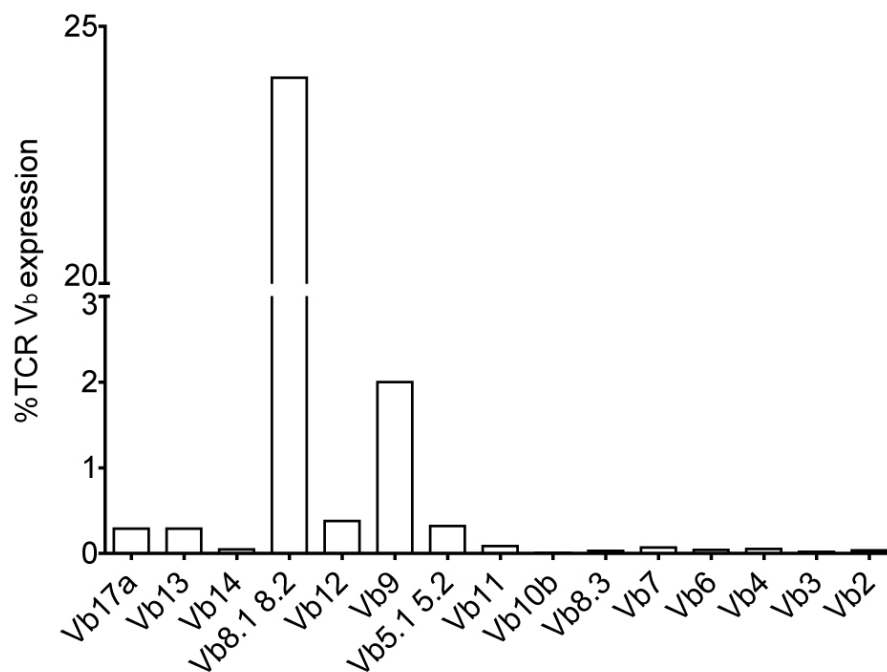


Figure III.5. Cross-reactive T cell lines have Narrowed TCR Repertoires. TCR V β profiling of CD8⁺ T cells from a GP34-A11R cross-reactive TCL (TCL #1) was performed. Briefly, CD8⁺ T cells from TCL#1 were stained with TCR V β antibodies purchased from BD Pharmingen. The percentage of TCR V β expressed is plotted.

For the tetramer staining assay, we monitored binding of LCMV-GP34 WT, VV-A11R WT, VV-A11R P4A, and VV-A11R P7A or control OVA tetramers on the LCMV-GP34 and VV-A11R cross-reactive (TCL #3), and VV-A11R singly-reactive (TCL #2) T cell lines (Figure III.6B). The tetramer staining patterns paralleled the results from the ICS assay. The GP34-A11R cross-reactive TCL #3 stains with WT GP34, WT A11R and A11R P7A tetramers, while the A11R singly-reactive TCL #2 stains only with the WT A11R tetramer (Figure III.6B). Taken together, these results show that cross-reactive TCRs that recognize LCMV-GP34 depend on the P4N for the cross-reactive recognition of VV-A11R.

Using the notion that the LCMV-cross-reactive T cell response directed towards VV-A11R is dominated by the P4N, we hypothesized that an increased LCMV-GP34, VV-A11R, cross-reactive T cell response would correspond with an increased dependence on the P4N. To address this, we used the GP34-A11R cross-reactive T cell line from Figure III.1 (TCL #1), which was nearly 100% reactive towards VV-A11R, and we selectively expanded the population that also recognizes LCMV-GP34 (23%) by stimulating *in vitro* with the LCMV-GP34 peptide for two additional passages (TCL #1-GP34, Figure III.6C, left panel). For comparison, we stimulated the same T cell line using the VV-A11R peptide for two additional passages (TCL #1-A11R, Figure III.6C, right panel). We tested for functional responses by performing an ICS for IFN γ production in response to WT, P4A or P7A variants of the LCMV-GP34 or the VV-A11R peptides, with OVA used as a control (Figure III.6C). Cross-reactive T cells stimulated with A11R only responded to LCMV-GP34 WT (~25%, plain bars), VV-

A11R WT (~100%, horizontally striped bars) and VV-A11R p7A (~25%, vertically striped bars). After the same TCL was expanded *in vitro* with the LCMV-GP34 peptide to select for the LCMV-GP34 and VV-A11R cross-reactive T cells, we observed an increase in IFN γ production in response to LCMV-GP34 WT and VV-A11R P7A. By skewing the T cell response in favor of LCMV-GP34 reactivity in this entirely VV-A11R cross-reactive TCL, we observed a proportional decrease in the dependence on the P7 residue in the VV-A11R peptide. These results indicate that VV-A11R cross-reactive T cells that respond towards LCMV-GP34 do not require the P7 residue.

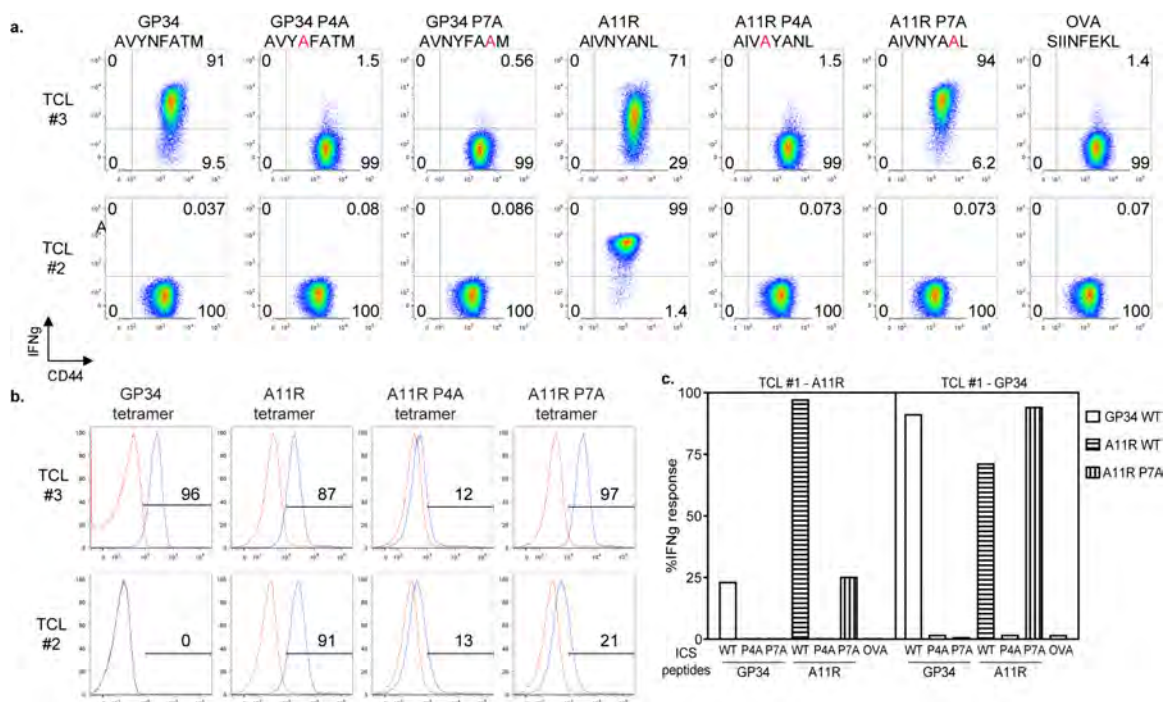


Figure III.6. Recognition Determinants for GP34-A11R Cross-reactive T cell receptors. GP34-A11R cross-reactive (TCL #3) and A11R singly-reactive (TCL #2) T cell lines were generated as described for Figure III.1. *A.* Cross-reactive T cell lines were tested for IFN γ production against WT, p4A or p7A variant peptides from LCMV-GP34 and VV-A11R along with the control-peptide, OVA. The results are represented as dot plots and are representative of three independent experiments. *B.* Single MHC tetramer staining experiments were performed on both the GP34-A11R cross-reactive (TCL #3) and the A11R singly-reactive (TCL #2) T cell lines. Briefly, WT LCMV-GP34, VV-A11R (WT, p4A, p7A) and control-OVA peptide-MHC tetramers were tested at 125 nM with the results represented as histograms. In each histogram, the indicated tetramer (blue trace) was overlaid with the control-OVA tetramer (red trace). *C.* The GP34-A11R cross-reactive T cell line from Figure III.1 (TCL #1) was re-stimulated *in vitro* using LCMV-GP34 peptide-pulsed targets, to selectively expand the GP34-A11R cross-reactive population (TCL #1 - GP34). For comparison, TCL #1 was also re-stimulated *in vitro* using VV-A11R peptide-pulsed targets (TCL #1 - A11R). After two rounds of stimulation, CD8 $^{+}$ T cells were analyzed for IFN γ production in response to WT, P4A and P7A variants of both LCMV-GP34 peptide and VV-A11R peptide along with the control-OVA peptide. The data is represented in the bar graph.

To address whether cross-reactive TCR recognition could also depend on contacts with the H-2K^b molecule, we tested previously identified LCMV- and VV-derived K^b epitopes which have the same important P4N or the P7 residue with either LCMV-GP34 or VV-A11R (Table III.2). These peptides have all been tested for T cell responses in ICS assays, which measured IFN γ production on T cells from either acutely LCMV-infected mice or GP34-A11R cross-reactive TCLs. Cross-reactive T cell responses have not been observed with any of these peptides (data not shown), indicating that the shared aspects leading to cross-reactive T cell responses depend predominantly on peptide contacts with TCR. This result highlights the importance of the P4N that is shared between LCMV-GP34 and VV-A11R.

Table III.2. Tested K^b-binding epitopes which share either the P4N residue or the P7 residue with LCMV-GP34 or VV-A11R

Source	Protein	Sequence
VV	E7R ₁₃₀₋₁₃₇	STNLFNNL
VV	A3L ₂₇₀₋₂₇₇	KS ^Y NYMLL
LCMV	Nucleoprotein ₂₀₅₋₂₁₂	YTVKYPNL
LCMV	Glycoprotein ₁₁₈₋₁₂₅	ISHNFCNL
LCMV	L ₇₇₅₋₇₈₂	SSF ^N NGTL

III.C.3. Analysis of the K^b-VV-A11R and K^b-LCMV-GP34 Molecular Surfaces

To understand the dependence of P4N for cross-reactive T cell recognition, we determined the crystal structures of K^b-VV-A11R (PDB ID# 3TIE) and K^b-LCMV-GP34 (PDB ID# 3TID) complexes, using data extending to 2.2Å and 1.7Å resolution respectively (Table III.3). The overall structures of K^b-VV-A11R and K^b-LCMV-GP34 differ very little with an RMSD of 0.472 Å. A side profile comparison of the antigen binding cleft from K^b-VV-A11R and K^b-LCMV-GP34 reveal that both VV-A11R and LCMV-GP34 are bound and presented similarly in K^b (Figure III.7A,B). Both peptides at P4 and P7 have solvent exposed side chains, which protrude away from the K^b heavy chain and are available for TCR contact (Figure III.7A,B). The main chain at P6 also appears solvent accessible, while side chains at P2, P3, P5 and P8 are buried in the K^b molecule (Figure III.7A,B). In the top views of K^b-VV-A11R and K^b-LCMV-GP34 (Figure III.7D,E), it is clear that most of the surfaces of LCMV-GP34 and VV-A11R are virtually identical when presented by K^b, particularly at the asparagine at P4, which appears to be in the same conformation (Figure III.7G). The P7 side chain is a notable exception, with differences clearly observed when the K^b-VV-A11R and the K^b-LCMV-GP34 structures are overlaid (Figure III.7G).

Table III.3. Data Collection and Refinement Statistics for K^b-GP34 and K^b-A11R

Data Collection	K^b-LCMV-GP34 (AVYNFATM)	K^b-VV-A11R (AIVNYANL)
Space group	C2	P21
Wavelength	1.0809	1.0809
Unit cell parameters	a= 172.261, b= 47.649, c= 70.539 Å, β= 106.39°	a= 69.264 , b= 84.710 , c= 87.895 Å, β= 98.12°
Resolution (Å)	50-1.7	50-2.2
R _{sym} (%)	5(26)	10(28)
I/sI	22.1 (7.8)	15.1 (5.7)
Completeness (%)	98 (96.7)	99.4 (99.3)
Redundancy	3.8 (3.8)	6.2 (6.3)
Refinement		
Resolution (Å)	40-1.7	40-2.2
No. reflections	59,404	50,967
Rwork/Rfree (%)	0.167/0.190	0.177/0.219
No. atoms		
Protein	3081	6160
Water	665	464
Average B-factor (Å ²)	20.7	37.4
R.M.S. Deviations		
Bond length (Å)	0.006	0.008
Bond angles (°)	1.036	1.054
Ramachandran Plot		
Most favored (%)	98.9	98.5
Allowed (%)	1.1	1.4
Disallowed (%)	0	0.1

As a comparison, we overlaid the previously reported crystal structure of the highly defined and studied K^b-OVA, which was not recognized by T cells cross-reactive with LCMV-GP34 or VV-A11R. Similar to the K^b-LCMV-GP34 and the K^b-VV-A11R structures, the OVA peptide has solvent accessible side chains at P4, P6 and P7, whereas the P2, P3, P5 and P8 residues are all buried in K^b (Figure III.7C). The K^b-OVA surface appears quite different than those of K^b-LCMV-GP34 and the K^b-VV-A11R, with bulky side chains placed at P6 and P7. These might sterically inhibit interactions with the TCR (Figure III.7F,H). Furthermore, the P4N, which is shared by all the peptides in OVA, adopts a different rotamer as compared to VV-A11R and LCMV-GP34 (Figure III.7F,H). The combination of the bulky side chains at P6 and P7 with the P4N in a different conformation may help to explain the absence of a cross-reactive T cell response towards OVA. In summary, the structures of K^b-VV-A11R and K^b-LCMV-GP34 have markedly similar surfaces for TCR recognition and contrast greatly with that of K^b-OVA.

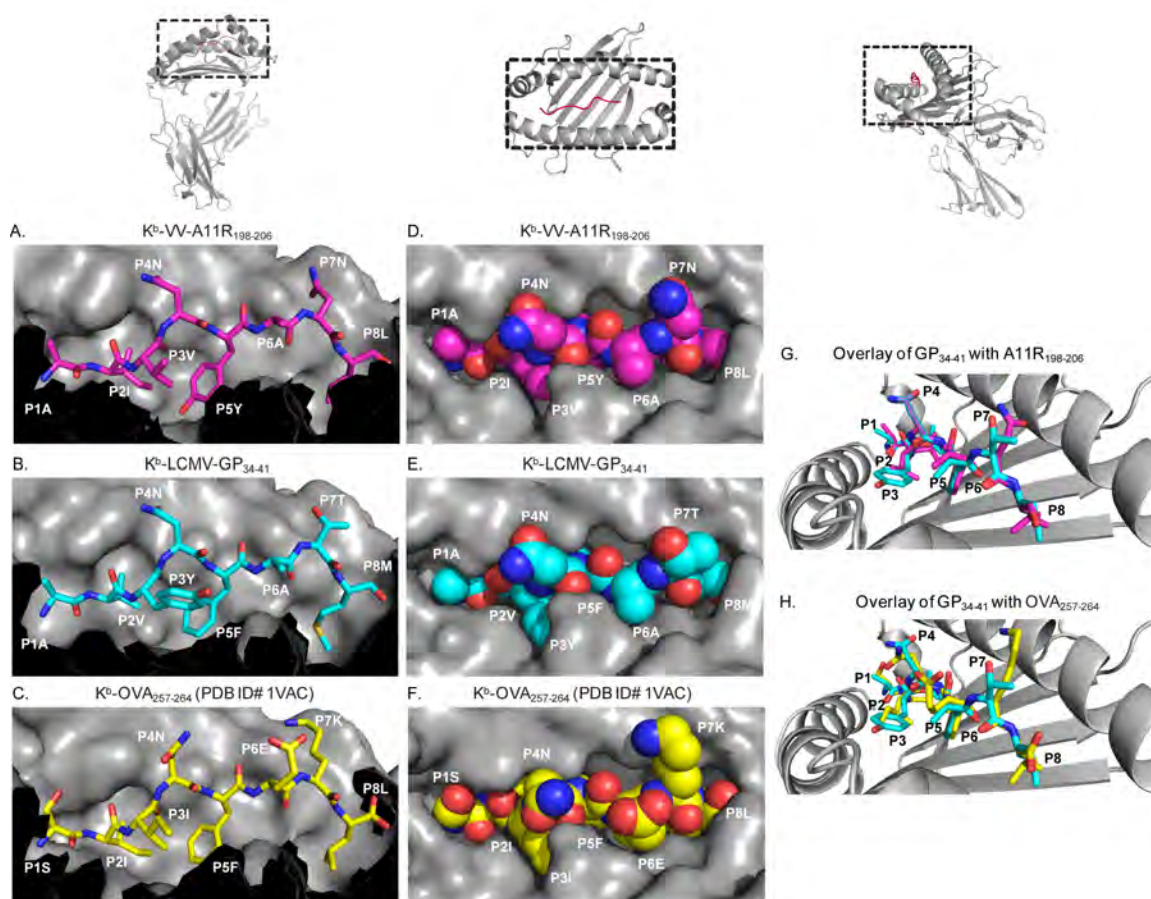


Figure III.7. Analysis of the K^b -VV-A11R and K^b -LCMV-GP34 Molecular Surfaces. A-C. The peptide-MHC structures of K^b -VV-A11R₁₉₈₋₂₀₆, K^b -LCMV-GP₃₄₋₄₁, and K^b -OVA₂₅₇₋₂₆₄ (PDB ID# 1VAC) are shown from a side profile view. In each panel, the peptide is represented as a stick model, while the H-2K^b molecule is represented by its surface. Residues T143, K144, K146, W147, A150, G151, E152, R155, L156, A158, Y159, T163, and C164 from H-2K^b are excluded. D-F. The peptide-MHC structures of K^b -VV-A11R₁₉₈₋₂₀₆, K^b -LCMV-GP₃₄₋₄₁, and K^b -OVA₂₅₇₋₂₆₄ (PDB ID# 1VAC) are represented as surfaces and viewed from above. The peptides are colored magenta for VV-A11R₁₉₈₋₂₀₆, cyan for LCMV-GP₃₄₋₄₁ and yellow for OVA₂₅₇₋₂₆₄ with the H-2K^b molecule shown in grey. The residues in the peptide are labeled as “P” followed by the peptide position. G. The peptide-MHC structures of K^b -VV-A11R₁₉₈₋₂₀₆ and K^b -LCMV-GP₃₄₋₄₁ have been overlaid for comparison. The presented view is looking down towards the N terminus of the peptide. The peptide in each structure is represented as stick model and colored using the same coloring scheme used in a-c, while the H-2K^b molecule is shown as cartoon and colored grey. H. The peptide-MHC structures of K^b -OVA₂₅₇₋₂₆₄ and K^b -LCMV-GP₃₄₋₄₁ have been overlaid for comparison using the same view from f. Pymol was used to generate all the images.

III.C.4. Skewing of Cross-reactive T cell Responses against VV-A11R and LCMV-GP34

The functional and structural data presented thus far support the idea that the cross-reactive T cell response against VV-A11R is dominated by the P4 asparagine. We hypothesized that VV-A11R cross-reactive T cell responses would be selected against by *in vitro* stimulation with a P4A variant which lacks the important asparagine contact. To test for this, we generated T cell lines from three LCMV-immune mice (Figure III.8A) and expanded them *in vitro* using either the LCMV-GP34 WT peptide or the LCMV-GP34 P4A mutant peptide (TCLs #4,5,6). In each case, expansion with the LCMV-GP34 P4A peptide selects against a cross-reactive VV-A11R T cell response. Interestingly, the cognate response towards LCMV-GP34 was maintained, perhaps through selecting for T cells which recognize the P7T residue.

Next, we wanted to utilize the requirement for the P4N in our system to generate a novel cross-reactive T cell response. To address this, we utilized the OVA peptide, which contains a P4N, but has never been found to be cross-reactive. Our structural analysis suggests that the cross-reactive T cell response against OVA might be absent because of the bulky residues at P6 and P7 in OVA (SIINFEKL), which might sterically inhibit TCR docking. To address this, we generated OVA variants with the P6 and P7 residues from LCMV-GP34 (OVA-AT, SIINFATL), or with both P6 and P7 as alanines (OVA-AA, SIINFAAL). We performed an ICS assay on a GP34-A11R cross-reactive T cell line (TCL #7) to test for the recognition of VV-A11R, LCMV-GP34, OVA, OVA-AA and OVA-AT (Figure III.8B). The results show that while the native OVA peptide

does not crossreact, 41% of the CD8⁺ T cells respond towards the modified OVA-AT peptide (Figure III.8B). Because >90% of T cells respond to both VV-A11R and LCMV-GP34, most cells that respond against VV-A11R or LCMV-GP34 must also crossreact against OVA-AT. Interestingly, we found that OVA-AA is not cross-reactive, indicating that the cross-reactive recognition of OVA-AT requires the P7T. Because the hybrid OVA peptides have not been reported previously, we needed to exclude the possibility that these cross-reactive responses were unique to our *in vitro* T cell line. To test if the hybrid OVA peptides could be recognized *ex vivo*, we performed an ICS assay on splenocytes from acute-LCMV infected mice or naïve mice as controls (Figure III.8C). T cell responses were observed towards the OVA-AT peptide, with IFN γ production measured at ~3%. T cell responses were not observed towards the OVA-AA peptide, matching the results *in vitro* from the GP34-A11R cross-reactive TCL (Figure III.8D). T cell responses towards VV-A11R (~2%) and LCMV-GP34 (~10%) were elevated, but within the range that has been previously observed (data not shown). Taken together, these results highlight the pervasive nature of cross-reactive T cell responses, as even the null OVA peptide can be made cross-reactive simply through substitution of side chains that may inhibit TCR engagement.

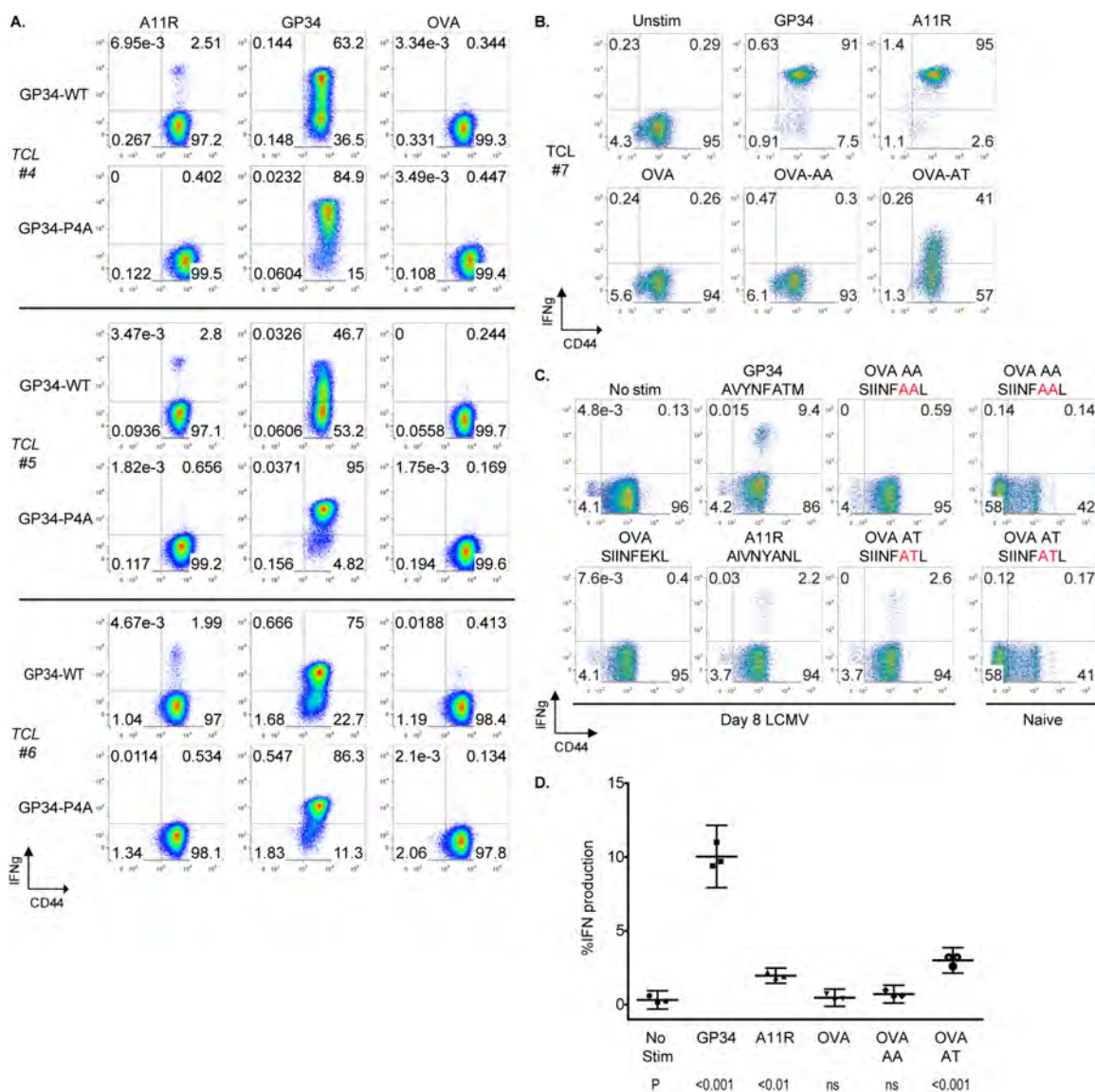


Figure III.8. Skewing of Cross-reactive Responses against both VV-A11R and LCMV-GP34. *A.* T cell lines (TCL #4,5,6) were generated using the splenocytes from three LCMV-immune mice. T cells were expanded *in vitro* for four passages by stimulation with either WT-GP34 or GP34 p4A peptide-pulsed targets. T cell lines were analyzed for IFN γ production in response to VV-A11R peptide, LCMV-GP34 peptide and OVA peptide with the results presented as dot plots. *B.* Cross-reactive T cell lines were tested for IFN γ production against LCMV-GP34, VV-A11R, OVA or the OVA hybrid peptides, OVA-AA and OVA-AT. The results are represented as dot plots and are representative of three independent experiments. *C.* CD8⁺ T cells from acute LCMV-infected mice (n=3) or uninfected mice (n=2) were tested for IFN γ production in response to 1 μ M of the indicated peptides with the results presented in the graph.

III.D. Discussion

Protective heterologous immunity plays an important role in the immune response. The ligand requirements for T cell recognition of disparate epitopes from unrelated pathogens are unclear. In this study, we observed that LCMV-GP34 and VV-A11R tetramers compete with each other for TCR. This clearly indicates the presence of individually cross-reactive TCRs which can dually recognize both LCMV-GP34 and VV-A11R (Figure 1E). We compared the recognition determinants for LCMV-GP34 and VV-A11R by generating site-specific mutations in both epitopes at potential TCR contact residues. We tested the mutated peptides for IFN γ production on either acute LCMV-infected mice or cross-reactive TCLs and found different recognition patterns for LCMV-GP34 and VV-A11R. The cognate response towards LCMV-GP34 was dependent on the P4N and P7T, whereas the cross-reactive T cell response towards VV-A11R depended mainly on P4N. Interestingly, we found that the P4A variant of VV-A11R protected against cytotoxic T cell responses in acutely LCMV-infected mice, *in vivo*. Combined, our results clearly indicate that the P4N, which is shared between LCMV-GP34 and VV-A11R, mediates the LCMV-cross-reactive T cell response towards VV-A11R.

Analysis of the K^b-LCMV-GP34 and K^b-VV-A11R crystal structures revealed that these cross-reactive peptide-MHC complexes have nearly identical surface structures, with the P4N conserved in both structures. Structural mimicry was somewhat unexpected due to the sequence disparity between LCMV-GP34 (AVYNFATM) and VV-A11R (AIVNYANL), which share only three of eight residues (underlined). Consistent with overall structural similarity between K^b-LCMV-GP34 and K^b-VV-A11R,

which includes the conserved P4N, our functional data indicate that the P4N is an important recognition determinant that is shared for the cognate response towards LCMV-GP34 as well as the cross-reactive T cell response towards VV-A11R. Using information about the requirement for P4N in the VV-A11R cross-reactive T cell response, we were able to selectively eliminate the VV-A11R cross-reactive T cell response while maintaining a non-cross-reactive cognate LCMV-GP34 T cell response by expanding T cells *in vitro* with the LCMV-GP34 P4A peptide. Additionally, we were able to predict and generate a novel cross-reactive T cell response by simply substituting the P6 and P7 residues of the null OVA peptide. These modifications probably facilitated recognition of the important P4N. Collectively, our results highlight that shared aspects of the molecular surface formed by peptide-MHC complexes can be utilized for cross-reactive T cell recognition. These findings highlight the pervasive nature of cross-reactive T cell responses, but more importantly, demonstrate that cross-reactive T cell responses can be controlled and even manipulated. The ability to skew cross-reactive T cell responses in a specific manner highlights the potential for vaccine design.

The CD8 memory population is not stable *in vivo*, as infections with cross-reactive viruses can elicit expansions of subsets of the antigen specific memory pool and result in memory pools with altered affinities to and protective capacities against the first-encountered pathogen (Cornberg, Chen et al. 2006; Chen, Cornberg et al. 2012). This is an important issue to evaluate when designing vaccines against viruses known to have highly mutable epitopes or epitopes cross-reactive with other pathogens. Of note, we have shown that altering the epitope used in an ICS assay by a peptide substitution can

sometimes lead to a much higher T cell response to that epitope, indicating that a cross-reactive response may sometimes be more detectable and effective than the response to a homologous peptide. Thus, by understanding the parameters of cross-reactivity one might be able to construct a vaccine with an altered peptide that would stimulate an improved response against the desired targeted epitope.

In conclusion, the results presented in this study highlight the pervasive nature of cross-reactive T cell responses. A detailed understanding of the LCMV-GP34 and VV-A11R cross-reactive T cell response revealed that the shared P4N residue is utilized for cross-reactive TCR recognition. Using our understanding of this system, we were able to selectively eliminate VV-A11R cross-reactive T cell responses or generate novel cross-reactive T cell responses to a variant of the OVA peptide. A better mechanistic understanding of protective heterologous immune responses is needed to improve vaccine design strategies.

Chapter IV:

Conclusions and Future Directions

The work presented in this thesis was directed at understanding the molecular mechanisms of CD8⁺ T cell recognition and cross-reactivity. Chapter II described the development of bi-specific MHC heterodimers and its advantages as a staining reagent for cross-reactive CD8⁺ T cells. Chapter III described the molecular mechanism of a cross-reactive CD8⁺ T cell response that occurs between LCMV-GP₃₄₋₄₁ and VV-A11R₁₉₈₋₂₀₅. In this chapter, I will provide additional discussion, overall conclusions and future directions for the results presented.

IV. A. The Bi-specific MHC Heterodimer

The results in Chapter II describe a novel bi-specific MHC heterodimer approach, which can be used to monitor cross-reactive T cells capable of recognizing two different peptide-MHC complexes. Conventionally, MHC tetramers are used for phenotypic characterization of T cells. However, when we first employed two MHC tetramers to identify cross-reactive T cells, we observed MHC tetramer cross-competition. The cross-competition between the MHC tetramers indicates that individually-cross-reactive TCRs are capable of recognizing both LCMV-GP34 and VV-A11R, which disproves the notion that expression of two different TCRs on a single cell (Hardardottir, Baron et al. 1995; He, Janeway et al. 2002) underlies the cross-reactive T cell response between LCMV-GP34 and VV-A11R. In the scenario where two different TCRs could be expressed on

the surface of a single T cell, the binding of the two different MHC tetramers would be mutually exclusive.

The observation that two MHC tetramers compete for cross-reactive TCRs, resulting in reduced tetramer staining for the lower affinity peptide-MHC and TCR complex, complicates the use of MHC tetramers for the identification of cross-reactive T cells. However, the observed MHC tetramer competition can be avoided. For example, if the concentrations of the two tetramers were titrated, it could be possible to use two MHC tetramers to identify cross-reactive T cells. While this is feasible for experimentation on cross-reactive T cells from *in vitro* T cells lines with relatively large numbers of cells to perform titration experiments, the numbers of T cells from human samples are much more limited. Additionally, due to the polyclonal nature of T cell responses, the avidities between different TCRs may vary, which would make MHC tetramer titration experiments a necessity for each and every experiment targeted at visualizing cross-reactive T cells. Therefore, we developed bi-specific MHC heterodimers through heterobifunctional cross-linking. We observed that our heterobifunctional cross-linking strategy does not perturb the integrity of the peptide-MHC complex or its interaction with TCR. Most importantly, our bi-specific MHC heterodimers were found to be specific for T cells that have individual TCRs which are cross-reactive for LCMV-GP34 and VV-A11R.

There were some issues with the heterobifunctional cross-linking strategy, which have not been mentioned. As previously noted, we observed that the cross-linker-modified peptide-MHC monomers were particularly sensitive to side reactions, especially

upon storage. In addition to the tendency for the hydrazide-reactive cross-linker (MHPH) to self-react, we observed that the presence of the Alexa fluorophores prior to cross-linking, induced non-specific dimerization. This complicated our initial strategy, which was to uniformly label the peptide-MHC complexes with an amine-reactive Alexa fluorophore, followed by cross-linker addition onto the MHC monomers using a free thiol placed at the C-terminus of the MHC class I heavy chain. Through trial and error, we discovered that the nonspecific dimerization did not occur if heterobifunctional cross-linking preceded Alexa-labeling of the MHC monomers. Despite the unexpected side reactions, we observed that the hydrazide moiety found on MHPH would preferentially react with the aldehyde of the MTFB cross-linker.

To control for non-specific dimerization, we utilized “control” MHC heterodimers which consist of a cognate peptide-MHC monomer paired with a null peptide-MHC monomer. In the scenario where self-dimerization should occur, a “homo”-dimer consisting of two MHPH-modified monomers or MTFB-modified monomers might be generated, which would appear as a single peak ~90 kDa on a gel filtration profile. While mass spectroscopy experiments clearly indicated the presence of both peptides in the bi-specific MHC heterodimer (Figure II.6), the precise amount of either peptide was unknown. For example, within a single MHC heterodimer preparation, there could be some heterodimers formed by heterobifunctional cross-linking and some undesirable “homo”-dimers formed by nonspecific dimerization. Freshly prepared recombinant MHC molecules have been found to release peptide, which can be re-presented by cell surface bound MHC molecules (Schott, Bertho et al. 2002). A concern that pertains to

MHC heterodimers is that peptide from recombinant MHC complexes might be transferred between component MHC monomers within an MHC heterodimer and form undesired MHC “homo” dimers. However, because staining is not observed from the “control” MHC heterodimers, we assume that peptide transfer is not an issue, perhaps due to the unstable nature of recombinant MHC Class I complexes, which dissociate in the absence of peptide (Garboczi, Hung et al. 1992). In summary, the “control” MHC heterodimers served an important role in determining if any nonspecific “homo”-dimerization was occurring.

While the MHPH-MTFB cross-linking reaction is readily reproducible, the efficiency of this reaction was found to vary amongst different batches of either cross-linker. The reduced cross-linking efficiency jeopardizes the final yield of labeled MHC heterodimer, which complicates the use of the MHPH-MTFB cross-linking pair. Ideally, a more efficient and bio-orthogonal reaction is more desirable. A potential candidate is the alkyne-azide cross-linking pair, better known as a “click” reaction. Recent studies have indicated that the “click” reaction is unprecedented in terms of specificity and bio-orthogonality. The rapid reaction rate combined with the absence of water hydrolysis greatly enhances the efficiency of the heterobifunctional cross-linking (Best 2009). Recently, iodoacetamide azide and iodoacetamide alkyne, two “click” cross-linkers became available commercially (Invitrogen), which can be readily conjugated onto MHC class I complexes through a free thiol at the C-terminus of the MHC class I heavy chain.

In addition to the adaptation towards the “click” cross-linker reagents, which are currently underway, other systems of T cell cross-reactivity need to be evaluated. For

example, humans infected with EBV-associated mononucleosis have T cells which cross-react with influenza A virus (Clute, Watkin et al. 2005). Additionally, T cells cross-reactive between hepatitis C virus and influenza A virus have been found to influence the severity of HCV-induced liver pathology (Urbani, Amadei et al. 2005). The adaptation of the bi-specific MHC heterodimer in these systems may help to better clarify the precise role of cross-reactive T cells. A feasible experiment could be to use the MHC heterodimer to deplete cross-reactive T cells, in order to evaluate the effect of depletion on the immune response. Similar work with the depletion of regulatory T cells has been done previously (Dietze, Zelinsky et al. 2011). Overall, the precise function of cross-reactive T cells has been challenging to address, which is mostly attributed to the absence of viable reagents.

IV.B. Generating T cell cross-reactivity

For a conventional immune response, where T cells recognize foreign peptides presented by self-MHC molecules, there are three parameters that a useful T cell repertoire must fulfill in order to maximize reactivity towards foreign antigens. An effective T cell repertoire must be able to recognize and respond towards a large variety of different peptide-MHC antigens so that pathogenic antigens will not go undetected; an effective T cell repertoire must be specifically geared towards foreign antigens; and the frequency of T cells reacting towards a foreign antigen must be sufficiently large in order to mount a rapid response (Wilson, Wilson et al. 2004). In order to meet these criteria for an effective T cell repertoire, mathematical calculations estimate that a single T cell

should cross-react towards as many as 10^6 different peptide-MHC ligands (Mason 1998). It has been shown that only three to four different peptide residues are positioned to serve as TCR contact residues (Bjorkman, Saper et al. 1987; Fremont, Matsumura et al. 1992; Stern, Brown et al. 1994; Wilson, Wilson et al. 2004), which implies that any peptide containing these three to four residues might be cross-reactive. Of the total possible nonamer peptides consisting of the 20 natural amino acids (20^9), upwards of 10^6 different peptides might contain such a sequence, which is in agreement with the mathematical estimates (Wilson, Wilson et al. 2004).

The dynamics and the energetics of ligand-receptor interactions for T cells could further explain why T cell recognition is promiscuous. The half life of TCR-MHC interactions are thought to be dictated by the off-rate, which has been reported to be largely dependent on TCR contact with the MHC alpha helices, without regard for the bound peptide (Wu, Tuot et al. 2002). Furthermore, during selection, it has been found that an effective, but incomplete T cell repertoire can result from positive selection using a single thymic peptide (Ignatowicz, Kappler et al. 1996). The resulting T cell repertoire is cross-reactive towards peptides that are unrelated in sequence to the single thymic peptide initially used during positive selection (Ignatowicz, Rees et al. 1997).

On the structural level, it has been found that the overall peptide-MHC composite surface recognized by TCR encompasses almost 2500 square angstroms (Garcia 1999; Garcia, Teyton et al. 1999). However, peptide-specific interactions comprise only 25% of this overall composite surface, whereas MHC-specific interactions comprise 75% (Garcia, Teyton et al. 1999). Therefore, it's likely that similar or perhaps even different

MHC alleles could adopt similar structures which might lead to promiscuous T cell recognition.

In contrast to conventional T cell responses, there exist large subsets of T cells which recognize peptides in complex with MHC alleles that were not encountered during thymic development. This mode of T cell recognition is commonly referred to as alloreactivity and is a clinical problem known as transplant rejection and graft versus host disease (Felix and Allen 2007). Alloreactive T cells are found in 100-fold to 1,000-fold higher precursor frequencies as compared to the frequency of T cells specific for foreign antigens presented by self-MHC alleles (Suchin, Langmuir et al. 2001).

While it may have been initially a surprise that alloreactive T cells are found in such high numbers, there is no process which selects against T cells from responding towards the hundreds of different MHC alleles that are not expressed by a given host. Furthermore, because 75% of the composite peptide-MHC surface recognized by TCR is based on interactions with MHC (Garcia, Teyton et al. 1999), structural similarities between different MHC molecules may lead to alloreactive T cell responses. For example, it has been found that the specificity of alloreactive T cells is linked to polymorphisms in the MHC alpha helices which contact TCRs (Lombardi, Barber et al. 1991).

IV.C. Cross-reactive T cell responses toward LCMV-GP₃₄₋₄₁ and VV-A11R₁₉₈₋₂₀₅

The results in chapter III describe the molecular mechanism for the protective cross-reactive CD8⁺ T cell response between LCMV-GP34 and VV-A11R. MHC

tetramer cross-competition experiments clearly indicate that the cross-reactive T cell response between LCMV-GP34 and VV-A11R is mediated by individually cross-reactive TCRs, capable of recognizing both ligands simultaneously (Figure III.1). To address the mechanism for cross-reactive TCR engagement, the recognition determinants for LCMV-GP34 and VV-A11R were compared by generating single site mutations in both epitopes, at the predicted TCR-contact residues. The mutated peptides were tested in functional assays, which showed that the recognition determinants for LCMV-GP34 and VV-A11R differ both in the context of an acute LCMV infection (Figure III.5) and in GP34-A11R cross-reactive T cell lines (Figure III.6). The cognate response towards LCMV-GP34 was found to require both the P4 and P7 residues, while the cross-reactive T cell response towards VV-A11R largely required the P4N residue. These results provide evidence that the shared P4N mediates the LCMV-cross-reactive T cell response towards VV-A11R.

Given the sequence disparity between LCMV-GP34 and VV-A11R epitopes, which differ at 5 out of the 8 positions, structural mimicry was an unexpected explanation for the cross-reactive response. However, analysis of the crystal structures of K^b-LCMV-GP34 and K^b-VV-A11R revealed that the two complexes are structural mimics. The residues which are most exposed in both structures were found at the P4 and the P7 residues. Not coincidentally, the P4N residue is identically placed in both structures with respect to MHC, such that the P4N from both structures can be overlaid on top of one another (Figure III.7). Interestingly, the OVA peptide also contains a P4N (SIINFEKL), but cross-reactive T cell responses have never been observed towards OVA. Other peptides sharing the P4N or the P7 residue from LCMV and VV were also tested and

found to be non-reactive in our system, suggesting that the cross-reactive T cell response between LCMV-GP34 and VV-A11R contains a unique recognition pattern that is not dependent on residues from the MHC molecule (Table III.4).

Overlay of both K^b-LCMV-GP34 and K^b-VV-A11R structures with the previously reported K^b-OVA structure (Figure III.7) indicates that the P4N in OVA adopts a different rotamer as compared to our K^b-LCMV-GP34 and K^b-VV-A11R structures. Additionally, the overlay highlighted major structural differences at the P6 and P7 residues, such that the OVA peptide contains a large glutamate residue followed by a lysine residue at P6 and P7, respectively. In regard to cross-reactive TCR recognition, incorporation of a lysine at the P7 residue abrogated cross-reactive T cell responses (Figure III.5), which suggests that the bulky glutamate and lysine residues in OVA might inhibit binding of cross-reactive TCR.

Interestingly, substitution of the P6 and P7 residues from LCMV-GP34 (AVYNFATM) into a hybrid version of the OVA peptide (SIINFATL) generated cross-reactive T cell responses in the context of a primary LCMV infection as well as in GP34-A11R cross-reactive T cell lines. The formation of cross-reactive T cell responses towards this hybrid OVA peptide suggests that the OVA peptide might share structural aspects necessary for cross-reactive TCR recognition. Whether the P6 and P7 residues in the null OVA peptide inhibit LCMV-VV cross-reactive T cell responses towards the P4N or the P6 and P7 residues from LCMV-GP34 can sufficiently mediate LCMV-VV cross-reactive T cell responses needs to be further examined. Taken together, our results

highlight that shared structural features from two disparate peptide-MHC ligands from unrelated viruses can mediate heterologous immunity.

The mode(s) by which a cross-reactive TCR can engage LCMV-GP34 and VV-A11R is only speculative in the absence of the peptide-MHC-TCR co-crystal structures. Needless to say, the co-crystal structures of K^b-LCMV-GP34 and K^b-VV-A11R in complex with cross-reactive TCR is required and currently being pursued. Nevertheless, our data clearly indicates that the P1, P6 and P7 residue requirements differ for TCR recognition of LCMV-GP34 and VV-A11R (Figure III.5), which reveals the manner by which cross-reactive TCRs might engage these ligands.

If a co-crystal structure of cross-reactive TCR in complex with either K^b-LCMV-GP34 or K^b-VV-A11R were available, I would expect two different possibilities for cross-reactive TCR engagement. Cross-reactive TCR may bind the K^b-LCMV-GP34 and K^b-VV-A11R complexes using the same overall docking strategy as seen for conventional “diagonal” TCR engagement of peptide-MHC ligands (Garboczi, Ghosh et al. 1996; Garcia, Degano et al. 1996) or using two completely different binding modes, such that the TCR might be globally repositioned to engage one ligand as compared to the other.

In the case where cross-reactive TCRs bind using the same overall docking strategy, cross-reactive TCR binding to LCMV-GP34 and VV-A11R may depend on the P4N and the P7T residues for recognition of LCMV-GP34 or the P4N and P1A residues for recognition of VV-A11R, with other peptide residues making less pronounced interactions contributing to TCR engagement. In other words, specific interactions are

likely to occur at the residues, which have been found to be important TCR contacts, with other residues contributing minimally. Alternatively, if cross-reactive TCRs utilize different binding modes for engaging K^b-LCMV-GP34 and K^b-VV-A11R, I would expect a repositioning of TCR in a manner that still allows TCR contact with the conserved P4N residue in both LCMV-GP34 and VV-A11R. Cross-reactive TCRs might be seated over the p4N and the C-terminus of the LCMV-GP34 peptide, which correlates with the requirement of the P7T residue in recognition of LCMV-GP34 (Figure III.5). For VV-A11R, cross-reactive TCR might be seated over the N-terminus of VV-A11R in a manner that would contact the required P4N residue as well as the P1A residue, corresponding to the requirement of these residues for VV-A11R recognition (Figure III.5).

In regard to isolating the cross-reactive TCR gene sequences, TCR V β repertoire analysis was performed on both TCL #1-A11R (Figure III.4) and TCL #1-GP34 (data not shown). The results revealed that selecting for the LCMV-GP34 cross-reactive T cell population within the largely VV-A11R-reactive TCL enriched for the TCR V β 8.1 8.2+ population (data not shown). The increase in LCMV-GP34 cross-reactivity following stimulation with LCMV-GP34 peptide correlated with an increase in the TCR V β 8.1 8.2+ population (~80%) (data not shown). It might be possible to isolate the TCR gene sequences from frozen vials of these GP34-A11R cross-reactive T cells (TCL #1-GP34), which could be clonal due to protracted expansion time *in vitro* (expresses >80% TCR V β 8.1 8.2). An alternate approach to isolate the cross-reactive TCR is to expand GP34-A11R cross-reactive T cells from either “newer” GP34-A11R cross-reactive T cell lines

or perhaps directly from LCMV-immune mice (~1% cross-reactive towards VV-A11R, Figure III.1A) and utilize single cell cloning by serial dilution. Previous serial dilution attempts using cross-reactive T cells (from GP34-A11R cross-reactive TCLs) in the presence of peptide-pulsed B6 splenocytes as stimulators were unsuccessful, but recent attempts using RMA-S cells as stimulators showed more promise.

In summary, the function(s) of cross-reactive T cells may be difficult to establish *in vivo*. Hopefully, these issues will be addressed by selective depletion of cross-reactive T cell populations using bi-specific MHC heterodimers. An intriguing approach to evaluating the role of cross-reactive T cells *in vivo* is through exclusion of the heterologous epitopes from viruses, which might inhibit cross-reactive T cell responses (Welsh and Fujinami 2007). In the case of GP34-A11R cross-reactivity, exclusion of important contact residues (P4N) necessary for only cross-reactive T cell responses might be a better approach as cognate-epitope responses could be maintained. The exclusion of these epitopes from vaccines has been suggested to avoid potential immunopathology generated by the elicited heterologous immune responses (Selin, Varga et al. 1998; Welsh and Fujinami 2007).

IV.E. Immunopathology

It has been known for almost 60 years that humans vaccinated against influenza produce antibodies against the immunizing virus, but in addition, produce antibodies of higher titer against a different strain of influenza, that was first encountered during childhood. This phenomenon was named original antigenic sin because the immune

response is dominated by cross-reactive memory cells generated by the primary infection and are re-activated in the presence of the challenging pathogen (Fazekas de St and Webster 1966). Original antigenic sin does not discriminate between beneficial versus detrimental immune responses.

Despite the focus of this thesis being centered on protective immunity, immunopathology is also an important consequence, which has been documented in a variety of different human and mouse systems (Chen, Fraire et al. 2001; Urbani, Amadei et al. 2005; Rothman 2009). Immunopathology is thought to be promoted by expansion of low affinity, cross-reactive T cells, which have greater affinity for the cross-reactive antigen as compared to the infectious antigen, leading to poor pathogen clearance (Mongkolsapaya, Dejnirattisai et al. 2003). The expansion of these cross-reactive T cells can lead to cytokine release and immune-mediated tissue damage, which has been shown to occur via activation-induced cell death of CD4⁺ and CD8⁺ T cells (Aichele, Brduscha-Riem et al. 1997). In the case of subsequent dengue infections, where high antigenic load occurs, high-affinity T cells are thought to be preferentially driven into apoptosis, which could help to promote immunopathology by expanding the frequency of cross-reactive T cells with lower affinity for the infecting pathogen (Mongkolsapaya, Dejnirattisai et al. 2003).

Alternatively, failure to mount cytotoxic T cell responses by memory T cells towards infected target cells might be due to a shift in cytokine production (Rothman 2009). In the case of dengue, stimulation of memory T cells with heterologous dengue virus serotypes promotes greater relative production of a pro-inflammatory cytokine

TNF α , as compared to a potential antiviral cytokine IFN γ (Rothman 2009). The shift in cytokine production from antiviral cytokine IFN γ , towards pro-inflammatory cytokine TNF α , has been found to hamper the ability of low affinity T cells to effectively clear virus (Von Herrath, Coon et al. 1997), which might further promote immunopathology for the reasons described earlier. Taken together, these points illustrate how cross-reactive memory T cells can promote immunopathology and be detrimental to the host.

IV.F. Contribution of the CD8 co-receptor

Compelling evidence has been found for the roles of the CD8 co-receptor, which includes the stabilization of the MHC-TCR complex (Garcia, Scott et al. 1996; Daniels and Jameson 2000; Wooldridge, van den Berg et al. 2005) and initiation of signaling cascades by the protein tyrosine kinase Lck during subsequent cell signaling (O'Rourke and Mescher 1993). While numerous studies in human and mouse systems have been conducted to address the precise role of CD8 in T cell recognition, it still remains unclear.

Whether CD8 is required or not during T cell recognition has remained a controversial issue. T cells have been observed to engage high affinity peptide-MHC ligands in the absence of CD8 co-engagement (Kerry, Buslepp et al. 2003), which suggests that CD8 only serves to fine tune T cell recognition. Meanwhile, other studies showed that CD8 co-engagement is required for T cell recognition (Delon, Gregoire et al. 1998; Daniels and Jameson 2000; Dutoit, Guillaume et al. 2003; Gakamsky, Luescher et al. 2005).

In addition, if CD8 co-engagement is required for T cell recognition, some have argued over the precise timing for CD8 co-engagement of MHC-TCR complexes. It is commonly believed that CD8 co-engagement recruits the protein tyrosine kinase Lck into the immunological synapse, which initiates downstream T cell activation pathways (Janeway 2001). However, a recent report has shown that the association of the CD8 co-receptor to the MHC-TCR complex occurs after initial TCR engagement and T cell triggering (Jiang, Huang et al. 2011). Contrary to the norm, it was indicated in this study that the protein tyrosine kinase Lck recruits CD8 to the same peptide-MHC molecule, engaged by TCR.

Despite the conflicting results surrounding the precise role or timing of CD8 co-engagement, our observation that control peptide-MHC heterodimers (cognate peptide-MHC monomer cross-linked to a noncognate peptide-MHC monomer) are not capable of binding to cross-reactive TCRs clearly indicates that the minimal requirements for dimeric TCR engagement is two CD8 co-receptor interactions combined with the two cognate peptide-MHC and TCR interactions (Figure II.9B).

Recent work on thymocytes, using unlabeled peptide-MHC heterodimers, demonstrated that positive selection requires T cell interaction with two cognate peptide-MHC complexes (Juang, Ebert et al. 2010). Meanwhile, this same study revealed that negative selection proceeds with a self peptide-MHC molecule linked to a cognate peptide-MHC molecule (Juang, Ebert et al. 2010). Given the differential ligand requirements for selection, it could be interesting to evaluate the precise number of CD8 contacts required during selection or other processes such as reactivation of memory T

cells, which was found to require CD8 for only certain effector functions (Kerry, Maile et al. 2005).

To address the requirements for CD8 co-engagement during immunological processes such as selection, a bi-specific MHC heterodimer could be assembled such that one peptide-MHC monomer, containing an intact CD8 binding site, could be cross-linked to another peptide-MHC monomer, containing a mutated CD8 binding site to either enhance or inhibit CD8 co-engagement (Wooldridge, van den Berg et al. 2005).

Enhancing the CD8 co-engagement might increase the overall avidity of the CD8-MHC-TCR interaction. During selection, increasing the overall avidity of the MHC-TCR-CD8 interaction of a developing T cell might promote apoptosis (Chidgey and Boyd 1997).

Decreased CD8 binding on more mature T cells has been observed using MHC tetramers (Daniels, Devine et al. 2001). However, a clear link between glycosylation and CD8 co-engagement is unclear using MHC tetramers, where glycosylation could also affect TCR clustering (Demetriou, Granovsky et al. 2001). The results in Chapter V.C (in appendices) highlights that glycosylation modulates the ability of naïve T cells to bind to MHC monomers, likely through altering CD8 co-engagement. The reduced CD8 co-engagement on naïve CD8⁺ T cells in the presence of glycan adducts provides a mechanistic explanation for how glycosylation affects T cell engagement of peptide-MHC ligands and highlights that glycosylation provides an additional level of control over T cell recognition.

In addressing the role of CD8, I found that the widely used mutation of the conserved CD8 binding site (D227K) on the MHC class I $\alpha 3$ domain, compromises the

integrity of the MHC class I complex (Figure V.C.2B). If the D227K mutation compromises the stability of all MHC class I alleles, those studies need to be re-evaluated. In the future, a different or stable K^b complex containing a mutated CD8 binding site needs to be generated to further evaluate the role of CD8 co-engagement. Our monomer binding assay using WT and CD8-null MHC monomers could be then repeated using the same desialylation and resialylation protocols to specifically address whether T cell engagement altered by glycosylation pattern changes can be attributed to glycan moieties on CD8.

Chapter V. Appendix

V.A. Protocols used in this Thesis

V.A.1	Agarose Gel Electrophoresis	137
V.A.2	Biotinylation Yield Test for MHC Class I Complexes	139
V.A.3	Bradford Assay	140
V.A.4	Buffer Exchange of Refolded Peptide-MHC Class I Complexes	142
V.A.5	Counting Tissue Culture Cells	145
V.A.6	DNA Sequencing	146
V.A.7	Freezing T Cell Lines	147
V.A.8	Generation and Maintenance of Antigen-Specific T Cell Lines	148
V.A.9	Growing BL21 Expressing MHC Class I Proteins in a 10L Fermentor	150
V.A.10	HQ on the Biocad Sprint HPLC	152
V.A.11	Inclusion Body Preparation for MHC Class I Subunits	154
V.A.12	Intracellular Cytokine Staining	156
V.A.13	MHC Class I Heterogeneous Cross-linking using MHPH and MTFB	157
V.A.14	Modifying Free Cysteines on Proteins using Maleimides	158
V.A.15	Modifying Primary Amines on Proteins using N-hydroxysuccinimide (NHS) Esters	159
V.A.16	Pouring LB-Amp Plates	160
V.A.17	Preparing MHC Class I Tetramers	161
V.A.18	Refolding of MHC Class I Complexes	162
V.A.19	SDS-PAGE	163
V.A.20	Single Cell Suspensions from Mouse Organs	165
V.A.21	Site Directed Mutagenesis	166
V.A.22	Staining CD8+ T cells with MHC Class I Tetramers	167
V.A.23	Stock Solutions	168
V.A.24	Transforming Competent Bacteria	169

V.A.1. AGAROSE GEL ELECTROPHORESIS

Protocol modified from Jennifer Stone

Procedure:

1. Prepare 100 ml of a 1% agarose solution. (Measure 1 g agarose into a glass beaker or flask and add 100 ml 1X TBE or TAE.)
2. Microwave or stir on a hot plate until agarose is dissolved and solution is clear. Note: the solution may boil rapidly after microwaving, so be careful handling it.
3. Allow solution to cool to about 55°C before pouring. (Ethidium bromide can be added at this point to a concentration of 0.5 µg/ml.)
4. Prepare clean gel tray by sealing ends with tape or other custom-made dam.
5. Place comb in gel tray about 1 inch from one end of the tray and position the comb vertically such that the teeth are about 1-2 mm above the surface of the tray.
6. Pour 50°C gel solution into tray to a depth of about 5 mm. Allow gel to solidify about 20 minutes at room temperature. Excess agarose can be stored at room temperature and re-melted in a microwave.
7. To run, gently remove the comb, place tray in electrophoresis chamber, and cover (just until wells are submerged) with electrophoresis buffer (the same buffer used to prepare the agarose).
8. To prepare samples for electrophoresis, add 1 µl of 6x gel loading dye for every 5 µl of DNA solution. Mix well. Load 5-12 µl of DNA per well (for minigel).
9. Electrophorese at 50-150 volts until dye markers have migrated an appropriate distance, depending on the size of DNA to be visualized.
10. If the gel was not stained with ethidium during the run, stain the gel in 0.5 µg/ml ethidium bromide until the DNA has taken up the dye and is visible under short-wave UV light, if the DNA will not be used further, or with a hand-held long-wave light if the DNA is to be cloned.

Materials:**Agarose Gel Solution**

Agarose in TBE or TAE (1%)
1x TBE or TAE Buffer

50x TAE Buffer

242 g Tris Base
57.1 g Glacial Acetic Acid
100 mL 0.5M EDTA, pH 8
Fill to 1L with ddH₂O

6x Gel Loading Buffer

0.25% Bromophenol Blue
0.25% Xylene Cyanol FF
33% Glycerol
18% 50x TAE Buffer
49% ddH₂O

Gel loading dye

10 mg/ml Ethidium Bromide

10x TBE

108 g Tris Base
55 g Boric Acid
40 mL 0.5 M EDTA, pH 8

V.A.2.BIOTINYLATION YIELD TEST FOR MHC CLASS I COMPLEXES

Protocol modified from Jennifer Stone

Procedure:

1. Set up reducing SDS-PAGE using a 12% polyacrylamide gel.
2. Assemble the following samples in reducing SDS loading buffer and boil your samples. Make sure to add enough reducing SDS loading buffer to account for the addition of streptavidin or PBS in step 3. Samples b-d should be brought to the same final volume.
 - a. Protein MW standards
 - b. 2 μ g Biotinylated MHC class I + PBS or other buffer
 - c. 2 μ g Biotinylated MHC class I + 2 μ g Streptavidin
 - d. 2 μ g Streptavidin
3. Cool all boiled samples to at least room temperature. Then add an excess of streptavidin (2 μ g) to the samples and an equivalent volume of PBS or similar buffer to the unbiotinylated monomer sample. Allow all samples to sit at least 10-15 minutes to allow for the streptavidin-biotin interaction to occur.
4. Run samples on gel (140V for 1 hour), then stain with coomassie. I usually rinse the gel after coomassie staining with deionized water and then add the destain.
 - a. Note, when destaining, tie two kimwipes (single knot) and immerse in the destaining solution. The kimwipes will bind up the coomassie.
5. The band corresponding to the biotinylated heavy chain of your MHC class I should disappear in sample C, and larger bands will appear indicating the presence of streptavidin-MHC oligomers.
6. The yield of biotinylation can be determined by determining the fraction of MHC class I heavy chain remaining after streptavidin was added.
7. Sample of biotinylated yield test for an MHC class I complex can be found in Figure II.3

V.A.3. BRADFORD ASSAY

Protocol modified from Jennifer Stone

Materials:

Dye stock: Coomassie Blue G (Cat# 42655) (100 mg) is dissolved in 50 mL of methanol. (If turbid, the solution is treated with Norit (100 mg) and filtered through a glass-fiber filter.) The solution is added to 100 mL of 85% H₃PO₄, and diluted to 200 mL with water. The solution should be dark red. The final reagent concentrations are 0.5 mg/mL Coomassie Blue G, 25% methanol, and 42.5% H₃PO₄. The solution is stable indefinitely in a dark bottle at 4°C.

Assay reagent: The assay reagent is prepared by diluting 1 volume of the dye stock with 4 volumes of distilled H₂O. The solution should appear brown, and have a pH of 1.1. It is stable for weeks in a dark bottle at 4°C.

Protein Standards: Protein standards should be prepared in the same buffer as the samples to be assayed. A convenient standard curve can be made using bovine serum albumin (BSA) with concentrations of 0, 250, 500, 1000, 1500, 2000 µg/mL for the standard assay, and 0, 10, 20, 30, 40, 50 µg/mL for the microassay.

Standard Protein Assay Procedure (For 200 - 2000 µg/mL protein):

1. Prepare six standard solutions (1 mL each) containing 0, 250, 500, 1000, 1500 and 2000 µg/mL BSA.
2. Set the spectrophotometer to collect the spectra over a wavelength range from 400 to 700 nm and over an absorbance range of 0 to 2 Absorbance units, and overlay the collected spectra.
 - a. Use a 4 mL plastic cuvette filled with distilled water to blank the spectrophotometer over this wavelength range.
 - b. Empty the plastic cuvette into a test tube and shake out any remaining liquid. Then add 2.0 mL Assay reagent and 0.04 mL of protein standard solution, starting with the lowest protein concentration and working up, or one of the samples to be assayed.
3. Cover with Parafilm and gently invert several times to mix.
4. Record the absorbance spectrum of the sample from 400 to 700 nm, and note the absorbance at 595 nm.
5. Repeat the steps above for each of the protein standards and for the samples to be assayed.
6. Examine the spectra of the standards and samples. If any spectrum has an absorbance at 595 nm greater than 2, or if any sample has an absorbance greater than the greatest absorbance for any of the standards, dilute the sample by a known amount and repeat the assay.

7. At one wavelength, approximately 575 nm, all of the spectra should have the same absorbance. (Such an intersection is called an isosbestic point and is a defining characteristic of solutions containing the same total concentration of an absorbing species with two possible forms. If any spectrum does not intersect the other spectra at or near the isosbestic point, it should be adjusted or rejected and repeated.
8. Prepare a graph of Absorbance at 595 nm vs [Protein] for the protein standards.
9. Examine the graphed points and decide if any should be rejected.
 - a. Often a single point can be rejected without invalidating the standard curve, but if more than one point appears questionable the assay should be repeated.
 - b. The Bradford assay gives a hyperbolic plot for absorbance versus protein concentration, but within a range of relatively low protein concentrations, the hyperbolic curve can be approximated reasonably well by a straight line.
10. To determine the protein concentration of a sample from its absorbance, use the standard curve to find the concentration of standard that would have the same absorbance as the sample.

Microassay Procedure (For <50 $\mu\text{g}/\text{mL}$ protein):

1. Prepare five standard solutions (1 mL each) containing 0, 10, 20, 30, 40 and 50 $\mu\text{g}/\text{mL}$ BSA
2. To a 1.4 mL plastic cuvette, add
 - a. 0.2 mL Dye stock
 - b. 0.8 mL of one of the protein standard solutions or samples to be assayed (containing <100 μg of protein for <50 $\mu\text{g}/\text{mL}$ standards)
3. Cover with Parafilm and gently invert several times to mix.
4. Follow the procedure described above for the standard assay procedure.

V.A.4. BUFFER EXCHANGE OF REFOLDED PEPTIDE-MHC CLASS I COMPLEXES

Protocol developed with Keith Daniels

Materials:

6L of 20 mM Tris, pH 8.0
2L 1M NaOH
20L distilled water

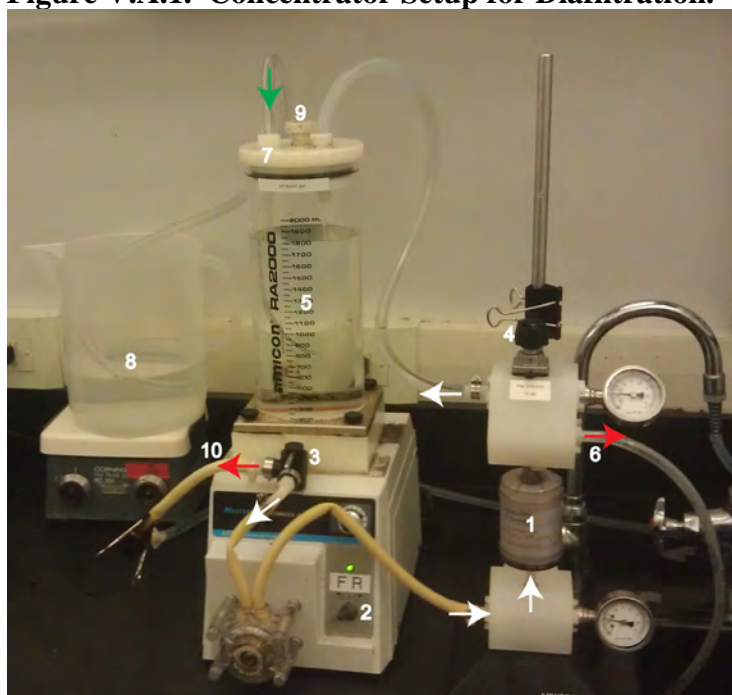
Procedure:

1. Prior to HQ chromatography, you need to get rid of excess arginine. Typically, we buffer exchange out the refolding mixture into Buffer A (20 mM Tris pH 8.0) for HQ chromatography.
2. Basic operations of the concentrator:
 - a. FLOW SWITCH – controls whether the pump is in FORWARD or REVERSE.
 - b. FLOW DIRECTION – controls whether the contents from the RESERVOIR are recirculated and pumped into the filter OR pumped through the COLLECTION line which is used for recovery or waste.
 - c. PRESSURE KNOB – controls how much pressure is generated, which determines how much “flow through” is forced through the 10k MWCO cartridge, which retains your protein on the membrane. Pressure can be adjusted by turning clockwise for more pressure and counterclockwise for less pressure. Try to keep the pressure under 10 PSI as indicated on the lower pressure gauge.
3. Set up your CARTRIDGE in the concentrator. We use the Prep/ScaleTM-TFF 1ft² cartridge (PLGC 10k regenerated cellulose, Millipore CDUF001LG).
4. As a general rule, before and after concentrating, clean the CARTRIDGE (and the system) by recirculating 1L 1M NaOH for 30 minutes or more without any pressure. Set the FLOW SWITCH to FORWARD and make sure the FLOW DIRECTION is for recirculating.
5. After cleaning, rinse the concentrator out thoroughly with at least 2L of distilled water (repeat a few times) under 10 PSI pressure (bottom pressure gauge). In a pinch, you can simply rinse and discard 3-4 times. Just make sure to pH the liquid that exits through the OUTLET to ensure that excess NaOH has been flushed out of the system.
6. For buffer exchange, I prefer to use diafiltration, which is a convenient “hands-free” technique. Seven diafiltration volumes will remove 99.9% of salt. (i.e. 300 mL of MHC class I refolding and 2100 mL of buffer A)
7. Filter your refolding mixture through a 0.2 μM filter and pour contents into the RESERVOIR. Set the FLOW SWITCH to FORWARD and make sure the

FLOW DIRECTION is set to recirculation. Pressurize the system to 10 psi (bottom pressure gauge) by turning the PRESSURE KNOB clockwise.

8. For diafiltration, you need to set up a closed system on the concentrator, meaning the same volume of liquid leaving the system through the OUTLET will need to be replaced by new buffer entering the RESERVOIR, via tubing through the INLET at the top of the RESERVOIR (see picture below).
 - a. Prepare 3L of 20 mM Tris pH 8.0 for the BUFFER RESERVOIR.
 - b. The tubing needed to run this “closed system” is 0.25 inch I.D., 0.5 inch O.D., 0.125 inch wall PVC tubing. (Fisher Scientific 14-169-7E).
9. Concentrate your protein in the RESERVOIR to about 300 mL so that you can set up diafiltration with 3L (10x diafiltration volumes). Thread in the tubing from your BUFFER RESERVOIR into the INLET at the top of the RESERVOIR and close off the system by turning the TOP KNOB clockwise to open the O-ring which makes a seal inside of the RESERVOIR.
10. Wait until the liquid from the BUFFER RESERVOIR is being drawn into the RESERVOIR via the INLET tube at an approximate rate at which liquid exits the RESERVOIR through the OUTLET before walking away.
11. Allow all of the 3L of the BUFFER RESERVOIR to circulate through the system (~1.5L/hour at 10 psi).
12. To recover the concentrated protein, pump contents off of the membrane and back into the RESERVOIR by pumping in REVERSE. Change the FLOW DIRECTION from recirculating into the RESERVOIR to the COLLECTION line to recover final product. I typically collect my protein right into 0.2 μ M filter and filter the refolding in preparation for HQ chromatography.
13. After you are done, clean out the concentrator as described earlier using 1M NaOH, followed by rinses with water and remove your CARTRIDGE.

Figure V.A.1. Concentrator Setup for Diafiltration.



- 1-CARTRIDGE
- 2-FLOW SWITCH
- 3-FLOW DIRECTION
- 4-PRESSURE KNOB
- 5-RESERVOIR
- 6-OUTLET
- 7-INLET
- 8-BUFFER RESERVOIR
- 9-TOP KNOB
- 10-COLLECTION LINE

V.A.5. COUNTING TISSUE CULTURE CELLS

Protocol from Jennifer Stone

Count cells touching top or left line

Do NOT count cells touching right or bottom line

Volume = 0.1 μ L

**Dilute cells 1:2 with trypan blue, e.g. add 10 μ L cell suspension to 10 μ L trypan blue.

**Add mixture to hemacytometer under the coverslip (takes about 10 μ L)

**Count cells in 2 squares the size of the red outlined portion—add numbers together

**Multiply result by 10^4 to get # cells/mL

EXAMPLE:
 square 1: 31 cells
 square 2: 34 cells
 TOTAL= 65 cells in 0.1 mL
 Density= 0.65×10^6 cells/mL

Note: Make sure you have enough cells in each of the squares (typically 20-40 cells/red square). I usually count four squares and take the average to get better counts.

V.A.6. DNA SEQUENCING

Protocol modified from Walter Kim

Note: Before Genewiz offered their DNA sequencing services, we used to run our own PCR reactions and dye cleanup.

Reaction procedure:

1. Do forward and reverse sequencing reactions separately
2. For the reaction mixture
 - a. Add 4 μL ultrapure water
 - b. Add 2 μL plasmid DNA (stock [] from mini prep)
 - c. Add 2 μL of primer
 - i. 10 μM primer concentration, stock [100 μM]
 - d. Add 2 μL BigDye V3.0 or V3.1
3. On PCR machine, run SEQ program
 - a. Runs for 4-6 hours
4. Add 1 μL 2% SDS to each reaction and incubate for 5 minutes at 95 degrees (plate method)

DyeEx cleanup Procedure:

1. Vortex DyeEx column gently
2. Twist $\frac{1}{4}$ turn and snap off bottom and place spin column in 2 mL collection column for 3 minutes @ 3000 rpm
 - a. Remove foil from both sides of plate, spin for 3 minutes at 750-1000xg
3. Snap off bottom of column and spin for 3 minutes @ 3000 rpm
4. Transfer column to centrifuge tube
5. Add 10 μL of DNA mixture directly to gel (slanted) without touching sides of tube
6. Spin column in centrifuge tube for 3 minutes @ 3000 rpm
 - a. Transfer contents to microcentrifuge tube and use a speed vac to evaporate liquid
7. Bring to CFAR facility for sequencing

V.A.7. FREEZING T CELL LINES

Protocol modified from Keith Daniels and Michael Brehm

Materials:

Freezing Media:

90% Fetal Calf Serum

10% Dimethyl Sulfoxide

Procedure:

1. Critical note: before freezing down your antigen-specific T cell lines, realize that the specificity may be different upon thawing.
2. Prepare fresh freezing media as specified above.
3. Spin cells down at 1500 x g for 5 minutes and aspirate the supernatant.
4. Suspend cells to 1e7 cells/ml in freezing media.
5. Aliquot into cryovials kept on ice (~1 ml/vial).
6. Place in Nalgene Cryo 1°C Freezing Container (Cat# 5100-0001) and make sure there's alcohol in the freezing container to allow for a -1°C/minute decrease in temperature. Store in -80°C freezer overnight.
7. Move into liquid nitrogen cell dewar within 24 hours.

V.A.8. GENERATION AND MAINTENANCE OF ANTIGEN-SPECIFIC T CELL LINES

Protocol modified from Michael Brehm

Materials:

- RMA cells (Roche virus transformed lymphocyte derived from B6 mice), expressing K^bD^b
- T cell media
 - RPMI, 10% FCS, 1% P/S, 5 mL HEPES, 5 mL L-Glut, 5 mL nonessential amino acids, 5 mL sodium pyruvate, 2.5 mL 0.01M BME
 - All purchased from Invitrogen (except BME)
- RP10
 - RPMI, 10% FCS, 1% P/S, 5 mL HEPES, 5 mL L-Glut
- 1 uM peptide (VV-A11R₁₉₈₋₂₀₅, LCMV-GP₃₄₋₄₁)
- Filtered tips to prevent cross contamination of peptide
- 0.8% Sterile Ammonium Chloride or Sigma RBC lysis buffer (Cat #R7757)
- 12 well plates (4 mL well volume ideal)
- BD T-Cell Culture Supplement without conA (IL-2 culture supplement), rat (BD Cat# 354115)

Procedure:

1. Spin down RMA cells for 5 minutes 1200 rpm and resuspend in T cell media to 10 million cells/mL
2. Pulse cells with peptide by adding 5 uL (200 ug/mL stock) peptide for every 10 million cells/mL
3. Incubate for 1 hour in CO₂ incubator, leaving 50 mL conical caps loosened
4. Irradiate pulsed cells for 3000 rads
 - a. Wash irradiated cells with 25 mL T cell media and resuspend in 1 million/mL
5. Mash up spleens with 3 mL syringe top (inside of mesh) and add 5 mL of 0.8% Ammonium Chloride OR Sigma Lysis buffer for 5 minutes
 - a. Add 25 mL of media to stop the lysis and spin down 1200 rpm for 5 minutes, discard supernatant
6. Count and resuspend splenocytes in 3.33 million/mL
7. Want a 10:1 ratio of splenocytes:stimulator RMA cells
8. Add 1 million cells (1 mL) of pulsed, irradiated cells to culture and 10 million (3 mL) of splenocytes to the culture
9. Check culture every 3-4 days, add 1 mL of T cell media if necessary

Restimulation procedure:

1. Spin down stimulator RMA for 5 minutes 1200 rpm and resuspend in T cell media to 10 million cells/mL
2. Pulse cells with peptide by adding 5 uL (200 ug/mL stock) peptide for every 10 million cells/mL
3. Incubate for 1 hour in CO₂ incubator, leaving 50 mL conical caps loosened
4. Irradiate pulsed cells for 3000 rads
 - a. Tighten cap on conical tube and place tube in irradiator
 - i. To operate irradiator, turn on, put samples in and set time and make sure the timer starts counting upwards
 - ii. Set to automatic
 - iii. When completed, follow procedure to exit (COMMAND, ARM, YES)
 - b. Wash irradiated cells with 25 mL T cell media and resuspend in 1 million/mL
 - i. Can use between 500,000 and 1 million stimulator cells per well
5. Harvest the cells by taking up the full 4 mLs in each well, and then pipet down in a circular motion to get all of the cells, do this twice for each well and then add to a 50 mL conical
6. After harvest, add 1 mL PBS and put back into incubator for 5-10 minutes while harvesting other plate(s)
 - a. Take 4 mLs of the harvested cell mixture and use that to harvest the 1 mL of PBS added + cells and add to 50 mL conical
 - b. Adding PBS will help remove the cells that are stuck to the bottom of the well, this is more important for latter passages
7. Spin down harvested cells for 5 minutes at 1200 rpm
8. Reseed cell lines based on density, which is determined visually (seed 1:2 or 2:3 for the first 3 passages and 1:3 or 1:4 for later passages)
9. Resuspend pelleted cells using T cell media containing 10% T stim without ConA
 - a. Make cocktail with T cell media so that cells can be resuspended into 3 mLs each well
10. Add 1 mL of pulsed RMA stimulators (between 500,000-1 million) with reseeded T cells and incubate for 3-4 days

V.A.9. GROWING BL21 EXPRESSING MHC CLASS I IN A 10 L FERMENTOR

Protocol modified from Jennifer Stone and Guoqi Li

Procedure:

Day 1:

1. Streak an LB-amp (chloramphenicol also if cells are pLys^s or chloramphenicol if cotransforming with BirA) plate in the evening using a glycerol stock containing the transformed BL21 cells of interest.
2. Incubate at 37°C overnight.

Day 2:

1. Put streaked plate at 4°C in morning, sealed with parafilm.
2. Autoclave the following items: Assembled fermentor filled with 8 L of distilled water, 1 L 1x LB broth, 1 L 10x LB broth, 1 L of distilled H₂O and least 150 mL 20 % glucose.
3. Inoculate autoclaved, 1 L 1x LB broth with a colony from your plate and grow overnight.

Day 3:

1. Set up the fermentor: For 10L: 1L 10x LB broth, 10 mL of 1000x Ampicillin, 100 mL 20 % glucose and 1-2 mLs antifoam. If the cells are pLys^s or if cotransforming with BirA, also add 10 mL 35 mg/mL chloramphenicol. Mix well. Remove 1 mL as a blank and store in a plastic cuvette with 1 μL 20 % NaN₃ to prevent growth.
2. Run the mixer on the fermentor at ~700 rpm, and run the air at 15 psi and 5 LPM. Watch for excessive foaming and add antifoam if more is needed.
3. Seed the fermentor with 1L of the overnight flask and allow the bacteria to grow depending on temperature (should take about 4-5 hours at room temperature to reach OD₆₀₀ = 0.7)
4. Take samples and check the OD₆₀₀ every hour or so until you get close to 0.7, and then check more frequently. Do not overgrow!
5. When the OD₆₀₀ reaches 0.7, take a 1 mL sample “not induced or N.I.” Spin down and re-suspend in 1x urea-SDS loading buffer. Freeze at -20°C.
6. Add IPTG to 0.75 mM final concentration. If performing *in vivo* biotinylation (i.e. co-transformed BirA + MHC class I plasmids), also add biotin to 50 μM. For a 10L fermentor, I add 10 mL of 0.75M IPTG stock (1000x) and 10 mL of 50 mM Biotin (1000x).
7. Grow for another 2-6 hours depending on the temperature. I induce MHC class I at room temperature for 4 hours.
8. Take a 1 mL sample for “induced.” If you want, you can take an “induced” sample every hour during induction as in the gel below. Spin down and re-suspend in 1x urea-SDS loading buffer. Freeze at -20 °C until you are ready to check the “not induced” and “induced” samples on a gel by SDS-PAGE.

- Spin down all the cells at 8000 x g and discard the supernatant. For inclusion bodies, you may freeze the pellet at -20°C , or proceed with the inclusion body prep through the DNase step and freeze at -20°C .

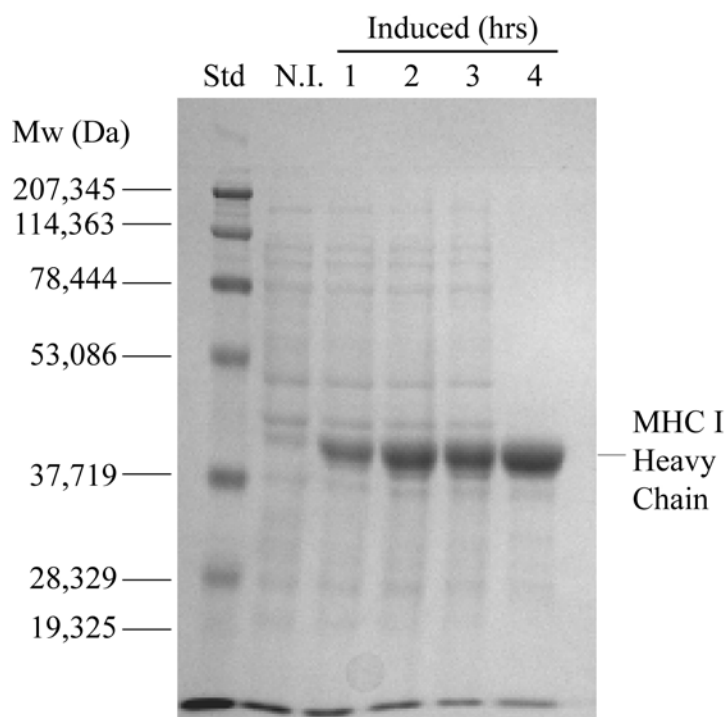


Figure V.A.2. MHC Class I Heavy Chain Expression. MHC Class I HC expression was monitored during the growth of a 10 L fermentor at room temperature. 12% SDS-PAGE gel of non-induced versus 0.75 mM IPTG-induced samples are shown. Molecular weight markers are labeled on the left.

V.A.10. HQ ON THE BIOCAD SPRINT HPLC

Protocol modified from Jennifer Stone

Setting up the biocad:

1. Start Biocad program (icon on desktop)
2. In the CONTROL PANEL window, select CONFIG, select EDIT CONFIG
3. To change values, double-click on the current value
 - a. Buffer A = 20 mM Tris pH 8.0
Buffer B = 20 mM Tris pH 8.0 + 1 M NaCl
 - b. Column type = ZS MHC class I, max flow rate 15 mL/minute, set high pressure to 1000 psi (if you don't know the pressure, ask someone who does know).
 - c. Only change pressure and column type
 - d. Make sure under DETECTOR that lamp is on

Equilibrating Buffer Lines:

1. Set the wavelength at 214nm to detect for the disappearance of azide (water azide)
2. Set to 10 mL/minute and pump 100% Buffer A until leveled
3. Set to 10 mL/minute and pump 100% Buffer B until leveled
4. If there are bubbles in the lines, they must be purged
 - a. Fix tubing onto a large 60 mL syringe from the PURGE KNOB
 - b. Loosen the PURGE KNOB on the biocad
 - c. Remove the bubbles with the 60 mL syringe
 - d. Re-tighten the PURGE KNOB on the biocad

Equilibrating Column:

1. Hook up column by twisting off bottom and top screw nubs gently
2. Using the flow rate (5 mL/minute), equilibrate using 100% Buffer A and 100% Buffer B independently
3. To equilibrate your column, you have to run a gradient wash. To open up any method, go to the Control Panel window, select WINDOW and METHOD EDITOR.
4. To run a method, go to FILE, OPEN and locate your method. My methods can be found in Biocad, People, Zu, Methods, "gradientwash" and choose RUN METHOD. It's not necessary to save the profile from the wash.
5. Select UPDATE METHOD WITH SYSTEM CONFIG when the biocad asks you as long as system config is correct.

Loading Buffer Exchanged Refolding Mix onto HQ column:

1. Before or after equilibrating your HQ column (I prefer before so that the contents of the F line don't enter the column), make sure to flush out the F line with Buffer B followed by Buffer A.
 - a. The F line is where you can load large volumes of protein. You can also inject into the biocad, but your method must have the injection step built in.
2. Load your buffer exchanged refolding mixture onto the column by selecting 100% and F and make sure you hit SET. You can then choose your FLOW RATE and hit START. I prefer to load at a slower flow rate such as 5 mL/minute as compared to the flow rate in the actual method (8 mL/minute).
 - a. I prefer to collect the flow through just in case something happens during the run.
3. Make sure the fraction collector is positioned properly. If you don't know what this means, ask someone. A note about the fraction collector, it's old. I typically reset the fraction collector before each run to prevent errors from occurring mid-run. I've had the fraction collector stop mid-run or not start at all, so beware.
4. After your refolding mixture is loaded, go to the METHOD EDITOR window. Select FILE, OPEN and my HQ method is located in Biocad, People, Zu, Methods, "KbFinject" and choose a location to save your results and hit RUN METHOD. A typical MHC Class I anion exchange profile can be found in Figure V.D.1A.
 - a. A 1 L refolding mixture should yield approximately between 15-25 mgs of refolded MHC Class I monomer

5. V.A.11. INCLUSION BODY PREPARATION FOR MHC CLASS I SUBUNITS

Protocol modified from Mia Rushe

Procedure (for pellet from 10 L culture):

1. Spin down cells at 5000 x g—collect supernatant into a container, sterilize with 1% Wescodyne for 10-20 minutes, and then dump down the sink.
2. With a rubber spatula, re-suspend fresh bacteria into a single plastic container with ~200 mL Sucrose Solution.
3. Chop the solution briefly in a homogenizer or polytron. **Do not sonicate!
4. Most of our cells are not pLys^s, so add 1 mg dry lysozyme per mL suspension (0.2 g) and stir for 10 minutes. If cells are pLys^s, just stir for 10 minutes.
5. While stirring, add 500 mL Deoxycholate-Triton Solution. Solution will become very viscous due to cell lysis and DNA release.
6. Add 1 mL of 4 M MgCl₂ Solution to make 5 mM final concentration.
7. Add 2 mL DNase Solution. Stir until the solution is the viscosity of water.
8. Freeze overnight at -20°C.
9. Thaw solution in warm water bath.
10. Stir an additional 10 minutes after thawing to allow the DNase to work again.
11. Spin down in 2 centrifuge bottles at 8000 x g for 20 minutes. Discard supernatant.
12. Re-suspend pellets in 300 mL or more each Triton Solution. Chop briefly, keeping the pellets on ice as much as possible. Spin down at 8000 x g for 20 minutes and discard supernatant.
13. Repeat step 12 three or more times.
14. Re-suspend pellets into 300 mL or more each Tris Solution. Chop briefly, keeping the pellets on ice as much as possible. Spin down at 8000 x g for 20 minutes and discard supernatant.
15. Repeat step 14 two or more times.
16. Re-suspend/dissolve the pellets and chop in ~ 200 mL Urea Solution.
17. Spin down at 20°C, 15,000 x g for 30 minutes. Filter through a 0.2 µm filter.

*Solutions (**Note: Do not add DTT until just before use!):*

Solution Name	Stock	For 1 L, 1x	For 1 L 10x
Sucrose			
50 mM Tris, pH 8.0	1 M Tris, pH 8.0	50 mL	
25% Sucrose	Dry, FW = 342.3	250 g	N/A
1 mM EDTA	0.5 M EDTA	2 mL	
0.1% NaN ₃	20 % NaN ₃	5 mL	
10 mM DTT	Dry, FW = 154.04	1.54 g	
Deoxycholate-Triton			
1 % Deoxycholic Acid	Dry, FW = 414.6	10 g	100 g
1 % Triton X-100	100% solution	10 mL	100 mL
20 mM Tris, pH 7.5	1 M Tris, pH 7.5	20 mL	200 mL
100 mM NaCl	5 M NaCl	20 mL	200 mL
0.1% NaN ₃	20 % NaN ₃	5 mL	50 mL
10 mM DTT	Dry, FW = 154.04	1.54 g	N/A
Triton			
0.5 % Triton X-100	100% solution	5 mL	50 mL
50 mM Tris, pH 8.0	1 M Tris, pH 8.0	50 mL	500 mL
100 mM NaCl	5 M NaCl	20 mL	200 mL
1 mM EDTA	0.5 M EDTA	2 mL	20 mL
0.1% NaN ₃	20 % NaN ₃	5 mL	50 mL
1 mM DTT	Dry, FW = 154.04	0.154 g	N/A
Tris			
50 mM Tris, pH 8.0	1 M Tris, pH 8.0	50 mL	500 mL
1 mM EDTA	0.5 M EDTA	2 mL	20 mL
0.1% NaN ₃	20 % NaN ₃	5 mL	50 mL
1 mM DTT	Dry, FW = 154.04	0.154 g	N/A
Urea			
8 M Urea	Dry, FW = 60.06	480.48 g	N/A
25 mM MES, pH 6.0	Dry, FW = 213.3	5.33 g	
10 mM EDTA	0.5 M EDTA	20 mL	
0.1 mM DTT	Dry, FW = 154.04	15.4 mg	
DNase		*Make 50 mL, not 1 L	
75 mM NaCl	5 M NaCl	0.75 mL	N/A
50% Glycerol	100% Glycerol	25 mL	
2 mg/mL DNase	Dry	100 mg	
Sigma Cat# D25			

V.A.12. INTRACELLULAR CYTOKINE STAINING

Protocol modified from Keith Daniels

1. Prepare the cells normally and lyse Red Blood Cells using 0.84% NH₄Cl or Red Blood Cell lysis buffer (Sigma Cat# R7757).
2. Add 2e6 cells per culture well.
- 3a. For Spontaneous and Non-Specific Stimulation

Plate (Volume/well)	
Total Volume	200 µl
GolgiPlug	0.2 µl neat
CD3	0.1 µl of 0.5mg/ml stock
PMA	0.5 ul of a 20 µg/ml stock (50 ng/ml)
Ionomycin	1ul of a 100 µg/ml stock (500 ng/ml)

- 3b. For Specific Peptide Stimulation add 1ul of a 200ug/ml peptide solution per well

Plate	
Total Volume	200 µl
GolgiPlug	0.2 µl neat
IL-2 (neat)	0.004 µl of 1µg/ml (10U/ml) Stock
IL-2 (Diluted)	0.4 µl

4. Incubate at 37°C for 4 hours (PMA & Ionomycin or CD3) or 5 hours (Peptide Stimulation).
5. Wash 1x using Staining Buffer (PBS without Mg²⁺ or Ca²⁺; 1% FCS; 0.09% Sodium Azide) 200ul/well - Centrifuge for 5 min at 1200-1500 rpm.
6. Block Fc receptors using 2.4G2 antibody for 5 min at 4°C in 100ul of Staining Buffer.
7. Wash 1x - Add 100µl Staining Buffer and Centrifuge for 5 min at 1200-1500 rpm.
8. Stain cells for surface antigens using appropriate antibodies in 100ul of Staining Buffer for 20 min at 4°C.
9. Wash cells 2x with Staining Buffer.
10. Resuspend cells using 100ul per well of CytoFix/CytoPerm Solution for 20 min at 4°C.
11. Wash cells 2x in 1X Perm/Wash solution (Dilute 10X stock in dH₂O)
12. Resuspend cells in 100ul of Perm/Wash solution containing anti-cytokine antibodies.
13. Incubate for 25 min at 4°C in the dark.
14. Wash cells 2x with 1X Perm/Wash.
15. Wash cells 1x using Staining Buffer.
16. Put in a final Volume of 300ul of Staining Buffer for Analysis.

V.A.13. MHC CLASS I HETEROGENOUS CROSS-LINKING USING MHPH AND MTFB

Protocol modified from Solulink

Procedure:

1. Store small aliquots (~50 uL) stock solutions of cross-linker reagents 3-N-Maleimido-6-hydraziniumpyridine hydrochloride (MHPH, Solulink Cat# S-1009-010) and Maleimido Trioxa Formylbenzaldehyde (MTFB, Solulink Cat# S-1035-105) at 20 mM in DMF at -80° C.
2. Reduce cysteine containing proteins (A and B) in 5 mM DTT overnight
3. Calculate the amount of MHPH and MTFB cross-linker to add to the proteins using a 5:1 molar excess of cross-linker. Do not allow the final volume of DMF to exceed 5% of the total volume.
4. Right before adding the cross-linker, remove DTT using NAP-5 drip column (GE Healthcare Cat# 17-0853-02) and equilibrate protein into 100mM phosphate, pH 6.0, 150mM NaCl.
5. Add the appropriate amount of MHPH to protein A and MTFB to protein B, keeping them separated. Allow the reaction to proceed at room temperature for 2 hours.
6. Set up and equilibrate Superdex 200 column on biocad (GE Healthcare Cat#17-5175-01) using 100mM phosphate, pH 6.0, 150mM NaCl.
7. Purify away the free cross-linker from modified proteins over HPLC
 - o Make sure to perform a blank run in between as I've observed the free cross-linker eluting much later off of the Superdex 200 column
8. Check the peak fractions for protein concentration and pool and concentrate the peak fractions.
 - o Save a small sample for SDS-PAGE
9. Make sure that the concentration of protein A and protein B are MATCHED and range between 10 – 30 μ M.
10. Mix equal molar amounts of protein A-MHPH and protein B-MTFB in the same tube and add aniline catalyst (Acros Organics Cat#158190050) to 5mM. Allow the reaction to proceed for at least 2 hours at room temperature.
 - o Save a small sample for SDS-PAGE.
11. Purify the reaction mixture using a Superdex 200 column. Pool and concentrate the peak fractions.
 - o Save a small sample for SDS-PAGE.
12. Label the MHC (hetero/homo) dimers using the primary amines (see protocol for labeling primary amines).
13. Run the saved samples on an SDS-PAGE. See Figure II.5 for an example.

V.A.14. MODIFYING FREE CYSTEINES ON PROTEINS USING MALEIMIDES

Protocol modified from Jennifer Stone

Procedure:

11. If the protein is not freshly reduced, add DTT to 5 mM and incubate the protein overnight at room temperature.
 - a. If the protein has been stored in DTT and is freshly purified by anion exchange, there is no need to re-reduce. Skip to step 2.
12. Either column-purify, dialyze, or concentrate/switch buffers to remove DTT and put protein in reaction buffer (I've tested PBS, Tris and Phosphate pH 6-8. If the pH is too high, the maleimide reagent will also modify primary amines such as lysine residues).
 - a. I prefer to use the NAP5 drip columns (GE Healthcare cat# 17-0853-01) because the procedure is quick and easys.
 - b. The MHC class I complexes elute between 0.75 mL to 1.5 mL.
13. Immediately check the concentration of the protein, which should be no lower than 10 μ M, otherwise hydrolysis of maleimide will occur
14. Add the maleimide reagent to a final concentration so that you get between a 5-10 fold molar excess of maleimide to your freshly reduced protein.
 - a. Your maleimide stock solution should be made in DMSO at a concentration greater than 5-10 mM. The reason being is that you want to be able to dilute your DMSO and still have a high enough concentration to prevent hydrolysis. I typically do at least a 1:20 dilution into the protein solution.
15. Mix well and store the solution at room temperature for 1-2 hours. If the probe is fluorescent, store the solution in the dark to prevent fluorescence quenching.
16. After the incubation, you might consider adding DTT to a final concentration of 5 mM to quench any remaining unreacted maleimide, although I've found that this isn't necessary.
17. HPLC purify away the excess maleimide and DTT (if added in step 6) using a Superdex 200 column (GE Healthcare Cat# 17-5175-01) set up on the Biocad.
18. Pool and concentrate the peak fractions.
19. Measure the final concentration and, if applicable, the degree of labeling.

V.A.15. MODIFYING PRIMARY AMINES ON PROTEINS USING NHS ESTERS

Protocol modified from Pierce

Procedure:

20. Make sure your protein is stored in an amine-free buffer at pH 7.25-8.0.
Basically, avoid Tris or glycine buffers. I typically use phosphate or PBS at pH 8.0.
21. Check the concentration of the protein, which should be no lower than 10 μ M, otherwise the reaction will not go efficiently.
22. Add the NHS ester reagent to a final concentration of so that you get a 10-20-fold molar excess of NHS ester to your protein. Your NHS ester stock solution should be made using DMSO at a concentration around 4 mM. The reason being is that you want to be able to dilute your DMSO and still have a high enough concentration to prevent hydrolysis of the succinimidyl ester. I typically do at least a 1:20 dilution into the protein solution.
23. Mix well and store the solution at room temperature for 1-2 hours. If the probe is fluorescent, store the solution in the dark to prevent fluorescence quenching.
24. After the incubation, add a 50-fold molar excess of ethanolamine relative to the amount of NHS ester added, to quench any remaining unreacted NHS ester.
 - a. I've found that quenching with Tris, followed by multiple rounds of dialysis is insufficient to quench the NHS ester.
25. HPLC purify away the excess NHS ester using a Superdex 200 (GE Healthcare Cat# 17-5175-01) column set up on the biocad.
26. Pool and concentrate the peak fractions.
27. Measure the final concentration and, if applicable, the degree of labeling.

V.A.16. POURING LB-AMP PLATES

Protocol modified from Jennifer Stone

Procedure:

1. Dissolve 25 grams of LB mix in a final volume of 1 liter. Add 15 grams of Bacto-agar (not agarose). Cover top with foil and autoclave for 20-30 minutes.
2. After autoclaving, swirl vigorously in the flask to mix the molten agar. Cool the solution to 50°C. This is approximately when you can stand to hold the bottom of the flask for 10-20 seconds.
3. For ampicillin, add 100 mg of Ampicillin and swirl until it dissolves.
4. Make space to accommodate ~40 plates, unstacked, per liter of agar mix. Pour plates to a depth of approximately 3 mm. You can measure 20-25 mL per plate, but I prefer to pour.
 - a. If there are bubbles on the surface of the agar, these can be removed by briefly flaming the surface with a Bunsen burner.
5. Leave the plates out at room temperature and unstacked. Wait at least a few hours before stacking and putting the plates in the fridge.
6. Label the plates with the date and note the antibiotic.
7. Store the plates in a plastic sleeve at 4°C.

V.A.17. PREPARING MHC CLASS I TETRAMERS

Protocol modified from Jennifer Stone

Materials:

- K^b-pep: Biotinylated MHC class I complex of choice in PBS or Tris.
- SA-PE: Choice of fluorochrome conjugated streptavidin, I frequently use premium grade R-phycoerythrin conjugated streptavidin (Invitrogen Cat# XXX)
- PBS, 1x
- FACS buffer: 1x PBS, 2% FCS
- BD cytofix (Cat# XXXX)
- Fluorescent antibodies to cell-surface markers:
 - α -CD8 β PerCP Cy 5.5
 - α -CD44-FITC

Procedure for 50 μ L: This procedure is generally completed on ice and the reagent should be made up fresh for each stain. I typically use 300-500 nM of MHC tetramer for most tetramer stains.

1. Aliquot 1.5 μ g K^b-pep into an eppendorf tube.
2. In a separate tube, dilute 2 μ L R-phycoerythrin conjugated Streptavidin (SA-PE) with 4 μ L PBS
3. Add 2 μ L of diluted SA-PE mixture to the tube with K^b-pep and pipet-mix well
4. Wait 2 minutes
5. Add 2 μ L of diluted SA-PE mixture to the tube with K^b-pep and pipet-mix well
6. Wait 2 minutes
7. Add the rest of the diluted SA-PE mixture to the tube with K^b-pep and pipet-mix well
8. Wait 2 minutes and the complex should form between biotinylated K^b-pep and SA-PE: K^b-SAPE oligomer
9. Dilute K^b-SAPE oligomer with FACS buffer to a final volume of 50 μ L.
10. I've made an excel spreadsheet to expedite these calculations. It should be located in my protocol folder on the "S drive", named "MHC Class I calc".

V.A.18. REFOLDING OF MHC CLASS I COMPLEXES

Protocol modified from NIH Tetramer Facility

Procedure:

8. Pre-chill 1 L of Folding Buffer in a 1.5 L beaker to 4°C.
9. Add 5 mM reduced glutathione, 0.5 mM oxidized glutathione, and 0.2 mM PMSF to cold Folding Buffer, stirring quickly and try to avoid foaming!
10. Calculate 1 μ M heavy chain urea-solubilized subunit and add to 4 mL of Injection Buffer.
11. Calculate 2 μ M β_2 M urea-solubilized subunit and add to the same 4 mL Injection Buffer.
12. Weigh out 10-20 mg of peptide and dissolve in 0.5 mL DMSO.
13. Add peptide solution dropwise to rapidly stirring Folding Buffer.
14. Forcefully inject heavy chain and β_2 M to the stirring reaction through a 26-gauge needle as close to the stir-bar as you can. There may be some precipitation or light foaming.
15. Replace the mixture at 4°C and incubate overnight.
16. The following morning, inject **heavy chain and β_2 M** in Injection Buffer into the cold, quickly-stirring mixture as above. Replace at 4°C.
17. In the evening, once again inject **heavy chain and β_2 M** in Injection Buffer into the cold, quickly-stirring mixture as above. Replace at 4°C and incubate overnight

Solutions:

Folding Buffer (pH 8.0)

400 mM L-Arginine (Sigma A5949)
 100 mM Tris, pH 8.0
 2 mM EDTA

Injection Buffer (pH 4.2)

3 M Guanidine-HCL
 10 mM Sodium Acetate
 10 mM EDTA

Other Materials

Urea-solubilized heavy chain and light chain (β_2 M)
 Peptide of choice
 Reduced glutathione (Sigma G4705)
 Oxidized glutathione (Sigma G4501)
 100 mM Phenylmethylsulfonyl fluoride (PMSF - Sigma P7626)

V.A.19. SDS-PAGE

Protocol modified from Mia Rushe

Procedure:

1. Assemble the gel apparatus, being careful to avoid leakage.
2. Select the percentage of Separating Gel you would like to pour. (Lower percentage gels allow higher molecular weight proteins to separate further.)
3. Add the ingredients in the order listed - mix well between each step.
4. After the temed and APS, move quickly, since the acrylamide will try to begin polymerizing.
5. Pour about 2.5-3 mL of acrylamide mixture into the space between the gel plates.
6. Slowly layer a small amount of water on top of the acrylamide mixture using a syringe. The acrylamide polymerizes faster in anaerobic conditions.
7. Allow the Separating Gel to polymerize for about 45 minutes.
8. Remove the water layer from the top of the gel by tilting and using a paper towel.
9. Mix the ingredients for the Stacking Gel (shown below) in order, mixing after each one.
10. Layer the Stacking Gel mixture on top of the Separating Gel. Fill all the way to the top.
11. Insert a comb into the stacking gel to create lanes for loading your samples.
12. Allow the Stacking Gel to polymerize for about 45 minutes.
13. Remove the comb.
14. At this point, you can either place the gel into the electrophoresis chamber covered with SDS Running Buffer, load samples in 1x SDS Loading Buffer, and run the gel, or you can store the gel at 4°C by wrapping in several soaked paper towels and then surrounding it with Saran Wrap. The gel should keep stored this way for a week or two.
15. After running your samples, disassemble the apparatus and place the gel into Coomassie Stain (or use other stain protocol). Allow to shake for >1 hour at room temperature.
16. Remove the stain and rinse with deionized water. Place gel into Destain on shaker with two knotted kimwipes. Observe on light box.

SDS-PAGE Gel Recipes:**Stacking Gel**

<u>Component</u>	
30% Acrylamide	0.3 mL
ddH ₂ O	1.2 mL
4x Lower Buffer	0.5 mL
TEMED	5 µL
10% APS	20 µL

Separating Gel

<u>Component</u>	<u>7.5%</u>	<u>10%</u>	<u>12.5%</u>	<u>15%</u>
30% Acrylamide	1 mL	1.3 mL	1.7 mL	2 mL
ddH ₂ O	2 mL	1.7 mL	1.3 mL	1 mL
4x Lower Buffer	1 mL	1 mL	1 mL	1 mL
TEMED	10 µL	10 µL	10 µL	10 µL
10% APS	20 µL	20 µL	20 µL	20 µL

Solutions:4x Lower Buffer

181.7 g Tris Base
4.0 g SDS
Fill to 1L with ddH₂O
Adjust pH to 8.8

4x Upper Buffer

60.6 Tris Base
4.0 g SDS
Fill to 1L with ddH₂O
Adjust pH to 6.8

10x Running Buffer

30.3 g Tris Base
10.0 g SDS
144.0 g glycine
Fill to 1L with ddH₂O
Do not pH

5x Laemlli Loading Buffer

60 mM Tris, pH 6.8
100 mM DTT (for reducing)
1% SDS
10% Glycerol
0.001% Bromophenol Blue
in ddH₂O

Coomassie Blue Stain

0.25% CBBR-250
15% Methanol
10% Acetic Acid in ddH₂O
Note: Dissolve CBBR in
Methanol first, add Acetic
Acid in water and filter.

Destain

15% Methanol
10% Acetic Acid in ddH₂O

2x SDS Sample Buffer

6.67 g SDS
20 g Sucrose
0.3 g Tris Base
1.03 g DTT
Note: pH to 7.5 with HCl,
Add to 100 mL ddH₂O

V.A.20. SINGLE CELL SUSPENSIONS FROM MOUSE ORGANS

Protocol from Keith Daniels and Jennifer Stone

Materials:

RP10

RPMI media

10% FCS

1% P/S

1% HEPES

1% L-Glut (even if it's already included in RPMI)

Procedure:

1. Collect the mouse organs (lymph nodes, spleen, etc) in a Petri dish with 3-5 mL RP10 medium.
2. Crush the organs between the frosted handles of two glass slides (sterilized). Start with the smallest organs, as the solution will become cloudy and the small organs will be difficult to see later.
3. Spin down cells at 1500 rpm, 10 minutes. Ensure that a pellet has formed! Remove supernatant and retain in a separate tube.
4. Resuspend cells in 2-3 mL room temperature RBC lysis buffer (Sigma Cat# R7757) per mouse. Allow to sit 5 minutes and no longer. NOTE: If you have trouble with losing cells in this step, try a Ficoll gradient to isolate the white blood cells instead of lysing the RBC's.
5. Dilute with 10 mL/mouse RP10 medium and spin down at 1500 rpm, 10 minutes. Ensure that a pellet has formed. Remove supernatant and immediately resuspend pelleted cells in RP10 medium and count total number.

V.A.21. SITE DIRECTED MUTAGENESIS

Modified from Walter Kim

Procedure:

1. In a PCR tube, add the following:
 - a. 3 μL 100% DMSO (quiksolution), final in 50 μL is 6%
 - b. 0.5 μL plasmid DNA (miniprep)
 - c. Primer
 - i. I test 1 μL , 2 μL and 5 μL [10 μM] of both forward and reverse primers
 - d. 5 μL 10x PFU buffer
 - e. 2.5 μL 4 mM (20x) dNTP mix or 1 μL 10 mM (50x) dNTP mix (New England Biolabs Cat# N0447s)
 - f. Ultra pure ddH₂O to 49 μL
 - g. 1 μL PFUultra (2.5 Units/ μL) last to 50 μL
 - i. PFU ultra has exonucleases which can cleave ssDNA primers
2. Run QUIKC2 program on PCR
3. After program is run, add 1 μL Dpn I restriction enzyme (10 U/ μL)
 - a. Mix reaction by vortexing
 - b. Incubate for 1 hour at 37° to digest parental DNA
4. Transform 5 μL of DNA in 45 μL supercompetent XL1-blue *E. coli*
5. Incubate on ice for 5 minutes
6. Heat shock in 42°C water bath for 45 seconds
7. Incubate on ice for 5 minutes
8. Add 100 μL of S.O.C. (warmed to 42°C)
9. Place in 37°C rotator for 1 hour
10. Plate all (150 μL) of reaction mixture onto Amp plates around noon and grow plate overnight. Note that XL1-blue colonies are really small.

V.A.22. STAINING CD8+ T CELLS WITH MHC CLASS I TETRAMERS

Protocol modified from Jennifer Stone and Keith Daniels

Procedure:

1. Prepare the cells normally and lyse Red Blood Cells using 0.84% NH₄Cl or Red Blood Cell lysis buffer (Sigma Cat# R7757).
2. Block Fc receptors using 2.4G2 antibody for 5 min at 4°C in 100 µl of FACs buffer.
3. Wash once using 200 µl FACs buffer and centrifuge for 5 minutes at 1500 rpm.
 - a. You will want to have a final volume such that you use 40 µL cell suspension and add 10 µL of each tetramer.
4. Aliquot 40 µl cell suspension into one well of a 96-well round-bottom plate for each staining experiment.
5. Add 10 µl of MHC class I tetramer to the cell suspension in appropriate wells
6. Incubate the plate at 4°C for 40 minutes.
7. Prepare a cocktail of desired fluorescent antibodies. Typically use 1 µl or less of each antibody per sample and dilute with FACS Buffer so that you will add 50 µL cocktail per sample.
8. Add 50 µl of fluorescent antibody cocktail to each sample. Pipet mix well.
9. Incubate on ice for 20 minutes.
10. Add 100 µl cold FACS buffer to each sample. Spin plate at 4°C for 5 minutes, 1500 rpm.
11. Flick plate into sink. Look at the bottom of the plate to make sure cell pellets have are still present after plate flick.
12. Wash with 150 µl cold FACS buffer and pipet mix well. Spin plate at 4°C for 5 minutes, 1500 rpm.
13. Flick supernatant
14. Add 100 µl of BD cytofix to each sample to fix the samples
15. Wash with 150 µl cold FACS buffer and pipet mix well. Spin plate at 4°C for 5 minutes, 1500 rpm.
16. Flick supernatant.
17. Resuspend samples in 150 µl cold FACs buffer.
18. Analyze by flow cytometry immediately or the next day.

NOTE: Remember to include plenty of controls including single-stained cells for compensation adjustment, control tetramers, control cells if available

V.A.23. STOCK SOLUTIONS

Solution	1000x stock	grams	Final Volume	Solvent
Biotin	50 mM	0.12212	10 mL	ddH ₂ O with 1M NaOH
iPTG	0.75 M	1.7871	10 mL	ddH ₂ O
Ampicillin	100 mg/mL	1	10 mL	ddH ₂ O
Chloramphenicol	35 mg/mL	0.35	10 mL	100% Ethanol
Kanamycin	50 mg/mL	0.5	10 mL	ddH ₂ O
PMSF	0.2 M	34.84 mg	1 mL	100% ethanol

V.A.24. TRANSFORMING COMPETENT BACTERIA

Modified from Jennifer Stone and Walter Kim

Procedure:

1. Before starting, determine the fate for your transformed bacteria. If the transformation is being done to express plasmid DNA, I use XL1-blue *E. coli*. However, for protein expression, I always use BL21 *E. coli*.
2. For transformation, I prefer the “5-45-5” method as coined by Walter Kim. Briefly, it’s 5 minutes on ice, 45 seconds at 42°C followed by 5 minutes on ice.
3. Prepare enough LB-agar plates for all of your samples, containing the antibiotic you will be selecting for. You will also need sterile eppendorf tubes, pipet tips, and a spreader.
4. Thaw an aliquot of competent cells on ice. For co-transformation (i.e. BirA + MHC class I), use supercompetent cells.
5. Pre-heat a water bath to 42°C.
6. For each sample, add 1µL of miniprep DNA (approximately 1-50ng) to 50µL of competent cells in a sterile eppendorf tube. Ideally, you should perform at least two controls: a known plasmid with the antibiotic resistance tag you will be using (such as pLM1 for ampicillin resistance), and cells with no DNA added.
7. Incubate on ice 5 minutes.
8. Place tubes in the water bath at 42°C for 45 seconds.
9. Return the tubes to ice for another 5 minutes.
10. For co-transformation, add a 10x volume of S.O.C. recovery media (Invitrogen Cat# 15544-034), mix gently and incubate the transformed cells at 37°C for 1 hour. This allows recovery from the heat shock in the water bath. For transformation of a single plasmid, skip to step 11.
 - a. S.O.C. media can also be prepared using the ingredients below.
 - i. S.O.C. formulation per one liter (from Invitrogen)
 - 2% tryptone
 - 0.5% yeast extract
 - 10 mM sodium chloride
 - 2.5 mM potassium chloride
 - 10 mM magnesium chloride
 - 10 mM magnesium sulfate
 - 20 mM glucose
11. Plate the cells onto LB plates containing the antibiotic you are using to screen (for example, ampicillin). Use a disposable spreader.
12. Incubate plate overnight at 37°C. You should have colonies on your positive control plasmid plate (such as pLM1), and no colonies on your “no DNA” plate.
 - a. Note: If you get too many colonies or a “lawn” on your transformation plates, use a smaller volume of the transformation mixture to spread onto your plates.

13. To test protein induction in BL21 or other production strain, grow several colonies from the transformed plate in 5 mL of 1x LB medium, 100 $\mu\text{g/mL}$ ampicillin (or other selecting antibiotic), 0.2-0.5% glucose until the cultures reach an OD_{600} of ~ 0.7 . Take a "Not Induced" sample from each culture. Add IPTG to 0.75 mM final concentration and grow for another 1-3 hours at 37°C. Take an "Induced" sample of the same volume from each culture. Run an SDS gel of the samples against molecular weight markers to test protein induction in each culture.

V.B. Gene Constructs used in this Thesis
Modified from Jennifer Stone

Gene Construct	H-2K ^b bsp Mouse heavy chain with biotin signal peptide (bsp) tag
Plasmid	pLM1
Promoter	T7
Antibiotic Resistance	Ampicillin
Made by	NIH tetramer facility
Gene Sequence	<p>ATGGGACCACATTCGCTGAGGTATTTTCGTCACCGCCGTGTCCCGGCCCGGCCTCGGGGA GCCCCGGTACATGGAAGTCGGCTACGTGGACGACACGGAGTTTCGTGCGCTTCGACAGCG ACGCGGAGAATCCGAGATATGAGCCGCGGGCGCGGTGGATGGAGCAGGAGGGGCCGAG TATTGGGAGCGGGAGACACAGAAAGCCAAGGGCAATGAGCAGAGTTTCCGAGTGGACCT GAGGACCCTGCTCGGCTACTACAACCAGAGCAAGGGCGGCTCTCACACTATTCAGGTGA TCTCTGGCTGTGAAGTGGGGTCCGACGGGCGACTCCTCCGCGGGTACCAGCAGTACGCC TACGACGGCTGCGATTACATCGCCCTGAACGAAGACCTGAAAACGTGGACGGCGGCGGA CATGGCGGCGCTGATCACCAAACACAAGTGGGAGCAGGCTGGTGAAGCAGAGAGACTCA GGCCTACCTGGAGGGCACGTGCGTGGAGTGGCTCCGCAGATACCTGAAGAACGGGAAC GCGACGCTGCTGCGCACAGATTCCCCAAAGGCCCATGTGACCCATCACAGCAGACCTGA AGATAAAGTCACCCTGAGGTGCTGGGCCCTGGGCTTCTACCCTGCTGACATCACCCCTGA CCTGGCAGTTGAATGGGGAGGAGCTGATCCAGGACATGGAGCTTGTGGAGACCAGGCCT GCAGGGGATGGAACCTTCCAGAAGTGGGCATCTGTGGTGGTGCCTCTTGGGAAGGAGCA GTATTACACATGCCATGTGTACCATCAGGGGCTGCCTGAGCCCCCTCACCCCTGAGATGGG AGCCTCCTCCATCCGGATCCCTGCATCATATTCTGGATGCACAGAAAATGGTGTGGAAT CATCGTTAA</p>
Protein Sequence	<p>MGPHSLRYFVTAVSRPGLGEPYMEVGYVDDTEFVRFDSDAENPRYEPRARWMEQEGPE YWERETQKAKGNEQSFRVLDLRTLLGYYNQSKGGSHTIQVISGCEVGS DGRLLRQYQYA YDGC DYIALNEDLKTWTAADMAALITKHKWEQAGEAERLRAYLEGT CVEWLRRLKNGN ATLLRTDSPKAHVTHHSRPEDKVTLRCWALGFYPADITLTWQLNGEELIQDMELVETRP AGDGT FQK WASVVVPLGKEQYYTCHVYHQGLPEPLTLRWEPPPSGSLHHILDAQKMVWN HRSTOP</p>
Protein MW	34,271.4 Da
Protein extinction coefficient	78,900 at 280nm (unfolded)

Gene Construct	H-2K ^b cs Mouse heavy chain with uniquely reactive cysteine at the C-terminus
Plasmid	pLM1
Promoter	T7
Antibiotic Resistance	Ampicillin
Made by	Mia Rushe
Insert size	~860bp
Gene Sequence	<p>ATGGGACCACATTTCGCTGAGGTATTTTCGTCACCGCCGTGTCCCGGCCCGGCCTCGGGGA GCCCCGGTACATGGAAGTCGGCTACGTGGACGACACGGAGTTTCGTGCGCTTCGACAGCG ACGCGGAGAATCCGAGATATGAGCCGCGGGCGCGGTGGATGGAGCAGGAGGGGCCGAG TATTGGGAGCGGGAGACACAGAAAGCCAAGGGCAATGAGCAGAGTTTCCGAGTGGACCT GAGGACCCTGCTCGCTACTACAACCAGAGCAAGGGCGGCTCTCACACTATTCAGGTGAT CTCTGGCTGTGAAGTGGGGTCCGACGGGCGACTCCTCCGCGGGTACCAGCAGTACGCCT ACGACGGC_cGtGATTACATCGCCCTGAACGAAGACCTGAAAACGTGGACGGCGGGCGGAC ATGGCGGCGCTGATCACC_{AA}ACACAAGTGGGAGCAGGCTGGTGAAGCAGAGAGACTCAG GGCCTACCTGGAGGGCACGTGCGTGGAGTGGCTCCGCAGATACCTGAAGAACGGGAACG CGACGCTGCTGCGCACAGATTCCCCAAAGGCCATGTGACCCATCACAGCAGACCTGAA GATAAAGTCACCCTGAGGTGCTGGGCCCTGGGCTTCTACCCTGCTGACATCACCCTGAC CTGGCAGTTGAATGGGGAGGAGCTGATCCAGGACATGGAGCTTGTGGAGACCAGGCCTG CAGGGGATGGAACCTTCCAGAAGTGGGCATCTGTGGTGGTGCCTCTTGGGAAGGAGCAG TATTACACATGCCATGTGTACCATCAGGGGCTGCCTGAGCCCCTCACCTGAGATGGGA GCCTtgct_{aa}</p>
Protein Sequence	<p>MGP_HSLRYFVTAVSRPGLGEP_RYMEVGYVDDTEFVRFDSDAENPRYEPRARWMEQEGPE YWERETQKAKGNEQSF_RVDLRTLLGYYNQSKGGSHTIQV_ISGCEVGS_DGRLLR_GYQQYA YDGRDYIALNEDLKTWTAADMAALITKH_KWEQAGEAERLRAYLE_GTCVEWLR_RYLKNGN ATLLRTDSPKAHVTHHSR_PEDKVTLRCWALGFYPADITLTWQLN_GEELIQDMELVET_RP AGDGT_FQKWASVVVPLGKEQYYTCHVYHQGLPEPLTLR_WEP_CSTOP</p>
Protein MW	32,122 Da
Protein extinction coefficient	73,210 at 280nm (unfolded)

Gene Construct	Beta-2-Microglobulin Human light chain
Plasmid	pLM1
Promoter	T7
Antibiotic Resistance	Chloramphenicol
Made by	NIH tetramer facility
Gene Sequence	ATGATCCAGCGTACACCAAAGATTCAGGTTTACTCACGTCATCCAGCAGAGAATGGAAA GTCAAATTTCCCTGAATTGCTATGTGTCTGGGTTTCATCCATCCGACATTGAAGTTGACT TACTGAAGAATGGAGAGAGAATTGAAAAAGTGGAGCATTTCAGACTTGTCTTTCAGCAAG GACTGGTCTTTCATCTCTTGTACTACACTGAATTCACCCCACTGAAAAAGATGAGTA TGCCTGCCGTGTGAACCATGTGACTTTGTTCACAGCCAAGATAGTTAAGTGGGATCGAG ACATGTAA
Protein Sequence	MIQRTPKIQVYSRHPAENGKSNFLNCYVSGFHPSDIEVDLLKNGERIEKVEHSDLSFSK DWSFYLLYYTEFTPTEKDEYACRVNHVTLTSLQPKIVKWDRDMSTOP
Protein MW	12,148 Da
Protein extinction coefficient	20,003 at 280nm (unfolded)

V.C. Glycosylation Modulates Binding of MHC Class I Monomers onto Naïve CD8+ T cells

MHC class I tetramer binding is affected by glycosylation, which has been attributed to glycan moieties presented on cell surface glycoproteins such as TCR or CD8 co-receptor. These glycan adducts are thought to either restrict receptor (TCR/CD8) clustering (Demetriou, Granovsky et al. 2001) or alter CD8 co-engagement (Daniels and Jameson 2000; Daniels, Devine et al. 2001; Moody, Chui et al. 2001). However, due to the multivalent nature of MHC tetramers, reduced MHC tetramer staining after deglycosylation might be due to either reduced TCR clustering or CD8 co-engagement. As part of a collaborative project with Dr. Jonathan Schneck, the effect of glycosylation was investigated using differentially sialylated CD8+ T cells from naïve 2C-TCR transgenic mice.

To generate a desialylated T cell population, a broad range neuraminidase from *vibrio cholera* (Sigma N-6514) was utilized, which removes both N- and O-linked glycans. Briefly, naïve CD8+ T cells from 2C TCR-transgenic mice were kept at a density of 2×10^6 /mL and incubated with 8 μ L/mL neuraminidase for 30 minutes at 37°C degrees. The extent of desialylation was determined by a reduction in anti-CD43 staining (data not shown). To generate a resialylated T cell population, a sialyltransferase (Calbiotech Cat# 566227) was utilized to add back the O-linked glycans. Briefly, 1.5mM CMP-Sialic Acid (EMD Cat# 233264) was added with 0.2 Units of sialyltransferase to the desialylated T cells and incubated for 40 minutes at 37°C degrees. The extent of

resialylation was determined by an increase in anti-CD43 staining (data not shown). The differentially sialylated T cell sub-populations were stained with labeled peptide-K^b monomers for one hour at 4°C degrees. T cells were fixed for 5 minutes using 1% paraformaldehyde and then washed once with staining buffer to get rid of any nonspecifically bound monomer.

Unlike MHC tetramer binding, where glycosylation could affect either TCR clustering or CD8 co-engagement (Demetriou, Granovsky et al. 2001), MHC monomers can engage only a single TCR, which would not be affected by TCR clustering. For this reason, we hypothesized that any effect of glycosylation on MHC monomer binding might be attributable to altered CD8 co-engagement.

We observed that naïve desialylated CD8⁺ T cells bind MHC monomers more cooperatively as compared to naïve untreated CD8⁺ T cells (Figure V.C.1A, B). The monomer binding data for the desialylated CD8⁺ T cells fit a two-site binding equation, which indicates the simultaneous engagement of TCR and CD8 onto MHC monomers. Additionally, a curvilinear scatchard plot for the MHC monomer binding was observed for the naïve desialylated T cells, which indicates more cooperative binding following desialylation (Figure V.C.1B). Interestingly, adding back O-linked glycans onto the naïve desialylated T cells resulted in less cooperative MHC monomer binding (Figure V.C.1C), similar to what was observed for the naïve untreated CD8⁺T cells (Figure V.C.1A).

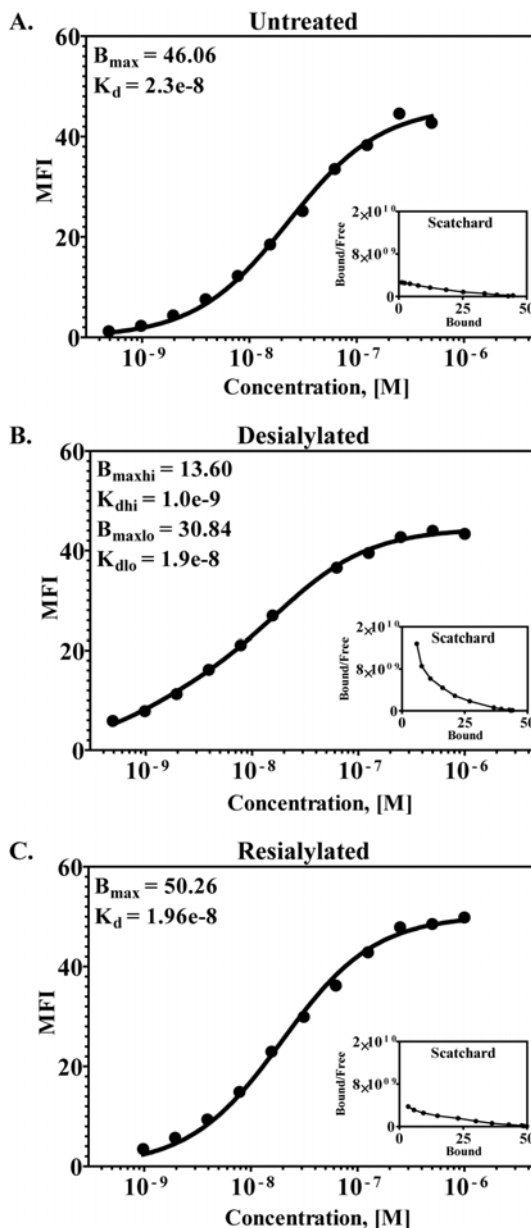


Figure V.C.1. Glycosylation Modulates MHC Class I Monomer Binding. CD8⁺ T cells from 2C TCR-transgenic mice were differentially glycosylated and tested for binding to Alexa 647-labeled peptide- K^b monomers. Specific MHC monomer binding to A. Naïve T cells (Untreated), B. naïve desialylated (Desialylated) and C. naïve resialylated after desialylation (Resialylated) T cells was calculated for each concentration by subtracting the observed binding (MFI) of the noncognate K^b OVA monomer from that of the cognate K^b SIY monomer. The specific binding data was fit using Graphpad to a one-site or two-site binding equation and plotted against concentration on a logarithmic scale. Scatchard analysis was performed and displayed as an inset.

To confirm that the effect of glycosylation on MHC monomer binding is due to altered CD8 co-engagement, we generated the widely used D227K mutation in the conserved MHC class I HC $\alpha 3$ domain (Daniels and Jameson 2000; Dutoit, Guillaume et al. 2003). Most studies have addressed the role of this CD8 mutation using MHC tetramers. However, binding of multivalent MHC tetramers may depend more on the higher affinity MHC-TCR interaction ($\sim 10 \mu\text{M}$) (Cole, Pumphrey et al. 2007) as compared to the CD8-MHC interaction ($\sim 100 \mu\text{M}$) (Moody, Xiong et al. 2001), which makes tetramer binding a complicated method to analyze CD8 co-engagement. For this reason, we performed MHC monomer binding assays on the high affinity OT-1 TCR system (Alam, Davies et al. 1999), which might tolerate the absence of CD8 co-engagement for MHC monomer binding.

Our results show that cognate K^{b} OVA monomers bind to naïve OT-1 T cells, with binding not observed for the noncognate K^{b} SIY monomer (Figure V.C.2A). However, we found that K^{b} OVA binding was abrogated in the absence of CD8 co-engagement, which initially appeared to be an interesting result. Upon reagent analysis, I observed that the K^{b} D227K monomers were more susceptible to protein aggregation under storage conditions that have been routinely used for the WT K^{b} monomers. For this reason, I analyzed the Alexa 647-labeled peptide- K^{b} complexes by size exclusion chromatography (data not shown) and 12% SDS-PAGE (Figure V.C.2B). The SDS-PAGE analysis revealed that the Alexa 647-labeled peptide- K^{b} complexes contain cleavage products, as indicated by protein bands appearing around 26 kDa and ~ 30 kDa. The cleavage products are most likely derived from the MHC Class I heavy chain, as the same relative

amount of $\beta_2\text{M}$ is detected for both the WT and D227K complexes. This finding indicates that the D227K mutation compromises the stability of the MHC class I HC or alternatively, makes it susceptible to proteolysis.

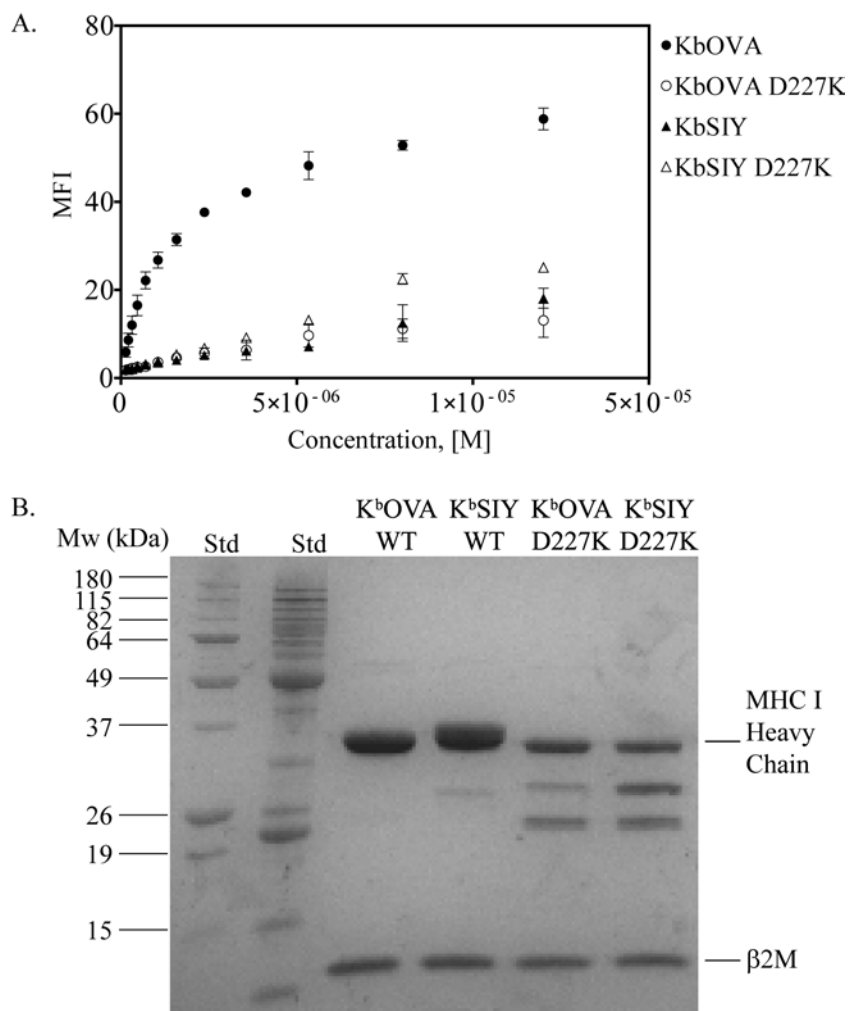


Figure V.C.2. Mutation of the Conserved CD8 Binding Site Compromises the Stability of the MHC Class I Complex. A. Naïve CD8⁺ T cells from OT-1 transgenic mice were tested for binding to Alexa 657-labeled peptide-K^b monomers, which contain either an intact or mutated (D227K) CD8 binding site. The monomer binding (MFI) was plotted against concentration. B. Alexa 647-labeled peptide-K^b monomers were analyzed by 12% SDS-PAGE. The bands corresponding to MHC class I heavy chain and β ₂M are indicated on the right hand side. Molecular weight markers are labeled on the left hand side.

V.D. In Cellular Assays the 9mer LCMV-GP₃₃₋₄₁ Peptide binds to H-2K^b as the 8mer LCMV-GP₃₄₋₄₁ Peptide

Canonically, the termini of MHC class I bound peptides associate with the MHC Class I heavy chain through hydrogen bonding at the amino terminus and hydrophobic interactions at the carboxyl terminus (Matsumura, Fremont et al. 1992; Rammensee 1995). However, a recent report has contradicted this view, and instead, has reported that the 9mer LCMV-GP₃₃₋₄₁ (KAVYNFATM) peptide can bind to the MHC Class I H-2K^b without hydrogen bonding interactions with the MHC class I molecule at the amino terminus (Achour, Michaelsson et al. 2002). In addition, this report indicated that the 9mer LCMV-GP₃₃₋₄₁ peptide binds to H-2K^b in a manner that allows for the P1K residue to be extended out of the amino terminal pocket on the MHC class I molecule. However, the crystallographic data which accompanies this report does not contain electron density for the P1K residue, which was attributed to the flexibility of this residue in the absence of an interaction with the MHC class I heavy chain (Achour, Michaelsson et al. 2002).

The cellular results that I have indicate that the 9mer LCMV-GP₃₃₋₄₁ peptide (KAVYNFATM) binds as the 8mer LCMV-GP₃₄₋₄₁ (AVYNFATM) peptide to the H-2K^b molecule. To determine if the 9mer LCMV-GP₃₃₋₄₁ peptide is presented by H-2K^b molecules, we first tested the refolding efficiency of the 8mer LCMV-GP₃₃₋₄₁ and the 9mer LCMV-GP₃₄₋₄₁ peptides onto H-2K^b molecules. We observe that the refolding efficiency of the 9mer K^bGP₃₃₋₄₁ complex is tenfold lower as compared to the native 8mer K^bGP₃₄₋₄₁ complex, as indicated by the anion exchange chromatography traces (Figure V.D.1). SDS-PAGE analysis of the labeled fractions from the anion exchange

chromatography show trace amounts of the K^b heavy chain and β_2 M light chain detected for the K^bGP₃₃₋₄₁ complex, whereas both subunits were readily observed for the K^bGP₃₄₋₄₁ complex (Figure V.D.1B). These results clearly demonstrate that the K^bGP₃₃₋₄₁ complex is refolded much less efficiently as compared to the K^bGP₃₄₋₄₁ complex.

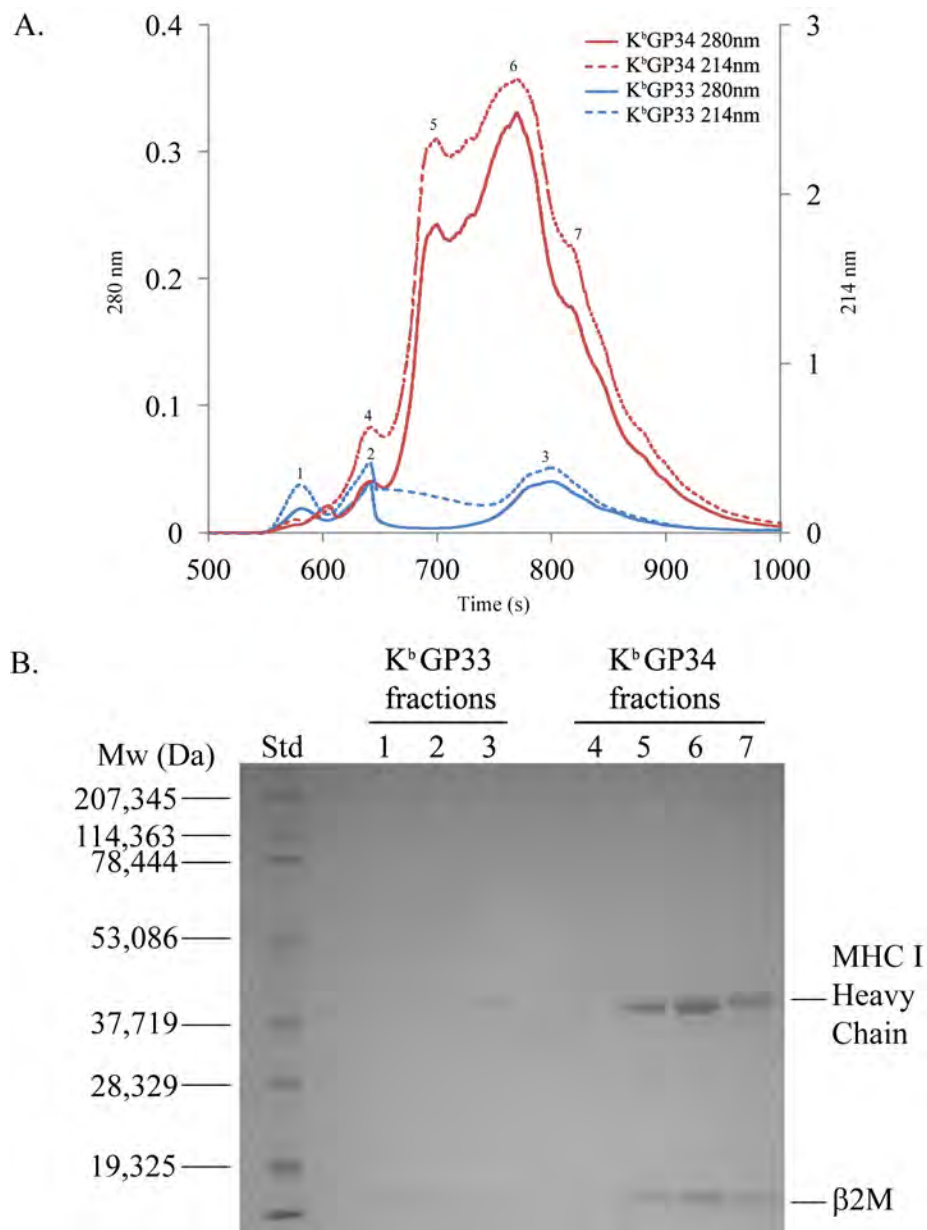


Figure V.D.1. The 9mer LCMV-GP₃₃₋₄₁ Peptide Refolds Inefficiently with H-2K^b. MHC Class I refolding was conducted as previously described using 95% pure peptide preparations (21st Century Biochemicals). A. Folded H-2K^b complexes were buffer exchanged into 20 mM Tris pH 8.0 and purified by anion exchange chromatography. The 280 nm and 214 nm wavelengths are displayed for both K^bGP₃₃₋₄₁ and K^bGP₃₄₋₄₁. B. Fractions from the anion exchange purification of both H-2K^b complexes were analyzed by 12% SDS-PAGE. The band corresponding to MHC Class I HC and β₂M light chain are indicated on the right hand side. The molecular weight markers are indicated on the left hand side.

Since the 9mer GP₃₃₋₄₁ peptide refolded inefficiently with the H-2K^b molecule, we hypothesized that the trace amounts of refolded K^b from the 9mer GP₃₃₋₄₁ peptide refolding, might actually be complexes of K^b with the shorter 8mer GP₃₄₋₄₁ peptide. This could occur if the 9mer GP₃₃₋₄₁ peptide was cleaved at the amino terminus. To determine if the 9mer GP₃₃₋₄₁ peptide is bound by H-2K^b molecules as the 8mer GP₃₄₋₄₁ peptide, we analyzed both refolded K^b complexes (from Figure V.D.2) by mass spectrometry. The results of the mass spectroscopy experiment indicate that K^bGP₃₃₋₄₁ complex mostly contains the 8mer GP₃₄₋₄₁ peptide (Mw = 916 da), as indicated by a peak at 938.7 da,, which contains a single sodium adduct. However, the longer GP₃₃₋₄₁ peptide (Mw = 1044.2 da) was also observed in the K^bGP₃₃₋₄₁ complex, which is indicated by a peak at 1066.2 da. Analysis of the K^bGP₃₄₋₄₁ complex showed in a single peak at 938.7 da, which corresponds to the sole presence of the 8mer GP₃₄₋₄₁ peptide with a single sodium adduct. Together, these results indicate that the 9mer GP₃₃₋₄₁ peptide may bind to H-2K^b molecules as either the 9mer GP₃₃₋₄₁ peptide or the truncated 8mer GP₃₄₋₄₁ peptide. However, given that the 9mer GP₃₃₋₄₁ peptide refolds very inefficiently with H-2K^b molecules, the trace amount of GP₃₃₋₄₁ peptide detected could be due to residual peptide from the refolding mixture. Further examination, including an *in vitro* peptide binding assay for K^b, will be needed to precisely determine if the 9mer GP₃₃₋₄₁ peptide is bound and presented by the H-2K^b molecule.

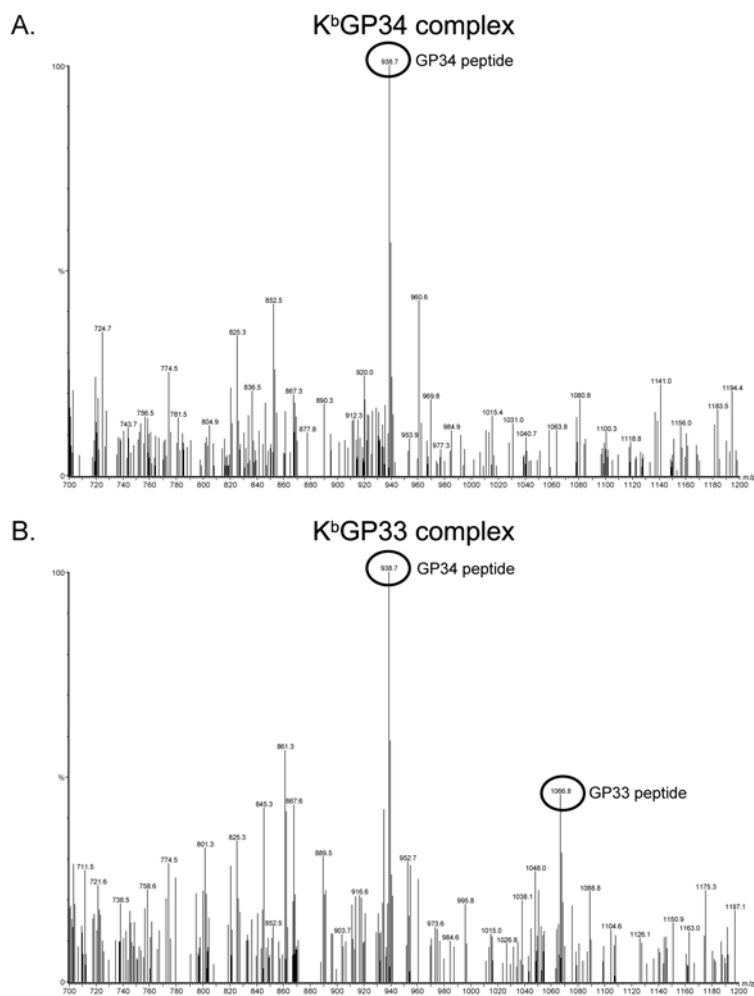


Figure V.D.2 The 9mer GP₃₃₋₄₁ Peptide Binds to H-2K^b Molecules as either GP₃₃₋₄₁ or the Truncated GP₃₄₋₄₁ Peptide. Mass spectroscopy using Matrix-Assisted Laser Desorption/Ionization (MALDI) of K^bGP₃₃₋₄₁ indicates that a portion of the 9mer GP₃₃₋₄₁ peptide is truncated, and bound to H-2K^b molecules as 8mer GP₃₄₋₄₁.

VI: Bibliography

- Achour, A., J. Michaelsson, et al. (2002). "A structural basis for LCMV immune evasion: subversion of H-2D(b) and H-2K(b) presentation of gp33 revealed by comparative crystal structure analyses." *Immunity* **17**(6): 757-768.
- Adams, P. D., P. V. Afonine, et al. (2010). "PHENIX: a comprehensive Python-based system for macromolecular structure solution." *Acta Crystallogr D Biol Crystallogr* **66**(Pt 2): 213-221.
- Aichele, P., K. Brduscha-Riem, et al. (1997). "Peptide antigen treatment of naive and virus-immune mice: antigen-specific tolerance versus immunopathology." *Immunity* **6**(5): 519-529.
- Alam, S. M., G. M. Davies, et al. (1999). "Qualitative and quantitative differences in T cell receptor binding of agonist and antagonist ligands." *Immunity* **10**(2): 227-237.
- Altman, J. D. and M. M. Davis (2003). "MHC-peptide tetramers to visualize antigen-specific T cells." *Curr Protoc Immunol* **Chapter 17**: Unit 17 13.
- Altman, J. D., P. A. Moss, et al. (1996). "Phenotypic analysis of antigen-specific T lymphocytes." *Science* **274**(5284): 94-96.
- Androlewicz, M. J., K. S. Anderson, et al. (1993). "Evidence that transporters associated with antigen processing translocate a major histocompatibility complex class I-binding peptide into the endoplasmic reticulum in an ATP-dependent manner." *Proc Natl Acad Sci U S A* **90**(19): 9130-9134.
- Badis, G., M. F. Berger, et al. (2009). "Diversity and complexity in DNA recognition by transcription factors." *Science* **324**(5935): 1720-1723.
- Banchereau, J., F. Briere, et al. (2000). "Immunobiology of dendritic cells." *Annu Rev Immunol* **18**: 767-811.
- Best, M. D. (2009). "Click chemistry and bioorthogonal reactions: unprecedented selectivity in the labeling of biological molecules." *Biochemistry* **48**(28): 6571-6584.
- Biron, C. A. (2001). "Interferons alpha and beta as immune regulators--a new look." *Immunity* **14**(6): 661-664.
- Bjorkman, P. J., M. A. Saper, et al. (1987). "Structure of the human class I histocompatibility antigen, HLA-A2." *Nature* **329**(6139): 506-512.
- Blattman, J. N., D. J. Sourdive, et al. (2000). "Evolution of the T cell repertoire during primary, memory, and recall responses to viral infection." *J Immunol* **165**(11): 6081-6090.
- Boehm, T. (2011). "Design principles of adaptive immune systems." *Nat Rev Immunol* **11**(5): 307-317.
- Boen, E., A. R. Crownover, et al. (2000). "Identification of T cell ligands in a library of peptides covalently attached to HLA-DR4." *J Immunol* **165**(4): 2040-2047.

- Boniface, J. J., J. D. Rabinowitz, et al. (1998). "Initiation of signal transduction through the T cell receptor requires the multivalent engagement of peptide/MHC ligands [corrected]." *Immunity* **9**(4): 459-466.
- Borbulevych, O. Y., K. H. Piepenbrink, et al. (2011). "Conformational melding permits a conserved binding geometry in TCR recognition of foreign and self molecular mimics." *J Immunol* **186**(5): 2950-2958.
- Borbulevych, O. Y., K. H. Piepenbrink, et al. (2009). "T cell receptor cross-reactivity directed by antigen-dependent tuning of peptide-MHC molecular flexibility." *Immunity* **31**(6): 885-896.
- Borbulevych, O. Y., S. M. Santhanagopalan, et al. (2011). "TCRs used in cancer gene therapy cross-react with MART-1/Melan-A tumor antigens via distinct mechanisms." *J Immunol* **187**(5): 2453-2463.
- Borst, J., J. E. Coligan, et al. (1984). "The delta- and epsilon-chains of the human T3/T-cell receptor complex are distinct polypeptides." *Nature* **312**(5993): 455-458.
- Bouso, P., A. Casrouge, et al. (1998). "Individual variations in the murine T cell response to a specific peptide reflect variability in naive repertoires." *Immunity* **9**(2): 169-178.
- Brandle, D., C. Muller, et al. (1992). "Engagement of the T-cell receptor during positive selection in the thymus down-regulates RAG-1 expression." *Proc Natl Acad Sci U S A* **89**(20): 9529-9533.
- Brunger, A. T. (2007). "Version 1.2 of the Crystallography and NMR system." *Nat Protoc* **2**(11): 2728-2733.
- Buchmeier, M. J., R. M. Welsh, et al. (1980). "The virology and immunobiology of lymphocytic choriomeningitis virus infection." *Adv Immunol* **30**: 275-331.
- Busch, D. H., I. Pilip, et al. (1998). "Evolution of a complex T cell receptor repertoire during primary and recall bacterial infection." *J Exp Med* **188**(1): 61-70.
- Call, M. E., J. Pyrdol, et al. (2002). "The organizing principle in the formation of the T cell receptor-CD3 complex." *Cell* **111**(7): 967-979.
- Cammarota, G., A. Scheirle, et al. (1992). "Identification of a CD4 binding site on the beta 2 domain of HLA-DR molecules." *Nature* **356**(6372): 799-801.
- Casrouge, A., E. Beaudoin, et al. (2000). "Size estimate of the alpha beta TCR repertoire of naive mouse splenocytes." *J Immunol* **164**(11): 5782-5787.
- Chaudhri, G., B. J. Quah, et al. (2009). "T cell receptor sharing by cytotoxic T lymphocytes facilitates efficient virus control." *Proc Natl Acad Sci U S A* **106**(35): 14984-14989.
- Chen, A. T., M. Cornberg, et al. (2012). "Loss of anti-viral immunity by infection with a virus encoding a cross-reactive pathogenic epitope." *PLoS Pathog* **8**(4).
- Chen, H. D., A. E. Fraire, et al. (2001). "Memory CD8+ T cells in heterologous antiviral immunity and immunopathology in the lung." *Nat Immunol* **2**(11): 1067-1076.
- Chen, H. D., A. E. Fraire, et al. (2003). "Specific history of heterologous virus infections determines anti-viral immunity and immunopathology in the lung." *Am J Pathol* **163**(4): 1341-1355.

- Chidgey, A. and R. Boyd (1997). "Agonist peptide modulates T cell selection thresholds through qualitative and quantitative shifts in CD8 co-receptor expression." *Int Immunol* **9**(10): 1527-1536.
- Classon, B. J., M. H. Brown, et al. (1992). "The hinge region of the CD8 alpha chain: structure, antigenicity, and utility in expression of immunoglobulin superfamily domains." *Int Immunol* **4**(2): 215-225.
- Clayton, L. K., M. Sieh, et al. (1989). "Identification of human CD4 residues affecting class II MHC versus HIV-1 gp120 binding." *Nature* **339**(6225): 548-551.
- Clement, C. C., E. S. Cannizzo, et al. (2010). "An expanded self-antigen peptidome is carried by the human lymph as compared to the plasma." *PLoS One* **5**(3): e9863.
- Clute, S. C., L. B. Watkin, et al. (2005). "Cross-reactive influenza virus-specific CD8+ T cells contribute to lymphoproliferation in Epstein-Barr virus-associated infectious mononucleosis." *J Clin Invest* **115**(12): 3602-3612.
- Cochran, J. R., T. O. Cameron, et al. (2001). "Receptor proximity, not intermolecular orientation, is critical for triggering T-cell activation." *J Biol Chem* **276**(30): 28068-28074.
- Cole, D. K., N. J. Pumphrey, et al. (2007). "Human TCR-binding affinity is governed by MHC class restriction." *J Immunol* **178**(9): 5727-5734.
- Colf, L. A., A. J. Bankovich, et al. (2007). "How a single T cell receptor recognizes both self and foreign MHC." *Cell* **129**(1): 135-146.
- Cornberg, M., A. T. Chen, et al. (2006). "Narrowed TCR repertoire and viral escape as a consequence of heterologous immunity." *J Clin Invest* **116**(5): 1443-1456.
- Cornberg, M., S. C. Clute, et al. (2010). "CD8 T cell cross-reactivity networks mediate heterologous immunity in human EBV and murine vaccinia virus infections." *J Immunol* **184**(6): 2825-2838.
- Cornberg, M., S. C. Clute, et al. (2010). "CD8 T Cell Cross-Reactivity Networks Mediate Heterologous Immunity in Human EBV and Murine Vaccinia Virus Infections." *J Immunol*.
- Cornberg, M., B. S. Sheridan, et al. (2007). "Protection against vaccinia virus challenge by CD8 memory T cells resolved by molecular mimicry." *J Virol* **81**(2): 934-944.
- Dai, S., E. S. Huseby, et al. (2008). "Crossreactive T Cells spotlight the germline rules for alphabeta T cell-receptor interactions with MHC molecules." *Immunity* **28**(3): 324-334.
- Daniels, M. A., L. Devine, et al. (2001). "CD8 binding to MHC class I molecules is influenced by T cell maturation and glycosylation." *Immunity* **15**(6): 1051-1061.
- Daniels, M. A., K. A. Hogquist, et al. (2002). "Sweet 'n' sour: the impact of differential glycosylation on T cell responses." *Nat Immunol* **3**(10): 903-910.
- Daniels, M. A. and S. C. Jameson (2000). "Critical role for CD8 in T cell receptor binding and activation by peptide/major histocompatibility complex multimers." *J Exp Med* **191**(2): 335-346.
- Degen, E., M. F. Cohen-Doyle, et al. (1992). "Efficient dissociation of the p88 chaperone from major histocompatibility complex class I molecules requires both beta 2-microglobulin and peptide." *J Exp Med* **175**(6): 1653-1661.

- Delon, J., C. Gregoire, et al. (1998). "CD8 expression allows T cell signaling by monomeric peptide-MHC complexes." *Immunity* **9**(4): 467-473.
- Demetriou, M., M. Granovsky, et al. (2001). "Negative regulation of T-cell activation and autoimmunity by Mgat5 N-glycosylation." *Nature* **409**(6821): 733-739.
- Dietze, K. K., G. Zelinsky, et al. (2011). "Transient depletion of regulatory T cells in transgenic mice reactivates virus-specific CD8+ T cells and reduces chronic retroviral set points." *Proc Natl Acad Sci U S A* **108**(6): 2420-2425.
- Dirksen, A., S. Dirksen, et al. (2006). "Nucleophilic catalysis of hydrazone formation and transimination: implications for dynamic covalent chemistry." *J Am Chem Soc* **128**(49): 15602-15603.
- Doyle, C. and J. L. Strominger (1987). "Interaction between CD4 and class II MHC molecules mediates cell adhesion." *Nature* **330**(6145): 256-259.
- Duffy, S., K. L. Tsao, et al. (1998). "Site-specific, enzymatic biotinylation of recombinant proteins in *Spodoptera frugiperda* cells using biotin acceptor peptides." *Anal Biochem* **262**(2): 122-128.
- Dustin, M. L. and A. C. Chan (2000). "Signaling takes shape in the immune system." *Cell* **103**(2): 283-294.
- Dutoit, V., P. Guillaume, et al. (2003). "Decreased binding of peptides-MHC class I (pMHC) multimeric complexes to CD8 affects their binding avidity for the TCR but does not significantly impact on pMHC/TCR dissociation rate." *J Immunol* **170**(10): 5110-5117.
- Emsley, P. and K. Cowtan (2004). "Coot: model-building tools for molecular graphics." *Acta Crystallogr D Biol Crystallogr* **60**(Pt 12 Pt 1): 2126-2132.
- Fahmy, T. M., J. G. Bieler, et al. (2001). "Increased TCR avidity after T cell activation: a mechanism for sensing low-density antigen." *Immunity* **14**(2): 135-143.
- Fahmy, T. M., J. G. Bieler, et al. (2002). "Probing T cell membrane organization using dimeric MHC-Ig complexes." *J Immunol Methods* **268**(1): 93-106.
- Falk, K., O. Rotzschke, et al. (1991). "Allele-specific motifs revealed by sequencing of self-peptides eluted from MHC molecules." *Nature* **351**(6324): 290-296.
- Fazekas de St. G. and R. G. Webster (1966). "Disquisitions of Original Antigenic Sin. I. Evidence in man." *J Exp Med* **124**(3): 331-345.
- Felix, N. J. and P. M. Allen (2007). "Specificity of T-cell alloreactivity." *Nat Rev Immunol* **7**(12): 942-953.
- Fremont, D. H., M. Matsumura, et al. (1992). "Crystal structures of two viral peptides in complex with murine MHC class I H-2Kb." *Science* **257**(5072): 919-927.
- Gakamsky, D. M., I. F. Luescher, et al. (2005). "CD8 kinetically promotes ligand binding to the T-cell antigen receptor." *Biophys J* **89**(3): 2121-2133.
- Gallucci, S. and P. Matzinger (2001). "Danger signals: SOS to the immune system." *Curr Opin Immunol* **13**(1): 114-119.
- Gao, G. F., J. Tormo, et al. (1997). "Crystal structure of the complex between human CD8alpha(alpha) and HLA-A2." *Nature* **387**(6633): 630-634.
- Garboczi, D. N., P. Ghosh, et al. (1996). "Structure of the complex between human T-cell receptor, viral peptide and HLA-A2." *Nature* **384**(6605): 134-141.

- Garboczi, D. N., D. T. Hung, et al. (1992). "HLA-A2-peptide complexes: refolding and crystallization of molecules expressed in *Escherichia coli* and complexed with single antigenic peptides." Proc Natl Acad Sci U S A **89**(8): 3429-3433.
- Garcia, K. C. (1999). "Molecular interactions between extracellular components of the T-cell receptor signaling complex." Immunol Rev **172**: 73-85.
- Garcia, K. C., M. Degano, et al. (1998). "Structural basis of plasticity in T cell receptor recognition of a self peptide-MHC antigen." Science **279**(5354): 1166-1172.
- Garcia, K. C., M. Degano, et al. (1996). "An alphabeta T cell receptor structure at 2.5 Å and its orientation in the TCR-MHC complex." Science **274**(5285): 209-219.
- Garcia, K. C., C. A. Scott, et al. (1996). "CD8 enhances formation of stable T-cell receptor/MHC class I molecule complexes." Nature **384**(6609): 577-581.
- Garcia, K. C., L. Teyton, et al. (1999). "Structural basis of T cell recognition." Annu Rev Immunol **17**: 369-397.
- Hardardottir, F., J. L. Baron, et al. (1995). "T cells with two functional antigen-specific receptors." Proc Natl Acad Sci U S A **92**(2): 354-358.
- He, X., C. A. Janeway, Jr., et al. (2002). "Dual receptor T cells extend the immune repertoire for foreign antigens." Nat Immunol **3**(2): 127-134.
- Hewitt, E. W. (2003). "The MHC class I antigen presentation pathway: strategies for viral immune evasion." Immunology **110**(2): 163-169.
- Hult, K. and P. Berglund (2007). "Enzyme promiscuity: mechanism and applications." Trends Biotechnol **25**(5): 231-238.
- Ignatowicz, L., J. Kappler, et al. (1996). "The repertoire of T cells shaped by a single MHC/peptide ligand." Cell **84**(4): 521-529.
- Ignatowicz, L., W. Rees, et al. (1997). "T cells can be activated by peptides that are unrelated in sequence to their selecting peptide." Immunity **7**(2): 179-186.
- Janeway, C. A., Jr. and R. Medzhitov (2002). "Innate immune recognition." Annu Rev Immunol **20**: 197-216.
- Janeway, C. A., Travers, P., Walport, M., Shlomchik, M. (2001). Immunobiology: The Immune System in Health and Disease. New York, Garland Science.
- Jiang, N., J. Huang, et al. (2011). "Two-stage cooperative T cell receptor-peptide major histocompatibility complex-CD8 trimolecular interactions amplify antigen discrimination." Immunity **34**(1): 13-23.
- Juang, J., P. J. Ebert, et al. (2010). "Peptide-MHC heterodimers show that thymic positive selection requires a more restricted set of self-peptides than negative selection." J Exp Med **207**(6): 1223-1234.
- Kappler, J. W., N. Roehm, et al. (1987). "T cell tolerance by clonal elimination in the thymus." Cell **49**(2): 273-280.
- Kern, P., R. E. Hussey, et al. (1999). "Expression, purification, and functional analysis of murine ectodomain fragments of CD8alphaalpha and CD8alphabeta dimers." J Biol Chem **274**(38): 27237-27243.
- Kern, P. S., M. K. Teng, et al. (1998). "Structural basis of CD8 coreceptor function revealed by crystallographic analysis of a murine CD8alphaalpha ectodomain fragment in complex with H-2Kb." Immunity **9**(4): 519-530.

- Kerry, S. E., J. Buslepp, et al. (2003). "Interplay between TCR affinity and necessity of coreceptor ligation: high-affinity peptide-MHC/TCR interaction overcomes lack of CD8 engagement." *J Immunol* **171**(9): 4493-4503.
- Kerry, S. E., R. Maile, et al. (2005). "Memory CD8 T cells require CD8 coreceptor engagement for calcium mobilization and proliferation, but not cytokine production." *Immunology* **114**(1): 44-52.
- Khanolkar, A., M. J. Fuller, et al. (2004). "CD4 T cell-dependent CD8 T cell maturation." *J Immunol* **172**(5): 2834-2844.
- Kim, S. K., M. Cornberg, et al. (2005). "Private specificities of CD8 T cell responses control patterns of heterologous immunity." *J Exp Med* **201**(4): 523-533.
- King, T. P., S. W. Zhao, et al. (1986). "Preparation of protein conjugates via intermolecular hydrazone linkage." *Biochemistry* **25**(19): 5774-5779.
- Kisselev, A. F., T. N. Akopian, et al. (1999). "The sizes of peptides generated from protein by mammalian 26 and 20 S proteasomes. Implications for understanding the degradative mechanism and antigen presentation." *J Biol Chem* **274**(6): 3363-3371.
- Kitagawa, T. and T. Aikawa (1976). "Enzyme coupled immunoassay of insulin using a novel coupling reagent." *J Biochem* **79**(1): 233-236.
- Kotturi, M. F., B. Peters, et al. (2007). "The CD8+ T-cell response to lymphocytic choriomeningitis virus involves the L antigen: uncovering new tricks for an old virus." *J Virol* **81**(10): 4928-4940.
- Kotturi, M. F., I. Scott, et al. (2008). "Naive precursor frequencies and MHC binding rather than the degree of epitope diversity shape CD8+ T cell immunodominance." *J Immunol* **181**(3): 2124-2133.
- Krogsgaard, M., Q. J. Li, et al. (2005). "Agonist/endogenous peptide-MHC heterodimers drive T cell activation and sensitivity." *Nature* **434**(7030): 238-243.
- Lanzavecchia, A. and F. Sallusto (2002). "Progressive differentiation and selection of the fittest in the immune response." *Nat Rev Immunol* **2**(12): 982-987.
- Laugel, B., H. A. van den Berg, et al. (2007). "Different T cell receptor affinity thresholds and CD8 coreceptor dependence govern cytotoxic T lymphocyte activation and tetramer binding properties." *J Biol Chem* **282**(33): 23799-23810.
- Leiden, J. M. and J. L. Strominger (1986). "Generation of diversity of the beta chain of the human T-lymphocyte receptor for antigen." *Proc Natl Acad Sci U S A* **83**(12): 4456-4460.
- Li, Y., Y. Huang, et al. (2005). "Structure of a human autoimmune TCR bound to a myelin basic protein self-peptide and a multiple sclerosis-associated MHC class II molecule." *EMBO J* **24**(17): 2968-2979.
- Lombardi, G., L. Barber, et al. (1991). "The specificity of alloreactive T cells is determined by MHC polymorphisms which contact the T cell receptor and which influence peptide binding." *Int Immunol* **3**(8): 769-775.
- Lowe, J. B. (2001). "Glycosylation, immunity, and autoimmunity." *Cell* **104**(6): 809-812.
- Macdonald, W. A., Z. Chen, et al. (2009). "T cell allorecognition via molecular mimicry." *Immunity* **31**(6): 897-908.
- Maile, D., Brostoff, J., Roth, D., Roitt, I., (2006). *Immunology*, Elsevier.

- Mariuzza, R. A. (2006). "Multiple paths to multispecificity." *Immunity* **24**(4): 359-361.
- Marrack, P. and J. Kappler (1988). "The T-cell repertoire for antigen and MHC." *Immunol Today* **9**(10): 308-315.
- Mason, D. (1998). "A very high level of crossreactivity is an essential feature of the T-cell receptor." *Immunol Today* **19**(9): 395-404.
- Masopust, D., V. Vezys, et al. (2001). "Preferential localization of effector memory cells in nonlymphoid tissue." *Science* **291**(5512): 2413-2417.
- Mathew, A., I. Kurane, et al. (1998). "Predominance of HLA-restricted cytotoxic T-lymphocyte responses to serotype-cross-reactive epitopes on nonstructural proteins following natural secondary dengue virus infection." *J Virol* **72**(5): 3999-4004.
- Matsumura, M., D. H. Fremont, et al. (1992). "Emerging principles for the recognition of peptide antigens by MHC class I molecules." *Science* **257**(5072): 927-934.
- Mazza, C., N. Auphan-Anezin, et al. (2007). "How much can a T-cell antigen receptor adapt to structurally distinct antigenic peptides?" *EMBO J* **26**(7): 1972-1983.
- McCoy, A. J., R. W. Grosse-Kunstleve, et al. (2007). "Phaser crystallographic software." *J Appl Crystallogr* **40**(Pt 4): 658-674.
- Medzhitov, R. and C. Janeway, Jr. (2000). "Innate immunity." *N Engl J Med* **343**(5): 338-344.
- Minor, W., M. Cymborowski, et al. (2006). "HKL-3000: the integration of data reduction and structure solution--from diffraction images to an initial model in minutes." *Acta Crystallogr D Biol Crystallogr* **62**(Pt 8): 859-866.
- Mongkolsapaya, J., W. Dejnirattisai, et al. (2003). "Original antigenic sin and apoptosis in the pathogenesis of dengue hemorrhagic fever." *Nat Med* **9**(7): 921-927.
- Moody, A. M., D. Chui, et al. (2001). "Developmentally regulated glycosylation of the CD8alpha-beta coreceptor stalk modulates ligand binding." *Cell* **107**(4): 501-512.
- Moody, A. M., Y. Xiong, et al. (2001). "The CD8alpha-beta co-receptor on double-positive thymocytes binds with differing affinities to the products of distinct class I MHC loci." *Eur J Immunol* **31**(9): 2791-2799.
- Moskophidis, D., F. Lechner, et al. (1993). "Virus persistence in acutely infected immunocompetent mice by exhaustion of antiviral cytotoxic effector T cells." *Nature* **362**(6422): 758-761.
- Mueller, D. L. (2010). "Mechanisms maintaining peripheral tolerance." *Nat Immunol* **11**(1): 21-27.
- Niederberger, N., K. Holmberg, et al. (2003). "Allelic exclusion of the TCR alpha-chain is an active process requiring TCR-mediated signaling and c-Cbl." *J Immunol* **170**(9): 4557-4563.
- Nugent, C. T., R. O. Renteria, et al. (2005). "Low binding capacity of murine tetramers mutated at residue 227 does not preclude the ability to efficiently activate CD8+ T lymphocytes." *Immunol Lett* **98**(2): 208-215.
- O'Rourke, A. M. and M. F. Mescher (1993). "The roles of CD8 in cytotoxic T lymphocyte function." *Immunol Today* **14**(4): 183-188.

- Ortmann, B., M. J. Androlewicz, et al. (1994). "MHC class I/beta 2-microglobulin complexes associate with TAP transporters before peptide binding." Nature **368**(6474): 864-867.
- Padovan, E., G. Casorati, et al. (1995). "Dual receptor T-cells. Implications for alloreactivity and autoimmunity." Ann N Y Acad Sci **756**: 66-70.
- Padovan, E., G. Casorati, et al. (1993). "Expression of two T cell receptor alpha chains: dual receptor T cells." Science **262**(5132): 422-424.
- Pamer, E. and P. Cresswell (1998). "Mechanisms of MHC class I--restricted antigen processing." Annu Rev Immunol **16**: 323-358.
- Pancer, Z. and M. D. Cooper (2006). "The evolution of adaptive immunity." Annu Rev Immunol **24**: 497-518.
- Parker, K. C., B. M. Carreno, et al. (1992). "Peptide binding to HLA-A2 and HLA-B27 isolated from Escherichia coli. Reconstitution of HLA-A2 and HLA-B27 heavy chain/beta 2-microglobulin complexes requires specific peptides." J Biol Chem **267**(8): 5451-5459.
- Potter, T. A., T. V. Rajan, et al. (1989). "Substitution at residue 227 of H-2 class I molecules abrogates recognition by CD8-dependent, but not CD8-independent, cytotoxic T lymphocytes." Nature **337**(6202): 73-75.
- Poussier, P. and M. Julius (1994). "Thymus independent T cell development and selection in the intestinal epithelium." Annu Rev Immunol **12**: 521-553.
- Puglielli, M. T., A. J. Zajac, et al. (2001). "In vivo selection of a lymphocytic choriomeningitis virus variant that affects recognition of the GP33-43 epitope by H-2Db but not H-2Kb." J Virol **75**(11): 5099-5107.
- Quigley, M., X. Huang, et al. (2007). "Extent of stimulation controls the formation of memory CD8 T cells." J Immunol **179**(9): 5768-5777.
- Rammensee, H. G. (1995). "Chemistry of peptides associated with MHC class I and class II molecules." Curr Opin Immunol **7**(1): 85-96.
- Rothman, A. L. (2009). "T lymphocyte responses to heterologous secondary dengue virus infections." Ann N Y Acad Sci **1171 Suppl 1**: E36-41.
- Rudd, P. M., M. R. Wormald, et al. (1999). "Roles for glycosylation of cell surface receptors involved in cellular immune recognition." J Mol Biol **293**(2): 351-366.
- Rudolph, M. G., R. L. Stanfield, et al. (2006). "How TCRs bind MHCs, peptides, and coreceptors." Annu Rev Immunol **24**: 419-466.
- Sadasivan, B., P. J. Lehner, et al. (1996). "Roles for calreticulin and a novel glycoprotein, tapasin, in the interaction of MHC class I molecules with TAP." Immunity **5**(2): 103-114.
- Sallusto, F., J. Geginat, et al. (2004). "Central memory and effector memory T cell subsets: function, generation, and maintenance." Annu Rev Immunol **22**: 745-763.
- Sallusto, F., D. Lenig, et al. (1999). "Two subsets of memory T lymphocytes with distinct homing potentials and effector functions." Nature **401**(6754): 708-712.
- Schatz, D. G., M. A. Oettinger, et al. (1989). "The V(D)J recombination activating gene, RAG-1." Cell **59**(6): 1035-1048.

- Schott, E., N. Bertho, et al. (2002). "Class I negative CD8 T cells reveal the confounding role of peptide-transfer onto CD8 T cells stimulated with soluble H2-Kb molecules." Proc Natl Acad Sci U S A **99**(21): 13735-13740.
- Schott, E. and H. L. Ploegh (2002). "Mouse MHC class I tetramers that are unable to bind to CD8 reveal the need for CD8 engagement in order to activate naive CD8 T cells." Eur J Immunol **32**(12): 3425-3434.
- Schwartz, R. H. (2003). "T cell anergy." Annu Rev Immunol **21**: 305-334.
- Selin, L. K., M. A. Brehm, et al. (2006). "Memory of mice and men: CD8+ T-cell cross-reactivity and heterologous immunity." Immunol Rev **211**: 164-181.
- Selin, L. K., M. Cornberg, et al. (2004). "CD8 memory T cells: cross-reactivity and heterologous immunity." Semin Immunol **16**(5): 335-347.
- Selin, L. K., S. R. Nahill, et al. (1994). "Cross-reactivities in memory cytotoxic T lymphocyte recognition of heterologous viruses." J Exp Med **179**(6): 1933-1943.
- Selin, L. K., S. M. Varga, et al. (1998). "Protective heterologous antiviral immunity and enhanced immunopathogenesis mediated by memory T cell populations." J Exp Med **188**(9): 1705-1715.
- Selin, L. K., K. Vergilis, et al. (1996). "Reduction of otherwise remarkably stable virus-specific cytotoxic T lymphocyte memory by heterologous viral infections." J Exp Med **183**(6): 2489-2499.
- Shen, Z. T., M. A. Brehm, et al. (2010). "Bi-specific MHC heterodimers for characterization of cross-reactive T cells." J Biol Chem **285**(43): 33144-33153.
- Shepherd, J. C., T. N. Schumacher, et al. (1993). "TAP1-dependent peptide translocation in vitro is ATP dependent and peptide selective." Cell **74**(3): 577-584.
- Shortman, K., M. Egerton, et al. (1990). "The generation and fate of thymocytes." Semin Immunol **2**(1): 3-12.
- Siegal, F. P., N. Kadowaki, et al. (1999). "The nature of the principal type 1 interferon-producing cells in human blood." Science **284**(5421): 1835-1837.
- Silvennoinen, L., J. Myllyharju, et al. (2004). "Identification and characterization of structural domains of human ERp57: association with calreticulin requires several domains." J Biol Chem **279**(14): 13607-13615.
- Sixt, M., N. Kanazawa, et al. (2005). "The conduit system transports soluble antigens from the afferent lymph to resident dendritic cells in the T cell area of the lymph node." Immunity **22**(1): 19-29.
- Smith-Garvin, J. E., G. A. Koretzky, et al. (2009). "T cell activation." Annu Rev Immunol **27**: 591-619.
- Sourdive, D. J., K. Murali-Krishna, et al. (1998). "Conserved T cell receptor repertoire in primary and memory CD8 T cell responses to an acute viral infection." J Exp Med **188**(1): 71-82.
- Spaulding, A. C., I. Kurane, et al. (1999). "Analysis of murine CD8(+) T-cell clones specific for the Dengue virus NS3 protein: flavivirus cross-reactivity and influence of infecting serotype." J Virol **73**(1): 398-403.
- Sprent, J. and C. D. Surh (2002). "T cell memory." Annu Rev Immunol **20**: 551-579.

- Stern, L. J., J. H. Brown, et al. (1994). "Crystal structure of the human class II MHC protein HLA-DR1 complexed with an influenza virus peptide." *Nature* **368**(6468): 215-221.
- Stone, J. D. and L. J. Stern (2006). "CD8 T cells, like CD4 T cells, are triggered by multivalent engagement of TCRs by MHC-peptide ligands but not by monovalent engagement." *J Immunol* **176**(3): 1498-1505.
- Suchin, E. J., P. B. Langmuir, et al. (2001). "Quantifying the frequency of alloreactive T cells in vivo: new answers to an old question." *J Immunol* **166**(2): 973-981.
- Suh, W. K., M. F. Cohen-Doyle, et al. (1994). "Interaction of MHC class I molecules with the transporter associated with antigen processing." *Science* **264**(5163): 1322-1326.
- Takahama, Y. (2006). "Journey through the thymus: stromal guides for T-cell development and selection." *Nat Rev Immunol* **6**(2): 127-135.
- Toebes, M., M. Coccoris, et al. (2006). "Design and use of conditional MHC class I ligands." *Nat Med* **12**(2): 246-251.
- Townsend, A., T. Elliott, et al. (1990). "Assembly of MHC class I molecules analyzed in vitro." *Cell* **62**(2): 285-295.
- Udaka, K., K. H. Wiesmuller, et al. (1996). "Self-MHC-restricted peptides recognized by an alloreactive T lymphocyte clone." *J Immunol* **157**(2): 670-678.
- Urbani, S., B. Amadei, et al. (2005). "Heterologous T cell immunity in severe hepatitis C virus infection." *J Exp Med* **201**(5): 675-680.
- Van Bleek, G. M. and S. G. Nathenson (1990). "Isolation of an endogenously processed immunodominant viral peptide from the class I H-2Kb molecule." *Nature* **348**(6298): 213-216.
- van der Merwe, P. A. and S. J. Davis (2003). "Molecular interactions mediating T cell antigen recognition." *Annu Rev Immunol* **21**: 659-684.
- Veiga-Fernandes, H., U. Walter, et al. (2000). "Response of naive and memory CD8+ T cells to antigen stimulation in vivo." *Nat Immunol* **1**(1): 47-53.
- Velloso, L. M., J. Michaelsson, et al. (2004). "Determination of structural principles underlying three different modes of lymphocytic choriomeningitis virus escape from CTL recognition." *J Immunol* **172**(9): 5504-5511.
- Von Herrath, M. G., B. Coon, et al. (1997). "Low-affinity cytotoxic T-lymphocytes require IFN-gamma to clear an acute viral infection." *Virology* **229**(2): 349-359.
- Walzl, G., S. Tafuro, et al. (2000). "Influenza virus lung infection protects from respiratory syncytial virus-induced immunopathology." *J Exp Med* **192**(9): 1317-1326.
- Wearsch, P. A. and P. Cresswell (2007). "Selective loading of high-affinity peptides onto major histocompatibility complex class I molecules by the tapasin-ERp57 heterodimer." *Nat Immunol* **8**(8): 873-881.
- Wedemeyer, H., E. Mizukoshi, et al. (2001). "Cross-reactivity between hepatitis C virus and Influenza A virus determinant-specific cytotoxic T cells." *J Virol* **75**(23): 11392-11400.
- Welsh, R. M., J. W. Che, et al. (2010). "Heterologous immunity between viruses." *Immunol Rev* **235**(1): 244-266.

- Welsh, R. M. and R. S. Fujinami (2007). "Pathogenic epitopes, heterologous immunity and vaccine design." Nat Rev Microbiol **5**(7): 555-563.
- Welsh, R. M., S. K. Kim, et al. (2006). "The privacy of T cell memory to viruses." Curr Top Microbiol Immunol **311**: 117-153.
- Wilson, D. B., D. H. Wilson, et al. (2004). "Specificity and degeneracy of T cells." Mol Immunol **40**(14-15): 1047-1055.
- Wooldridge, L., H. A. van den Berg, et al. (2005). "Interaction between the CD8 coreceptor and major histocompatibility complex class I stabilizes T cell receptor-antigen complexes at the cell surface." J Biol Chem **280**(30): 27491-27501.
- Wu, L. C., D. S. Tuot, et al. (2002). "Two-step binding mechanism for T-cell receptor recognition of peptide MHC." Nature **418**(6897): 552-556.
- Yin, Y. and R. A. Mariuzza (2009). "The multiple mechanisms of T cell receptor cross-reactivity." Immunity **31**(6): 849-851.
- Zimmerman, C., K. Brduscha-Riem, et al. (1996). "Visualization, characterization, and turnover of CD8+ memory T cells in virus-infected hosts." J Exp Med **183**(4): 1367-1375.